

Deep Learning in Asset Pricing*

Luyang Chen[†]Markus Pelger[‡]Jason Zhu[§]

December 15, 2024

Abstract

We use deep neural networks to estimate an asset pricing model for individual stock returns that takes advantage of the vast amount of conditioning information, while keeping a fully flexible form and accounting for time-variation. The key innovations are to use the fundamental no-arbitrage condition as criterion function, to construct the most informative test assets with an adversarial approach and to extract the states of the economy from many macroeconomic time series. Our asset pricing model outperforms out-of-sample all benchmark approaches in terms of Sharpe ratio, explained variation and pricing errors and identifies the key factors that drive asset prices.

Keywords: Conditional asset pricing model, no-arbitrage, stock returns, non-linear factor model, cross-section of expected returns, machine learning, deep learning, big data, hidden states, GMM

JEL classification: C14, C38, C55, G12

*We thank Doron Avramov, Daniele Bianchi (discussant), Svetlana Bryzgalova, John Cochrane, Lin William Cong, Victor DeMiguel, Kay Giesecke, Stefano Giglio, Robert Hodrick, Bryan Kelly (discussant), Serhiy Kozak, Martin Lettau, Anton Lines, Marcelo Medeiros (discussant), Scott Murray (discussant) and Neil Shephard and seminar and conference participants at Yale SOM, Stanford, UC Berkeley, the Utah Winter Finance Conference, the GSU-RSF FinTech Conference, the New Technology in Finance Conference, the LBS Finance Summer Symposium, the Fourth International Workshop in Financial Econometrics, the Western Mathematical Finance Conference and INFORMS for helpful comments. We thank the China Merchants Bank for generous research support.

[†]Stanford University, Institute for Computational and Mathematical Engineering, Email: lych@alumni.stanford.edu.

[‡]Stanford University, Department of Management Science & Engineering, Email: mpelger@stanford.edu.

[§]Stanford University, Department of Management Science & Engineering, Email: jzhu121@stanford.edu.

The fundamental question in asset pricing is to explain differences in average returns of assets. No-arbitrage pricing theory provides a clear answer - expected returns differ because assets have different exposure to the stochastic discount factor (SDF) or pricing kernel. The empirical quest in asset pricing for the last 40 years has been to estimate a stochastic discount factor that can explain the expected returns of all assets. There are four major challenges that the literature so far has struggled to overcome in a unified framework: First, the SDF could by construction depend on all available information, which means that the SDF is a function of a potentially very large set of variables. Second, the functional form of the SDF is unknown and likely complex. Third, the SDF can have a complex dynamic structure and the risk exposure for individual assets can vary over time depending on economic conditions and changes in asset-specific attributes. Fourth, the risk premium of individual stocks has a low signal-to-noise ratio, which complicates the estimation of an SDF that explains the expected returns of all stocks.

In this paper we estimate a general non-linear asset pricing model with deep neural networks for all U.S. equity data based on a substantial set of macroeconomic and firm-specific information. Our crucial innovation is the use of the no-arbitrage condition as part of the neural network algorithm. We estimate the stochastic discount factor that explains all stock returns from the conditional moment constraints implied by no-arbitrage. It is a natural idea to use machine learning techniques like deep neural networks to deal with the high dimensionality and complex functional dependencies of the problem. However, machine-learning tools are designed to work well for prediction tasks in a high signal-to-noise environment. As asset returns in efficient markets seem to be dominated by unforecastable news, it is hard to predict the risk premium with off-the-shelf methods. We show how to build better machine learning estimators by incorporating economic structure. Including the no-arbitrage constraint in the learning algorithm significantly improves the risk premium signal and makes it possible to explain individual stock returns. Empirically, our general model outperforms out-of-sample the leading benchmark approaches and provides a clear insight into the structure of the pricing kernel and the sources of systematic risk.

Our model framework answers three conceptual key questions in asset pricing. (1) What is the functional form of the SDF based on the information set? Popular models, for example the Fama-French five-factor model, impose that the SDF depends linearly on a small number of characteristics. However, the linear model seems to be mis-specified and the factor zoo suggests that there are many more characteristics with pricing information. Our model allows for a general non-parametric form with a large number of characteristics. (2) What are the right test assets? The conventional approach is to calibrate and evaluate asset pricing models on a small number of pre-specified test assets, for example the 25 size and book-to-market double-sorted portfolios of Fama and French (1992). However, an asset pricing model that can explain well those 25 portfolios does not need to capture the pricing information of other characteristic sorted portfolios or individual stock returns. Our approach constructs in a data-driven way the most informative test assets that are the hardest to explain and identify the parameters of the SDF. (3) What are the states of the economy? Exposure and compensation for risk should depend on the economic conditions. A simple

way to capture those would be for example NBER recession indicators. However, this is a very coarse set of information given the hundreds of macroeconomic time series with complex dynamics. Our model extracts a small number of state processes that are based on the complete dynamics of a large number of macroeconomic time series and are the most relevant for asset pricing.

Our estimation approach combines no-arbitrage pricing and three neural network structures in a novel way. Each network is responsible for solving one of the three key questions outline above. First, we can explain the general functional form of the SDF as a function of the information set using a feedforward neural network. Second, we capture the time-variation of the SDF on macroeconomic conditions with a recurrent Long-Short-Term-Memory (LSTM) network that identifies a small set of macroeconomic state processes. Third, a generative adversarial network constructs the test assets by identifying the portfolios and states with the most unexplained pricing information. These three networks are linked by the no-arbitrage condition that helps to separate the risk premium signal from the noise and serves as a regularization to identify the relevant pricing information.

Our paper makes several methodological contributions. We are the first to introduce an adversarial estimation approach to finance and show that it can be interpreted as a data-driven way to construct test assets. Estimating the SDF from the fundamental no-arbitrage moment equation is conceptionally a generalized method of moment (GMM) problem. The conditional asset pricing moments imply an infinite number of moment conditions. Our generative adversarial approach provides a method to find and select the most relevant moment conditions from an infinite set of candidate moments. Second, we introduce a novel way to use neural networks to extract economic conditions from complex time series. The SDF depends on the dynamic time series structure of a large number of potentially non-stationary time series. We are the first to propose LSTM networks to summarize the dynamics of a large number of macroeconomic time series in a small number of economic states. More specifically, our LSTM approach applies in a data-driven way the most appropriate transformation to many non-stationary time series and extracts a small number of hidden state processes. Third, we propose a problem formulation that can extract the risk premium in spite of its low signal-to-noise ratio. The no-arbitrage condition identifies the components of the pricing kernel that carry a high risk premia but have only a weak variation signal. Intuitively, most machine learning methods in finance¹ fit a model that can explain as much variation as possible, which is essentially a second moment object. The no-arbitrage condition is based on explaining the risk premia, which is based on a first moment. We can decompose stock returns into a predictable risk premium part and an unpredictable martingale component. Most of the variation is driven by the unpredictable component that does not carry a risk premium. When considering average returns the unpredictable component is diversified away over time and the predictable risk premium signal is strengthened. However, the risk premia of individual stocks is time-varying and an unconditional mean of stock returns might not capture the predictable component. Therefore, we consider unconditional means of stock returns instrumented with all possible combinations of

¹These models include Gu, Kelly, and Xiu (2020), Messmer (2017) or Kelly, Pruitt, and Su (2019).

firm-specific characteristics and macroeconomic information. This serves the purpose of pushing up the risk premium signal while taking into account the time-variation in the risk premium.

Our empirical analysis is based on a data set of all available U.S. stocks from CRSP with monthly returns from 1967 to 2016 combined with 46 time-varying firm-specific characteristics and 178 macroeconomic time series. It includes the most relevant pricing anomalies and forecasting variables for the equity risk premium. Our approach outperforms out-of-sample all other benchmark approaches, which include linear models and deep neural networks that forecast risk premia instead of solving a GMM type problem. We compare the models out-of-sample with respect to the Sharpe ratio implied by the pricing kernel, the explained variation and explained average returns of individual stocks. Our model has an annual out-of-sample Sharpe ratio of 2.6 compared to 1.7 for the linear special case of our model, 1.5 for the deep learning forecasting approach and 0.8 for the Fama-French five-factor model. At the same time we can explain 8% of the variation of individual stock returns and explain 23% of the expected returns of individual stocks, which is substantially higher than the other benchmark models. On standard test assets based on single- and double-sorted anomaly portfolios our asset pricing model reveals an unprecedented pricing performance. In fact, on all 46 anomaly sorted decile portfolios we achieve a cross-sectional R^2 higher than 90%.

Our empirical main findings are six-fold. First, economic constraints improve flexible machine learning models. We confirm Gu, Kelly, and Xiu (2020)'s insight that deep neural network can explain more structure in stock returns because of their ability to fit flexible functional forms with many covariates. However, when used for asset pricing, off-the-shelf simple prediction approaches can perform worse than even linear no-arbitrage models. It is the crucial innovation to incorporate the economic constraint in the learning algorithm that allows us to detect the underlying SDF structure. Although our estimation is only based on the fundamental no-arbitrage moments, our model can explain more variation out-of-sample than a comparable model with the objective to maximize explained variation. This illustrates that the no-arbitrage condition disciplines the model and yields better results among several dimensions.

Second, we confirm that non-linear and interaction effects matter as pointed out among others by Gu, Kelly, and Xiu (2020) and Bryzgalova, Pelger, and Zhu (2020). Our finding is more subtle and also explains why linear models, which are the workhorse models in asset pricing, perform so well. We find that when considering firm-specific characteristics in isolation, the SDF depends approximately linearly on most characteristics. Thus, specific linear risk factors work well on certain single-sorted portfolios. The strength of the flexible functional form of deep neural networks reveals itself when considering the interaction between several characteristics. Although in isolation firm characteristics have a close to linear effect on the SDF, the multi-dimensional functional form is complex. Linear models and also non-linear models that assume an additive structure in the characteristics (for example, additive splines or kernels) rule out interaction effects and cannot capture this structure.

Third, test assets matter. Even a flexible asset pricing model can only capture the asset pricing information that is included in the test assets that it is calibrated on. An asset pricing model

estimated on the optimal test assets constructed by the adversarial network has a 20% higher Sharpe ratio than one calibrated on unconditional individual stock returns. By explaining the most informative test assets we achieve a superior pricing performance on conventional sorted portfolios, e.g. size and book-to-market single- or double-sorted portfolios. In fact, our model has an excellent pricing performance on all 46 anomaly sorted decile portfolios.

Fourth, macroeconomic states matter. Macroeconomic time series data have a low dimensional “factor” structure, which can be captured by four hidden state processes. The SDF structure depends on these economic states that are closely related to business cycles and times of economic crises. In order to find these states we need to take into account the whole time series dynamics of all macroeconomic variables. The conventional approach to deal with non-stationary macroeconomic time series is to use differenced data that capture changes in the time series. However, using only the past change as an input loses all dynamic information and renders the macroeconomic time series essentially useless. Even worse, including conventionally standardized macroeconomic variables as predictors leads to worse performance than leaving them out overall, because they have lost most of their informational content and make it harder to separate the signal from the noise.

Fifth, our conceptional framework is complementary to multi-factor models. Multi-factor models are based on the assumption that the SDF is spanned by the those factors. We provide a unified framework to construct the SDF in a conditional multi-factor model, which in general does not coincide with the unconditional mean-variance efficient combination of the factors. We combine the general conditional multi-factor model of Kelly, Pruitt, and Su (2019) with our model. We show that using the additional economic structure of spanning the SDF with IPCA factors and combining it with our SDF framework can lead to an even better asset pricing model.

Sixth, our findings are robust to the time period under consideration, small capitalization stocks, the choice of the tuning parameters, and limits to arbitrage. The SDF structure is surprisingly stable over time. We estimate the functional form of the SDF with the data from 1967 to 1986, which has an excellent out-of-sample performance for the test data from 1992 to 2016. The risk exposure to the SDF for individual stocks varies over time because the firm-specific characteristics and macroeconomic variables are time-varying, but the functional form of the SDF and the risk exposure with respect to these covariates does not change. When, allowing for a time-varying functional form by estimating the SDF on a rolling window, we find that it is highly correlated with the benchmark SDF and only leads to minor improvements. The estimation is robust to the choice of the tuning parameters. The best performing models on the validation data all capture essentially the same asset pricing model. Our asset pricing model also performs well after excluding small and illiquid stocks from the test assets or the SDF.

Related Literature

Our paper contributes to an emerging literature that uses machine learning methods for asset pricing. In their pioneering work Gu, Kelly, and Xiu (2020) conduct a comparison of machine learning methods for predicting the panel of individual US stock returns and demonstrate the

benefits of flexible methods. Their estimates of the expected risk premia of stocks map into a cross-sectional asset pricing model. We use their best prediction model based on deep neural networks as a benchmark model in our analysis. We show that including the no-arbitrage constraint leads to better results for asset pricing and explained variation than a simple prediction approach. Furthermore, we clarify that it is essential to identify the dynamic pattern in macroeconomic time series before feeding them into a machine learning model and we are the first to do this in an asset pricing context. Messmer (2017) and Feng, He, and Polson (2018) follow a similar approach as Gu, Kelly, and Xiu (2020) to predict stock returns with neural networks. Bianchi, Büchner, and Tamoni (2019) provide a comparison of machine learning method for predicting bond returns in the spirit of Gu, Kelly, and Xiu (2020).² Freyberger, Neuhierl, and Weber (2020) use Lasso selection methods to estimate the risk premia of stock returns as a non-linear additive function of characteristics. Feng, Polson, and Xu (2019) impose a no-arbitrage constraint by using a set of pre-specified linear asset pricing factors and estimate the risk loadings with a deep neural network. Rossi (2018) uses Boosted Regression Trees to form conditional mean-variance efficient portfolios based on the market portfolio and the risk-free asset. Our approach also yields the conditional mean-variance efficient portfolio, but based on all stocks. Gu, Kelly, and Xiu (2019) extend the linear conditional factor model of Kelly, Pruitt, and Su (2019) to a non-linear factor model using an autoencoder neural network.³ We confirm their crucial insight that imposing economic structure on a machine learning algorithm can substantially improve the estimation. Bryzgalova, Pelger, and Zhu (2020) use decision trees to build a cross-section of asset returns, that is, a small set of basis assets that capture the complex information contained in a given set of stock characteristics. Their asset pricing trees generalize the concept of conventional sorting and are pruned by a novel dimension reduction approach based on no-arbitrage arguments. Avramov, Cheng, and Metzker (2020) raise the concern that the performance of machine learning portfolios could deteriorate in the presence of trading frictions.⁴ We discuss how their important insight can be taken into account

²Other related work includes Sirignano, Sadhwani, and Giesecke (2020) who estimate mortgage prepayments, delinquencies, and foreclosures with deep neural networks, Moritz and Zimmerman (2016) who apply tree-based models to portfolio sorting and Heaton, Polson, and Witte (2017) who automate portfolio selection with a deep neural network. Horel and Giesecke (2020) propose a significance test in neural networks and apply it to house price valuation.

³The intuition behind their and our approach can be best understood when considering the linear special cases. Our approach can be viewed as a non-linear generalization of Kozak, Nagel, and Santosh (2020) with the additional elements of finding the macroeconomic states and identifying the most robust conditioning instruments. Fundamentally, our object of interest is the pricing kernel. Kelly, Pruitt, and Su (2019) obtain a multi-factor factor model that maximizes the explained variation. The linear special case applies PCA to a set of characteristic based factors to obtain a linear lower dimensional factor model, while their more general autoencoder obtains the loadings to characteristic based factors that can depend non-linearly on the characteristics. We show in Section III.J how our SDF framework and their conditional multi-factor framework can be combined to obtain an even better asset pricing model.

⁴We have shared our data and estimated models with Avramov, Cheng, and Metzker (2020). In their comparison study Avramov, Cheng, and Metzker (2020) also include a portfolio derived from our GAN model. However, they do not consider our SDF portfolio based on ω but use the SDF loadings β to construct a long-short portfolio based on prediction quantiles. Similarly, they use extreme quantiles for a forecasting approach with neural networks to construct long-short portfolios, which is again different from our SDF framework. Thus, they study different portfolios and their numerical results do not directly apply to the machine learning portfolios considered in this paper.

when constructing machine learning investment portfolios. A promising direction is presented in Bryzgalova, Pelger, and Zhu (2020) who propose a novel framework to estimate an optimal machine learning portfolio subject to trading friction constraints.

The workhorse models in equity asset pricing are based on linear factor models exemplified by Fama and French (1993, 2015). Recently, new methods have been developed to study the cross-section of returns in the linear framework but accounting for the large amount of conditioning information. Lettau and Pelger (2020) extend principal component analysis (PCA) to account for no-arbitrage. They show that a no-arbitrage penalty term makes it possible to overcome the low signal-to-noise ratio problem in financial data and find the information that is relevant for the pricing kernel. Our paper is based on a similar intuition and we show that this result extends to a non-linear framework. Kozak, Nagel, and Santosh (2020) estimate the SDF based on characteristic sorted factors with a modified elastic net regression.⁵ Kelly, Pruitt, and Su (2019) apply PCA to stock returns projected on characteristics to obtain a conditional multi-factor model where the loadings are linear in the characteristics. Pelger (2020) combines high-frequency data with PCA to capture non-parametrically the time-variation in factor risk. Pelger and Xiong (2019b) show that macroeconomic states are relevant to capture time-variation in PCA-based factors.

Our approach uses the same fundamental insight as Bansal and Viswanathan (1993) who propose using the conditional GMM equations to estimate the SDF, but restrict themselves to a small number of conditioning variables. In order to deal with the infinite number of moment conditions we extend the classical GMM setup of Hansen (1982) and Chamberlain (1987) by an adversarial network to select the optimal moment conditions. A similar idea has been proposed by Lewis and Syrgkanis (2018) for non-parametric instrumental variable regressions. Our problem is also similar in spirit to the Wasserstein GAN in Arjosvky, Chintala, and Leon (2017) that provides a robust fit to moments. The Generative Adversarial Network (GAN) approach was first proposed by Goodfellow et al. (2014) for image recognition. In order to find the hidden states in macroeconomic time series we propose the use of Recurrent Neural Networks with Long-Short-Term-Memory (LSTM). LSTMs are designed to find patterns in time series data and have been first proposed by Hochreiter and Schmidhuber (1997). They are among the most successful commercial AIs and are heavily used for sequences of data such as speech (e.g. Google with speech recognition for Android, Apple with Siri and the “QuickType” function on the iPhone or Amazon with Alexa).

The rest of the paper is organized as follows. Section I introduces the model framework and Section II elaborates on the estimation approach. The empirical results are collected in Section III. Section IV concludes. The Internet Appendix collects additional empirical and simulation results.

⁵We show that the special case of a linear formulation of our model is essentially a version of their model and we include it as the linear benchmark case in our analysis.

I. Model

A. No-Arbitrage Asset Pricing

Our goal is to explain the differences in the cross-section of returns R for individual stocks. Let $R_{t+1,i}$ denote the return of asset i at time $t + 1$. The fundamental no-arbitrage assumption is equivalent to the existence of a stochastic discount factor (SDF) M_{t+1} such that for any return in excess of the risk-free rate $R_{t+1,i}^e = R_{t+1,i} - R_{t+1}^f$, it holds

$$\mathbb{E}_t [M_{t+1} R_{t+1,i}^e] = 0 \quad \Leftrightarrow \quad \mathbb{E}_t [R_{t+1,i}^e] = \underbrace{\left(-\frac{\text{Cov}_t(R_{t+1,i}^e, M_{t+1})}{\text{Var}_t(M_{t+1})} \right)}_{\beta_{t,i}} \cdot \underbrace{\frac{\text{Var}_t(M_{t+1})}{\mathbb{E}_t[M_{t+1}]}}_{\lambda_t},$$

where $\beta_{t,i}$ is the exposure to systematic risk and λ_t is the price of risk. $E_t[\cdot]$ denotes the expectation conditional on the information at time t . The stochastic discount factor is an affine transformation of the tangency portfolio.⁶ Without loss of generality we consider the SDF formulation

$$M_{t+1} = 1 - \sum_{i=1}^N \omega_{t,i} R_{t+1,i}^e = 1 - \omega_t^\top R_{t+1}^e.$$

The fundamental pricing equation $\mathbb{E}_t [R_{t+1}^e M_{t+1}] = 0$ implies the SDF weights

$$\omega_t = \mathbb{E}_t [R_{t+1}^e R_{t+1}^{e\top}]^{-1} \mathbb{E}_t [R_{t+1}^e], \quad (1)$$

which are the portfolio weights of the conditional mean-variance efficient portfolio.⁷ We define the tangency portfolio as $F_{t+1} = \omega_t^\top R_{t+1}^e$ and will refer to this traded factor as the SDF. The asset pricing equation can now be formulated as

$$\mathbb{E}_t [R_{t+1,i}^e] = \frac{\text{Cov}_t(R_{t+1,i}^e, F_{t+1})}{\text{Var}_t(F_{t+1})} \cdot \mathbb{E}_t [F_{t+1}] = \beta_{t,i} \mathbb{E}_t [F_{t+1}].$$

Hence, no-arbitrage implies a one-factor model

$$R_{t+1,i}^e = \beta_{t,i} F_{t+1} + \epsilon_{t+1,i}$$

with $\mathbb{E}_t [\epsilon_{t+1,i}] = 0$ and $\text{Cov}_t(F_{t+1}, \epsilon_{t+1,i}) = 0$. Conversely, the factor model formulation implies the stochastic discount factor formulation above. Furthermore, if the idiosyncratic risk $\epsilon_{t+1,i}$ is diversifiable and the factor F is systematic,⁸ then knowledge of the risk loadings is sufficient to

⁶ See Back (2010) for more details. As we work with excess returns we have an additional degree of freedom. Following Cochrane (2003) we use the above normalized relationship between the SDF and the mean-variance efficient portfolio. We consider the SDF based on the projection on the asset space.

⁷ Any portfolio on the globally efficient frontier achieves the maximum Sharpe ratio. These portfolio weights represent one possible efficient portfolio.

⁸ Denote the conditional residual covariance matrix by $\Sigma_t^\epsilon = \text{Var}_t(\epsilon_t)$. Then, sufficient conditions are $\|\Sigma_t^\epsilon\|_2 < \infty$ and $\frac{\beta^\top \beta}{N} > 0$ for $N \rightarrow \infty$ i.e. Σ_t^ϵ has bounded eigenvalues and β_t has sufficiently many non-zero elements.

construct the SDF:

$$\left(\beta_t^\top \beta_t\right)^{-1} \beta_t^\top R_{t+1}^e = F_{t+1} + \left(\beta_t^\top \beta_t\right)^{-1} \beta_t^\top \epsilon_{t+1} = F_{t+1} + o_p(1).$$

The fundamental problem is to find the SDF portfolio weights ω_t and risk loadings β_t . Both are time-varying and general functions of the information set at time t . The knowledge of ω_t and β_t solves three problems: (1) We can explain the cross-section of individual stock returns. (2) We can construct the conditional mean-variance efficient tangency portfolio. (3) We can decompose stock returns into their predictable systematic component and their non-systematic unpredictable component.

B. Generative Adversarial Methods of Moments

Finding the SDF weights is equivalent to solving a method of moment problem. The conditional no-arbitrage moment condition implies infinitely many unconditional moment conditions

$$\mathbb{E}[M_{t+1} R_{t+1,i}^e g(I_t, I_{t,i})] = 0$$

for any function $g(\cdot) : \mathbb{R}^p \times \mathbb{R}^q \rightarrow \mathbb{R}^d$, where $I_t \times I_{t,i} \in \mathbb{R}^{p+q}$ denotes all the variables in the information set at time t and d is the number of moment conditions. We denote by I_t all p macroeconomic conditioning variables that are not asset specific, e.g. inflation rates or the market return, while $I_{t,i}$ are q firm-specific characteristics, e.g. the size or book-to-market ratio of firm i at time t . The unconditional moment condition can be interpreted as the pricing error for a choice of portfolios and times determined by $g(\cdot)$. The challenge lies in finding the relevant moment conditions to identify the SDF.

A well-known formulation includes 25 moments that corresponds to pricing the 25 size and value double-sorted portfolios of Fama and French (1992). For this special case each g corresponds to an indicator function if the size and book-to-market values of a company are in a specific quantile. Another special case is to consider only unconditional moments, i.e. setting g to a constant. This corresponds to minimizing the unconditional pricing error of each stock.

The SDF portfolio weights $\omega_{t,i} = \omega(I_t, I_{t,i})$ and risk loadings $\beta_{t,i} = \beta(I_t, I_{t,i})$ are general functions of the information set, that is, $\omega : \mathbb{R}^p \times \mathbb{R}^q \rightarrow R$ and $\beta : \mathbb{R}^p \times \mathbb{R}^q \rightarrow R$. For example, the SDF weights and loadings in the Fama-French 3 factor model are a special case, where both functions are approximated by a two-dimensional kernel function that depends on the size and book-to-market ratio of firms. The Fama-French 3 factor model only uses firm-specific information but no macroeconomic information, e.g. the loadings cannot vary based on the state of the business cycle.

We use an adversarial approach to select the moment conditions that lead to the largest mispricing:

$$\min_{\omega} \max_g \frac{1}{N} \sum_{j=1}^N \left\| \mathbb{E} \left[\left(1 - \sum_{i=1}^N \omega(I_t, I_{t,i}) R_{t+1,i}^e \right) R_{t+1,j}^e g(I_t, I_{t,j}) \right] \right\|^2, \quad (2)$$

where the function ω and g are normalized functions chosen from a specified functional class. This is a minimax loss minimization problem. These types of problems can be modeled as a zero-sum game, where one player, the asset pricing modeler, wants to choose an asset pricing model, while the adversary wants to choose conditions under which the asset pricing model performs badly. This can be interpreted as first finding portfolios or times that are the most mispriced and then correcting the asset pricing model to also price these assets. The process is repeated until all pricing information is taken into account, that is the adversary cannot find portfolios with large pricing errors. Note that this is a data-driven generalization for the research protocol conducted in asset pricing in the last decades. Assume that the asset pricing modeler uses the Fama-French 5 factor model, that is M is spanned by those five factors. The adversary might propose momentum sorted test assets, that is g is a vector of indicator functions for different quantiles of past returns. As these test assets have significant pricing errors with respect to the Fama-French 5 factors, the asset pricing modeler needs to revise her candidate SDF, for example, by adding a momentum factor to M . Next, the adversary searches for other mispriced anomalies or states of the economy, which the asset pricing modeler will exploit in her SDF model.

Choosing the conditioning function g correspond to finding optimal instruments in a GMM estimation. The conventional GMM approach assumes a finite number of moments that identify a finite dimensional parameter. The moments are selected to achieve the most efficient estimator within this class. Nagel and Singleton (2011) use this argument to build optimal managed portfolios for a particular asset pricing model. Their approach assumes that the set of candidate test assets identify all the parameters of the SDF and they can therefore focus on which test asset provide the most efficient estimator. Our problem is different in two ways that rule out using the same approach. First, we have an infinite number of candidate moments without the knowledge of which moments identify the parameters. Second, our parameter set is also of infinite dimension, and we consequently do not have an asymptotic normal distribution with a feasible estimator of the covariance matrix. In contrast, our approach selects the moments based on robustness.⁹ By controlling the worst possible pricing error we aim to choose the test assets that can identify all parameters of the SDF.

Our conditioning function g generates a very large number of test assets to identify a complex SDF structure. The cross-sectional average is taken over the moment deviations, that is, pricing errors for $R_{t+1,j}^e g(I_t, I_{t,j})$, instead of considering the moment deviation for the d time-series $\frac{1}{N} \sum_{i=1}^N R_{t+1,i}^e g(I_t, I_{t,i})$ which would correspond to the traditionally sorted test assets. In the second case we would only have d test assets which limits the number of parameters and hence the complexity of the SDF that is identified. In contrast, our approach yields $d \cdot N$ test assets, which

⁹See Blanchet, Kang, and Murthy (2019) for a discussion on robust estimation with an adversarial approach.

allows us to fit a complex structure for the SDF, that is, we can consider non-linear models with many variables.¹⁰

Note that our moment conditions allow the SDF weights to be general functions of the information set, while equation 1 gives an explicit solution in terms of the conditional second and first moment of stock returns. Without strong parametric assumptions it is practically not possible to estimate reliably the inverse of a large dimensional conditional covariance matrix for stocks. Even in the unconditional setup the estimation of the inverse of a large dimensional covariance matrix is already challenging. In order to avoid this problem, we do not explicitly impose these restrictions on the SDF weights. Instead we use the insight that if our SDF explains the unconditional moments in equation 2 for any choice of g , then it must also satisfy equation 1. The generative adversarial formulation allows us to side-step solving explicitly an infeasible mean-variance optimization. In other words, if we allow the SDF weights to be general functions of the information set, but require this SDF to explain prices of any possible portfolio, then this SDF factor has to correspond to the conditional mean-variance efficient portfolio.

Once we have obtained the SDF factor weights, the loadings are proportional to the conditional moments $\mathbb{E}_t[F_{t+1}R_{t+1,i}^e]$. A key element of our approach is to avoid estimating directly conditional means of stock returns. Our empirical results show that we can better estimate the conditional co-movement of stock returns with the SDF factors, which is a second moment, than the conditional first moment. Note, that in the no-arbitrage one-factor model, the loadings are proportional to $\text{Cov}_t(R_{t+1,i}^e, F_{t+1})$ and $\mathbb{E}_t[F_{t+1}R_{t+1,i}^e]$, where the last one has the advantage that we avoid estimating the first conditional moment.

C. Alternative Models

We consider two special cases as alternatives: One model can take a flexible functional form but does not use the no-arbitrage constraint in the estimation. The other model is based on the no-arbitrage framework, but considers a linear functional form.

Instead of minimizing the violation of the no-arbitrage condition, one can directly estimate the conditional mean. Note that the conditional expected returns $\mu_{t,i}$ are proportional to the loadings in the one-factor formulation:

$$\mu_{t,i} := \mathbb{E}_t[R_{t+1,i}^e] = \beta_{t,i}\mathbb{E}_t[F_{t+1}].$$

Hence, up to a time-varying proportionality constant the SDF factor weights and loadings are equal to $\mu_{t,i}$. This reduces the cross-sectional asset pricing problem to a simple forecasting problem. Hence, we can use the forecasting approach pursued in Gu, Kelly, and Xiu (2020) for asset pricing.

¹⁰Obviously, instrumenting each stock with g only leads to more test assets if the resulting portfolios are not redundant. Empirically, we observe that there is a large variation in the vectors of characteristics cross-sectionally and over time. For example, if g is an indicator function for small cap stocks, the returns of $R_{t+1,j}^e g(I_t, I_{t,j})$ provide different information for different stocks j as the other characteristics are in most cases not identical and stocks have a small market capitalization at different times t .

The second benchmark model assumes a linear structure in the factor portfolio weights $\omega_{t,i} = \theta^\top I_{t,i}$ and linear conditioning in the test assets:

$$\frac{1}{N} \sum_{j=1}^N \mathbb{E} \left[\left(1 - \frac{1}{N} \sum_{i=1}^N \theta^\top I_{t,i} R_{t+1,i}^e \right) R_{t+1,j}^e I_{t,j} \right] = 0 \quad \Leftrightarrow \quad \mathbb{E} \left[\left(1 - \theta^\top \tilde{F}_{t+1} \right) \tilde{F}_{t+1}^\top \right] = 0,$$

where $\tilde{F}_{t+1} = \frac{1}{N} \sum_{i=1}^N I_{t,i} R_{t+1,i}^e$ are q characteristic managed factors. Such characteristic managed factors based on linearly projecting onto quantiles of characteristics are exactly the input to PCA in Kelly, Pruitt, and Su (2019) or the elastic net mean-variance optimization in Kozak, Nagel, and Santosh (2020).¹¹ The solution to minimizing the sum of squared errors in these moment conditions is a simple mean-variance optimization for the q characteristic managed factors that is, $\theta = \left(\mathbb{E} \left[\tilde{F}_{t+1} \tilde{F}_{t+1}^\top \right] \right)^{-1} \mathbb{E} \left[\tilde{F}_{t+1} \right]$ are the weights of the tangency portfolio based on these factors.¹² We choose this specific linear version of the model as it maps directly into the linear approaches that have already been successfully used in the literature. This linear framework essentially captures the class of linear factor models.

II. Estimation

A. Loss Function and Model Architecture

The empirical loss function of our model minimizes the weighted sample moments which can be interpreted as weighted sample mean pricing errors:

$$L(\omega | \hat{g}, I_t, I_{t,i}) = \frac{1}{N} \sum_{i=1}^N \frac{T_i}{T} \left\| \frac{1}{T_i} \sum_{t \in T_i} M_{t+1} R_{t+1,i}^e \hat{g}(I_t, I_{t,i}) \right\|^2. \quad (3)$$

for a given conditioning function $\hat{g}(\cdot)$ and information set. We deal with an unbalanced panel in which the number of time series observations T_i varies for each asset. As the convergence rates of the moments under suitable conditions is $1/\sqrt{T_i}$, we weight each cross-sectional moment condition by $\sqrt{T_i}/\sqrt{T}$, which assigns a higher weight to moments that are estimated more precisely and down-weights the moments of assets that are observed only for a short time period.

For a given conditioning function $\hat{g}(\cdot)$ and choice of information set the SDF factor portfolio weights are estimated by a feedforward network that minimizes the pricing error loss

$$\hat{\omega} = \min_{\omega} L(\omega | \hat{g}, I_t, I_{t,i}).$$

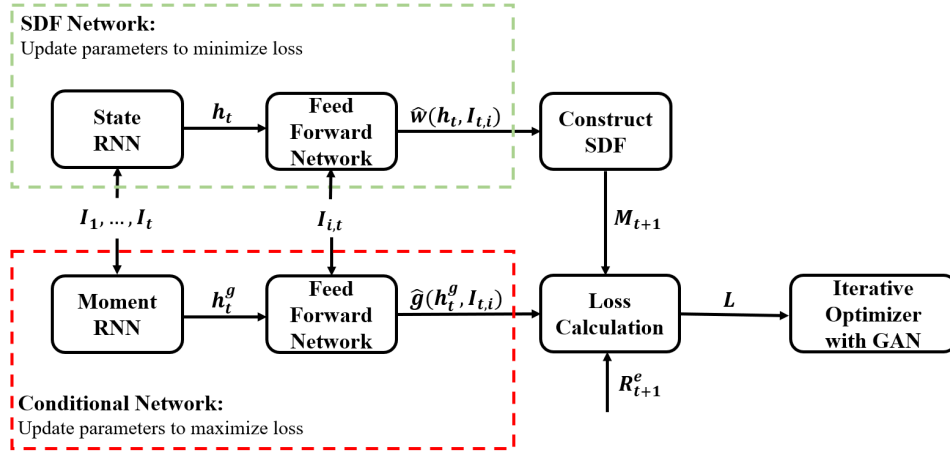
We refer to this network as the SDF network.

¹¹Kozak, Nagel, and Santosh (2020) consider also cross-products of the characteristics. They show that the PCA rotation of the factors improves the pricing performance. Lettau and Pelger (2020) extend this important insight to RP-PCA rotated factors. We consider PCA based factors in III.J. Our main analysis focuses on conventional long-short factors as these are the most commonly used models in the literature.

¹²As before we define as tangency portfolio one of the portfolios on the global mean-variance efficient frontier.

We construct the conditioning function \hat{g} via a conditional network with a similar neural network architecture. The conditional network serves as an adversary and competes with the SDF network to identify the assets and portfolio strategies that are the hardest to explain. The macroeconomic information dynamics are summarized by macroeconomic state variables h_t which are obtained by a Recurrent Neural Network (RNN) with Long-Short-Term-Memory units. The model architecture is summarized in Figure 1 and each of the different components are described in detail in the next subsections.¹³

Figure 1: GAN Model Architecture



This figure shows the model architecture of GAN (Generative Adversarial Network) with RNN (Recurrent Neural Network) with LSTM cells. The SDF network has two parts: (1) A LSTM estimates a small number of macroeconomic states. (2) These states together with the firm-characteristics are used in a FFN to construct a candidate SDF for a given set of test assets. The conditioning network also has two networks: (1) It creates its own set of macroeconomic states, (2) which it combines with the firm-characteristics in a FFN to find mispriced test assets for a given SDF M . These two networks compete until convergence, that is neither the SDF nor the test assets can be improved.

In contrast, forecasting returns similar to Gu, Kelly, and Xiu (2020) uses only a feedforward network and is labeled as FFN. It estimates conditional means $\mu_{t,i} = \mu(I_t, I_{t,i})$ by minimizing the average sum of squared prediction errors:

$$\hat{\mu} = \min_{\mu} \frac{1}{T} \sum_{t=1}^T \frac{1}{N_t} \sum_{i=1}^{N_t} (R_{t+1,i}^e - \mu(I_t, I_{t,i}))^2.$$

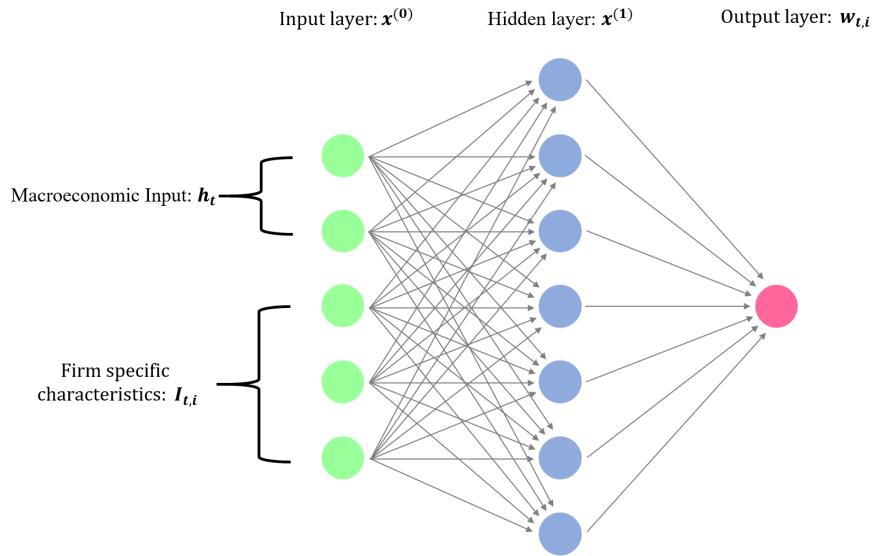
We only include the best performing feedforward network from Gu, Kelly, and Xiu (2020)'s comparison study. Within their framework this model outperforms tree learning approaches and other linear and non-linear prediction models. In order to make the results more comparable with Gu, Kelly, and Xiu (2020) we follow the same procedure as outlined in their paper. Thus, the simple forecasting approach does not include an adversarial network or LSTM to condense the macroeconomic dynamics.

¹³See Goodfellow, Bengio, and Courville (2016) for a textbook treatment.

B. Feedforward Network (FFN)

A feedforward network (FFN)¹⁴ is a universal approximator that can learn any functional relationship $y = f(x)$ between an input x and output variable y with sufficient data. We will consider four different FFN: For the covariates $x = [I_t, I_{t,i}]$ we estimate (1) the optimal weights in our GAN network ($y = \omega$), (2) the optimal instruments for the moment conditions in our GAN network ($y = g$), (3) the conditional mean return ($y = R_{t+1,i}^e$) and (4) the second moment ($y = R_{t+1,i}^e F_{t+1}$) to obtain the SDF loadings $\beta_{t,i}$.

Figure 2: Illustration of Feedforward Network with Single Hidden Layer



We start with a one-layer neural network. It combines the raw predictor variables (or features) $x = x^{(0)} \in \mathbb{R}^{K^{(0)}}$ linearly and applies a non-linear transformation. This non-linear transformation is based on an element-wise operating activation function. We choose the popular function known as the rectified linear unit (ReLU)¹⁵, which component-wise thresholds the inputs and is defined as

$$\text{ReLU}(x_k) = \max(x_k, 0).$$

The result is the hidden layer $x^{(1)} = (x_1^{(1)}, \dots, x_{K^{(1)}}^{(1)})$ of dimension $K^{(1)}$ which depends on the parameters $W^{(0)} = (w_1^{(0)}, \dots, w_{K^{(0)}}^{(0)})$ and the bias term $w_0^{(0)}$. The output layer is simply a linear

¹⁴FFN are among the simplest neural networks and treated in detail in standard machine learning textbooks, e.g. Goodfellow, Bengio, and Courville (2016).

¹⁵Other activation functions include sigmoid, hyperbolic tangent function and leaky ReLU. ReLU activation functions have a number of advantages including the non-saturation of its gradient, which greatly accelerates the convergence of stochastic gradient descent compared to the sigmoid/hyperbolic functions (Krizhevsky et al. (2012) and fast calculations of expensive operations.

transformation of the output from the hidden layer.

$$x^{(1)} = \text{ReLU}(W^{(0)\top} x^{(0)} + w_0^{(0)}) = \text{ReLU} \left(w_0^{(0)} + \sum_{k=1}^{K^{(0)}} w_k^{(0)} x_k^{(0)} \right)$$

$$y = W^{(1)\top} x^{(1)} + w_0^{(1)} \quad \text{with } x^{(1)} \in \mathbb{R}^{K^{(1)}}, W^{(0)} \in \mathbb{R}^{K^{(1)} \times K^{(0)}}, W^{(1)} \in \mathbb{R}^{K^{(1)}}.$$

Note that without the non-linearity in the hidden layer, the one-layer network would reduce to a generalized linear model. A deep neural network combines several layers by using the output of one hidden layer as an input to the next hidden layer. The details are explained in Appendix A.A. The multiple layers allow the network to capture non-linearities and interaction effects in a more parsimonious way.

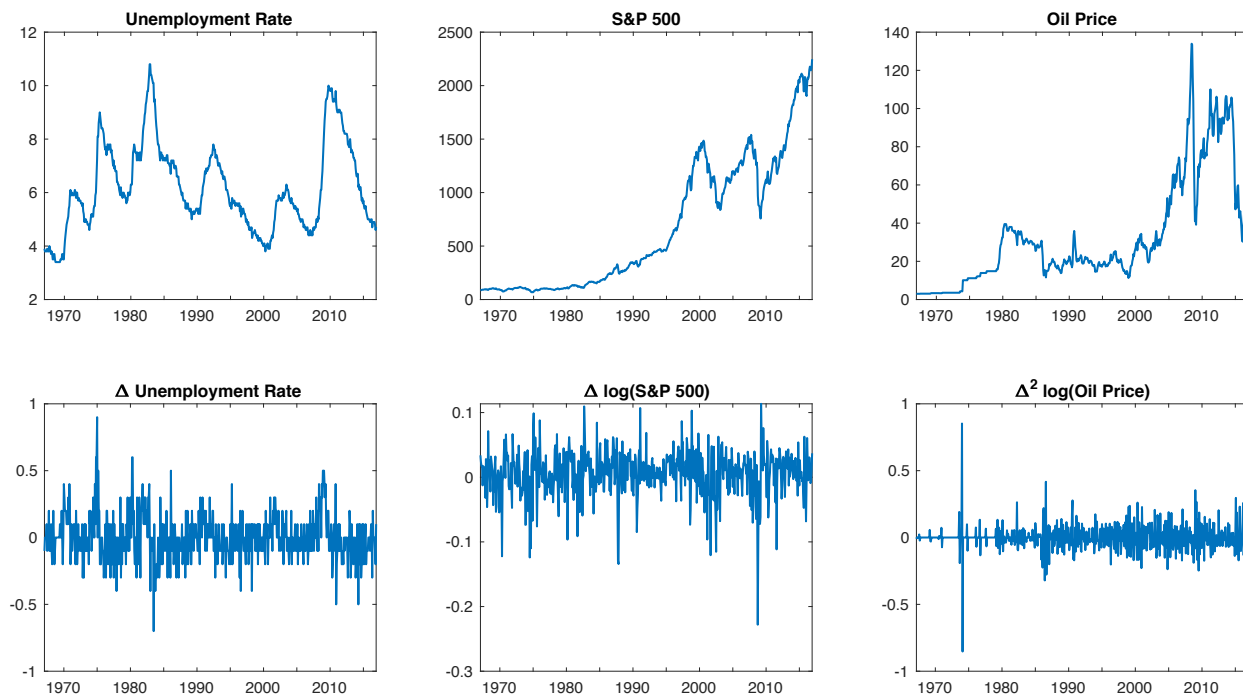
C. Recurrent Neural Network (RNN) with LSTM

A Recurrent Neural Network (RNN) with Long-Short-Term-Memory (LSTM) estimates the hidden macroeconomic state variables. Instead of directly passing macroeconomic variables I_t as features to the feedforward network, we apply a non-linear transformation to them with a specific RNN and only pass on a small number of hidden states. There are three reasons why this step is necessary.

First, many macroeconomic variables themselves are not stationary. Hence, we need to perform transformations as suggested in McCracken and Ng (2016), which typically take the form of some difference of the time-series. There is no reason to assume that the pricing kernel has a Markovian structure with respect to the macroeconomic information, in particular after transforming them into stationary increments. For example, business cycles can affect pricing but the GDP growth of the last period is insufficient to learn if the model is in a boom or a recession. Hence, lagged values of the macroeconomic state variables need to be included and we need to find a way to extract the relevant information from a potentially large number of lagged values. Second, a conventional RNN can take into account some time series behavior but can encounter problems with exploding and vanishing gradients when considering longer time lags. This is why we use Long-Short-Term-Memory cells. The LSTM is designed to find hidden state processes allowing for lags of unknown and potentially long duration in the time series, which makes it well-suited to detect business cycles. Third, the macroeconomic time series variables seem to be strongly dependent, that is, there is redundant information. Although the regularization in a neural network can in principle deal with redundant variables, the finite sample of stock returns is of a modest size compared to other machine learning applications. Hence, the large number of predictor variables proves to negatively impact the feedforward network performance. The RNN with LSTM summarizes the macroeconomic time series dynamics in a small number of hidden state processes that provide a more robust fit when used as an input to the feedforward network.

As an illustration, we show in Figure 3 three examples of the complex dynamics and non-stationarities in the macroeconomic time series that we include in our empirical analysis. We plot

Figure 3: Examples of Macroeconomic Variables



This figure shows examples of macroeconomic time series with standard transformations proposed by McCracken and Ng (2016).

the time series of the U.S. unemployment rate, the S&P 500 price and the oil price together with the standard transformations proposed by McCracken and Ng (2016) to remove the obvious non-stationarities. Using only the last observation of the differenced data obviously results in a loss of information and cannot identify the cyclical dynamic patterns. Hence, it is essential to include all past differences in an estimator that can infer the hidden states.

RNNs are a family of neural networks for processing sequences of data. They transform a sequence of input variables to another output sequence, with the same set of parameters at each step. A vanilla RNN model takes the current input variable x_t and the previous hidden state h_{t-1} and performs a non-linear transformation to get the current state h_t .

$$h_t = \sigma(W_h h_{t-1} + W_x x_t + w_0),$$

where σ is the activation function. Intuitively, we can think of a vanilla RNN as non-linear generalization of an autoregressive process where the lagged variables are transformations of the lagged observed variables. This type of structure is powerful if only the immediate past is relevant, but it is not suitable if the time series dynamics are driven by events that are further back in the past. Hence, we use the more complex LSTM model to capture long-term dependencies.

We can think of an LSTM as a flexible hidden state space model for a large dimensional system. The dynamics of the macroeconomic time series are driven by a small number of hidden states that aggregate cross-sectional and time series patterns. A popular approach to aggregate a cross-section

of macroeconomic time series is PCA.¹⁶ This aggregates the time series to a small number of latent factors that explain the correlation in the innovations in the time series, but PCA cannot identify the current state of the economic system. On the other hand, state space models, with the simple linear Gaussian state space model estimated by a Kalman filter as one of the most popular ones, are usually set up for a small number of time series under restrictive distributional assumptions. Our LSTM approach can deal with both the large dimensionality of the system and a very general functional form of the states while allowing for long-term dependencies. Appendix A.B provides a detailed explanation of the estimation method.

The output of the LSTM is a small number of state processes h_t which we use instead of the macroeconomic variables I_t as an input to our SDF network. Note, that for any \mathcal{F}_t -measurable sequence I_t , the output sequence h_t is again \mathcal{F}_t -measurable, so that the transformation creates no look-ahead bias. Furthermore, h_t contains all the macroeconomic information in the past, while I_t only uses current information.

D. Generative Adversarial Network (GAN)

The conditioning function g is the output of a second feedforward network. Enlightened by Generative Adversarial Networks (GAN), we chose the moment conditions that lead to the largest pricing discrepancy by having two networks compete against each other. One network creates the SDF M_{t+1} , and the other network creates the conditioning function.

We take three steps to train the model. Our initial first step SDF minimizes the unconditional loss. Second, given this SDF we maximize the loss by optimizing the parameters in the conditional network. Finally, given the conditional network and we update the SDF network to minimize the conditional loss.¹⁷ The logic behind this idea is that by minimizing the largest conditional loss among all possible conditioning functions, the loss for any function is small. Note that both, the SDF network and the conditional network each use a FFN network combined with an LSTM that estimates the macroeconomic hidden state variables, i.e. instead of directly using I_t as an input each network summarizes the whole macroeconomic time series information in the state process h_t (respectively h_t^g for the conditional network). The two LSTMs are based on the criteria function of the two networks, that is h_t are the hidden states that can minimize the pricing errors, while h_t^g generate the test assets with the largest mispricing:¹⁸

$$\{\hat{\omega}, \hat{h}_t, \hat{g}, \hat{h}_t^g\} = \min_{\omega, h_t} \max_{g, h_t^g} L(\omega | \hat{g}, h_t^g, h_t, I_{t,i}).$$

¹⁶See e.g. Ludvigson and Ng (2007).

¹⁷A conventional GAN network iterates this procedure until convergence. We find that our algorithm converges already after the above three steps, i.e. the model does not improve further by repeating the adversarial game. Detailed results on the GAN iterations are collected in the Internet Appendix.

¹⁸We allow for potentially different macroeconomic states for the SDF and the conditional network as the unconditional moment conditions that identify the SDF can depend on different states than the SDF weights.

E. Hyperparameters and Ensemble Learning

Due to the high dimensionality and non-linearity of the problem, training a deep neural network is a complex task. Here, we summarize the implementation and provide additional details in Appendix A.C. We prevent the model from overfitting and deal with the large number of parameters by using “Dropout”, which is a form of regularization that has generally better performance than conventional l_1/l_2 regularization. We optimize the objective function accurately and efficiently by employing an adaptive learning rate for a gradient-based optimization.

We obtain robust and stable fits by ensemble averaging over several fits of the models. A distinguishing feature of neural networks is that the estimation results can depend on the starting value used in the optimization. The standard practice which has also been used by Gu, Kelly, and Xiu (2020) is to train the models separately with different initial values chosen from an optimal distribution. Averaging over multiple fits achieves two goals: First, it diminishes the effect of a local suboptimal fit. Second, it reduces the estimation variance of the estimated model. All our neural networks including the forecasting approach are averaged over nine model fits.¹⁹ Let $\hat{w}^{(j)}$ and $\hat{\beta}^{(j)}$ be the optimal portfolio weights respectively SDF loadings given by the j^{th} model fit. The ensemble model is a weighted average of the outputs from models with the same architecture but different starting values for the optimization, that is $\hat{\omega} = \frac{1}{9} \sum_{j=1}^9 \hat{\omega}^{(j)}$ and $\hat{\beta} = \frac{1}{9} \sum_{j=1}^9 \hat{\beta}^{(j)}$. Note that for vector valued functions, for example the conditioning function g and macroeconomic states h , it is not meaningful to report their model averages as different entries in the vectors are not necessarily reflecting the same object in each fit.

We split the data into a training, validation and testing sample. The validation set is used to tune the hyperparameters, which includes the depth of the network (number of layers), the number of basis functions in each layer (nodes), the number macroeconomic states, the number of conditioning instruments and the structure of the conditioning network. We choose the best configuration among all possible combinations of hyperparameters by maximizing the Sharpe ratio of the SDF on the validation data.²⁰ The hyperparameters of the model with the highest validation Sharpe ratio are selected for the test data. Our optimal model has two layers, four economic states and eight instruments for the test assets. Our results are robust to the tuning parameters as discussed in Section III.H. In particular, our results do not depend on the structure of the network and the best performing networks on the validation data provide essentially an identical model with the same performance on the test data. The FFN for the forecasting approach uses the optimal hyperparameters selected by Gu, Kelly, and Xiu (2020). This has the additional advantage of making our results directly comparable to their results.

¹⁹An ensemble over nine models produces very robust and stable result and there is no effect of averaging over more models. The results are available upon request.

²⁰We have used different criteria functions, including the error in minimizing the moment conditions, to select the hyperparameters. The results are virtually identical and available upon request.

F. Model Comparison

We evaluate the performance of our model by calculating the Sharpe ratio of the SDF, the amount of explained variation and the pricing errors. We compare our GAN model with its linear special case, which is a linear factor model, and the deep-learning forecasting approach. The one factor representation yields three performance metrics to compare the different model formulations. First, the SDF is by construction on the globally efficient frontier and should have the highest conditional Sharpe ratio. We use the unconditional Sharpe ratio of the SDF portfolio $SR = \frac{\mathbb{E}[F]}{\sqrt{\text{Var}[F]}}$ as a measure to assess the pricing performance of models. The second metric measures the variation explained by the SDF. The explained variation is defined as $1 - \frac{\sum_{i=1}^N \mathbb{E}[\epsilon_i^2]}{\sum_{i=1}^N \mathbb{E}[R_i^e]}$ where ϵ_i is the residual of a cross-sectional regression on the loadings. As in Kelly, Pruitt, and Su (2019) we do not demean returns due to their non-stationarity and noise in the mean estimation. Our explained variation measure can be interpreted as a time series R^2 . The third performance measure is the average pricing error normalized by the average mean return to obtain a cross-sectional R^2 measure $1 - \frac{\frac{1}{N} \sum_{i=1}^N \mathbb{E}[\epsilon_i]^2}{\frac{1}{N} \sum_{i=1}^N \mathbb{E}[R_i]^2}$.

The output for our GAN model are the SDF factor weights $\hat{\omega}_{GAN}$. We obtain the risk exposure $\hat{\beta}_{GAN}$ by fitting a feedforward network to predict $R_{t+1}^e F_{t+1}$ and hence estimate $\mathbb{E}_t[R_{t+1}^e F_{t+1}]$. Note, that this loading estimate $\hat{\beta}_{GAN}$ is only proportional to the population value β but this is sufficient for projecting on the systematic and non-systematic component. The conventional forecasting approach, which we label FFN, yields the conditional mean $\hat{\mu}_{FFN}$, which is proportional to β and hence is used as $\hat{\beta}_{FFN}$ in the projection. At the same time $\hat{\mu}_{FFN}$ is proportional to the SDF factor portfolio weights and hence also serves as $\hat{\omega}_{FFN}$. Hence, the fundamental difference between GAN and FFN is that GAN estimates a conditional second moment $\beta_{GAN} = \mathbb{E}_t[R_{t+1}^e F_{t+1}]$, while FFN estimates a conditional first moment $\beta_{FFN} = \mathbb{E}_t[R_{t+1}^e]$ for cross-sectional pricing.

Note that the linear model, labeled as LS, is a special case with an explicit solution

$$\begin{aligned} \hat{\theta}_{LS} &= \left(\frac{1}{T} \sum_{t=1}^T \left(\frac{1}{N} \sum_{i=1}^N R_{t+1,i}^e I_{t,i} \right) \left(\frac{1}{N} \sum_{i=1}^N R_{t+1,i}^e I_{t,i} \right)^\top \right)^{-1} \left(\frac{1}{NT} \sum_{t=1}^T \sum_{i=1}^N R_{t+1,i}^e I_{t,i} \right) \\ &= \left(\frac{1}{T} \sum_{t=1}^T \tilde{F}_{t+1} \tilde{F}_{t+1}^\top \right)^{-1} \left(\frac{1}{T} \sum_{t=1}^T \tilde{F}_{t+1}^\top \right) \end{aligned}$$

and SDF factor portfolio weights $\omega_{LS} = \hat{\theta}_{LS}^\top I_{t,i}$. The risk exposure $\hat{\beta}_{LS}$ is obtained by a linear regression of $R_{t+1}^e F_{t+1}$ on $I_{t,i}$. As the number of characteristics is very large in our setup, the linear model is likely to suffer from over-fitting. The non-linear models include a form of regularization to deal with the large number of characteristics. In order to make the model comparison valid, we add a regularization to the linear model as well. The regularized linear model EN adds an elastic

net penalty to the regression to obtain $\hat{\theta}_{EN}$ and in the predictive regression for $\hat{\beta}_{EN}$:²¹

$$\hat{\theta}_{EN} = \arg \min_{\theta} \left(\frac{1}{T} \sum_{t=1}^T \tilde{F}_{t+1} - \frac{1}{T} \sum_{t=1}^T \tilde{F}_{t+1} \tilde{F}_{t+1}^{\top} \theta \right)^2 + \lambda_2 \|\theta\|_2^2 + \lambda_1 \|\theta\|_1.$$

The linear approach with elastic net is closely related to Kozak, Nagel, and Santosh (2020) who perform mean-variance optimization with an elastic net penalty on characteristic based factors.²² In addition we also report the maximum Sharpe ratios for the tangency portfolios based on the Fama-French 3 and 5 factor models.²³

For the four models GAN, FFN, EN and LS we obtain estimates of ω for constructing the SDF and estimates of β for calculating the residuals ϵ . We obtain the systematic and non-systematic return components by projecting returns on the estimated risk exposure $\hat{\beta}$:

$$\hat{\epsilon}_{t+1} = \left(I_N - \hat{\beta}_t (\hat{\beta}_t^{\top} \hat{\beta}_t)^{-1} \hat{\beta}_t^{\top} \right) R_{t+1}^e.$$

For each model we report (1) the unconditional Sharpe ratio of the SDF factor, (2) the explained variation in individual stock returns and (3) the cross-sectional mean²⁴ R^2 :

$$SR = \frac{\hat{\mathbb{E}}[F_t]}{\sqrt{\hat{Var}(F_t)}}, \quad EV = 1 - \frac{\left(\frac{1}{T} \sum_{t=1}^T \frac{1}{N_t} \sum_{i=1}^{N_t} (\hat{\epsilon}_{t+1,i})^2 \right)}{\left(\frac{1}{T} \sum_{t=1}^T \frac{1}{N_t} \sum_{i=1}^{N_t} (R_{t+1,i}^e)^2 \right)}, \quad XS-R^2 = 1 - \frac{\frac{1}{N} \sum_{i=1}^N \frac{T_i}{T} \left(\frac{1}{T_i} \sum_{t \in T_i} \hat{\epsilon}_{t+1,i} \right)^2}{\frac{1}{N} \sum_{i=1}^N \frac{T_i}{T} \left(\frac{1}{T_i} \sum_{t \in T_i} \hat{R}_{t+1,i} \right)^2}.$$

These are generalization of the standard metrics used in linear asset pricing.

We also evaluate our models on conventional characteristic sorted portfolios. The portfolio loadings are the average of the stock loadings weighted by the portfolio weights. In more detail, our models provide risk loadings β_t 's for each individual stock. The risk loadings β_t 's for the portfolios are obtained by aggregating the corresponding stock specific loadings. We obtain the systematic and error components with a cross-sectional regression on β_t at each point in time. This is similar to a standard cross-sectional Fama-MacBeth regression in a linear model with the main difference that the β_t 's are obtained from our SDF models on individual stocks. We normalize the

²¹The elastic net includes lasso and ridge regularization as a special case. We select the tuning parameters of the elastic net optimally on the validation data.

²²There are five differences to their paper. First, they use a modified ridge penalty based on a Bayesian prior. Second, they also include product terms of the characteristics. Third, their second moment matrix uses demeaned returns, i.e. the two approaches choose different mean-variance efficient portfolios on the globally efficient frontier. Fourth, we allow for different linear weights on the long and the short leg of the characteristic based factors. Fifth, they advocate to first apply PCA to the characteristics managed factors before solving the mean-variance optimization with elastic net penalty. Lettau and Pelger (2020) generalize the robust SDF recovery to the RP-PCA space. Bryzgalova, Pelger, and Zhu (2020) also include additional mean shrinkage in the robust SDF recovery and propose decision trees as an alternative to PCA. Bryzgalova, Pelger, and Zhu (2020) also show that mean-variance optimization with regularization can be interpreted as an adversarial approach with parameter uncertainty. We use conventional long-short factors as a benchmark as those are the most commonly used linear models in the literature. PCA based methods are deferred to Section III.J.

²³The tangency portfolio weights are obtained on the training data set and used on the validation and test data set.

²⁴We weight the estimated means by their rate of convergence to account for the differences in precision.

variation and mean of the systematic component by the corresponding variation and mean of all portfolios. This is the same procedure as for EV and $XS-R^2$ but on the portfolio instead of the stock level. For each individual decile or double-sorted portfolio we also normalize its systematic variation by its overall variation. For the individual quantiles we also report the pricing error $\hat{\alpha}_i$ normalized by the root-mean-squared average returns of all corresponding quantile sorted portfolios, that is,

$$\hat{\alpha}_i = \frac{\hat{\mathbb{E}}[\hat{\epsilon}_{t,i}]}{\sqrt{\frac{1}{N} \sum_{i=1}^N \hat{\mathbb{E}}[R_{t,i}]^2}}.^{25}$$

Appendix B includes a simulation that illustrates that all three evaluation metrics (SR, EV and $XS-R^2$) are necessary to assess the quality of an SDF. A model like FFN can achieve high Sharpe ratios by loading on some extreme portfolios but it does not imply that it captures the loading structure correctly.²⁶ Similarly, linear factors can achieve high Sharpe ratios but by construction cannot capture non-linear and interaction effects in the SDF loadings which is reflected in lower EV and $XS-R^2$. It does not matter how flexible the model is (e.g. FFN), by conditioning only on the most recent macroeconomic observations, general macroeconomic dynamics are ruled out, which seems to be the most strongly reflected in the Sharpe ratio. The no-arbitrage condition in the GAN model helps to deal with a low signal-to-noise ratio and correctly estimate the SDF loadings of stocks that have small risk premia which is reflected in the $XS-R^2$.

III. Empirical Results for U.S. Equities

A. Data

We collect monthly equity return data for all securities on CRSP. The sample period spans January 1967 to December 2016, totaling 50 years. We divide the full data into 20 years of training sample (1967 - 1986), 5 years of validation sample (1987 - 1991), and 25 years of out-of-sample testing sample (1992 - 2016). We use the one-month Treasury bill rates from the Kenneth French Data Library as the risk-free rate to calculate excess returns.

In addition, we collect the 46 firm-specific characteristics listed either on Kenneth French Data Library or used by Freyberger, Neuhierl, and Weber (2020).²⁷ All these variables are constructed either from accounting variables from the CRSP/Compustat database or from past returns from CRSP. We follow the standard conventions in the variable definition, construction and their updating. Yearly updated variables are updated at the end of each June following the Fama-French convention, while monthly changing variables are updated at the end of each month for the use in the next month. The full details on the construction of these variables are in the Internet Appendix. In Table A.II we sort the characteristics into the six categories *past returns*, *investment*, *profitability*, *intangibles*, *value* and *trading frictions*.

²⁵Note, that $XS-R^2 = 1 - \sum_{i=1}^N \hat{\alpha}_i^2$.

²⁶Pelger and Xiong (2019a) provide the theoretical arguments and show empirically in a linear setup why “proximate” factors that only capture the extreme factor weights correctly have similar time series properties as the population factors but their portfolio weights are not the correct loadings.

²⁷We use the characteristics that Freyberger, Neuhierl, and Weber (2020) used in the 2017 version of their paper.

The number of all available stocks from CRSP is around 31,000. As in Kelly, Pruitt, and Su (2019) or Freyberger, Neuhierl, and Weber (2020), we are limited to the returns of stocks that have all firm characteristics information available in a certain month, which leaves us with around 10,000 stocks. This is the largest possible data set that can be used for this type of analysis.²⁸

For each characteristic variable in each month, we rank them cross-sectionally and convert them into quantiles. This is a standard transformation to deal with the different scales and has also been used in Kelly, Pruitt, and Su (2019), Kozak, Nagel, and Santosh (2020) or Freyberger, Neuhierl, and Weber (2020) among others. In the linear model the projection $\tilde{F}_{t+1} = \frac{1}{N} \sum_{i=1}^N I_{t,i} R_{t+1,i}^e$ results in long-short factors with an increasing positive weight for stocks that have a characteristic value above the median and a decreasing negative weight for below median values.²⁹ We increase the flexibility of the linear model by including the positive and negative leg separately for each characteristic, i.e. we take the rank-weighted average of the stocks with above median characteristic values and similarly for the below median values. This results in two “factors” for each characteristic. Note, that our model includes the conventional long-short factors as a special case where the long and short legs receive the same absolute weight of opposite sign in the SDF. These factors are still zero cost portfolios as they are based on excess returns.³⁰

We collect 178 macroeconomic time series from three sources. We take 124 macroeconomic predictors from the FRED-MD database as detailed in McCracken and Ng (2016). Next, we add the cross-sectional median time series for each of the 46 firm characteristics. The quantile distribution combined with the median level for each characteristics is close to representing the same information as the raw characteristic information but in a normalized form. Third, we supplement the time series with the 8 macroeconomic predictors from Welch and Goyal (2007) which have been suggested as predictors for the equity premium and are not already included in the FRED-MD database.

We apply standard transformations to the time series data. We use the transformations suggested in McCracken and Ng (2016), and define transformations for the 46 median and the 8 time series from Welch and Goyal (2007) to obtain stationary time series. A detailed description of the macroeconomic variables as well as their corresponding transformations are collected in the Internet Appendix.

²⁸Using stocks with missing characteristic information requires data imputation based on model assumptions. Gu, Kelly, and Xiu (2019) replace a missing characteristic with the cross-sectional median of that characteristic during that month. However, this approach introduces an additional source of error and ignores the dependency structure in the characteristic space and thus creates artificial time-series fluctuation in the characteristics, which we want to avoid. Hence, we follow the same approach as in Freyberger, Neuhierl, and Weber (2020) and Kelly, Pruitt, and Su (2019) to use only stocks that have all firm characteristics available in a given month, which has the additional benefit of removing predominantly stocks with a very small market capitalization.

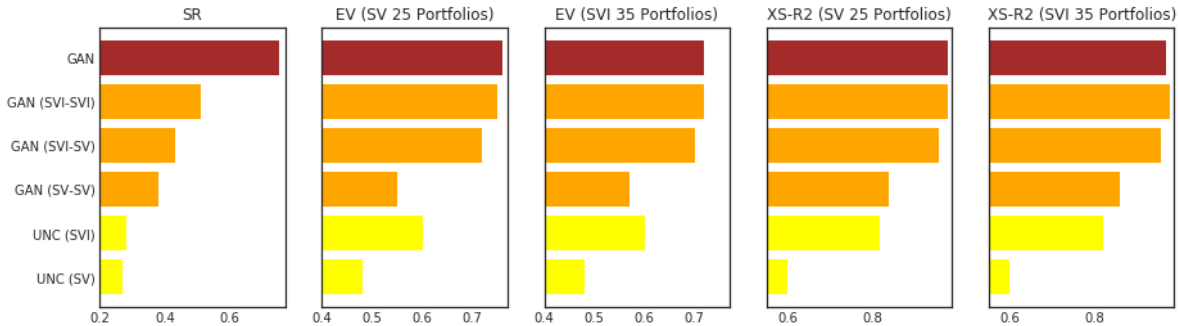
²⁹Kelly, Pruitt, and Su (2019) and Kozak, Nagel, and Santosh (2020) construct factors in this way.

³⁰In the first version of this paper we used the conventional long-short factors. However, our empirical results suggest that the long and short leg have different weights in the SDF and this additional flexibility improves the performance of the linear model. These findings are also in line with Lettau and Pelger (2020) who extract linear factors from the extreme deciles of single sorted portfolios and show that they are not spanned by long-short factors that put equal weight on the extreme deciles of each characteristic.

B. An Illustrative Example of GAN

We illustrate how GAN works with a simple example that uses only the three characteristics size (LME), book-to-market ratio (BEME) and investment (Investment) for all stocks in our sample but leaves out the macroeconomic information. We show that is not only crucial which characteristics are included in the SDF weights ω but also which are included in the test assets constructed by the conditioning function g . UNC denotes the model that is unconditional in the test assets, that is, the test assets are the individual stock returns and the objective function is based on the unconditional moments. We allow the SDF weights to depend on size and value information denoted by UNC (SV) or also include investment for UNC (SVI). The GAN model allows for test assets that depend on the characteristics, that is, g is a non-trivial function. We first list the characteristics included in the SDF weights ω and then those included in the test assets modeled by g . For example, GAN (SVI-SV) uses size, value and investment in ω , but only size and value in g . In order to keep this simple example interpretable, we restrict g to a scalar function. The loading β depends on the same information as the SDF weights ω . We also include the benchmark model that is estimated on all the data and discussed in more detail in the next subsection. We evaluate the asset pricing performance on two well-known sets of test assets: 25 double-sorted size and book-to-market portfolios (SV 25) and 35 portfolios that include in addition 10 decile portfolios sorted on investment (SVI 35). We infer the portfolio's β from the SDF loadings of the individual stocks and the portfolio weights.

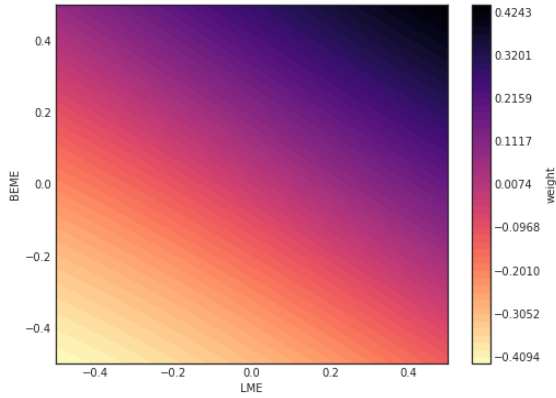
Figure 4: GAN Illustration



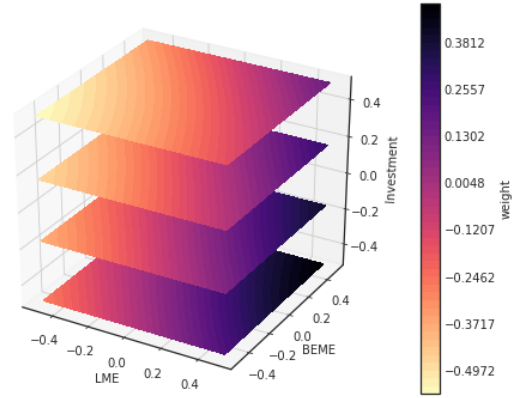
This figure shows the out-of-sample monthly Sharpe ratio (SR), explained time-series variation (EV) and cross-sectional R^2 for different SDF models. UNC (SV) and UNC (SVI) are unconditional models with respect to the test assets, that is, they use only size and value respectively size, value and investment for the SDF weights, but set g to a constant. The GAN models use a non-trivial g . GAN (SVI-SV) allows the SDF weight ω to depend on size, value and investment, but the test asset function g to depend only on size and investment. The model labeled as GAN is our benchmark model estimated with all characteristics and macroeconomic information. We evaluate the model on 25 double-sorted size and book-to-market portfolios (SV 25) and we add another 10 decile portfolios sorted on investment (SVI 35). The portfolios are value-weighted.

Figure 4 shows the out-of-sample Sharpe ratio, explained variation and cross-sectional R^2 . First, not surprisingly including more information in the SDF weights ω leads to a better asset pricing model. UNC (SVI) explains more variation and mean returns for portfolios sorted on investment but also for the size and book-to-market portfolios compared to UNC (SV). However, the key insight

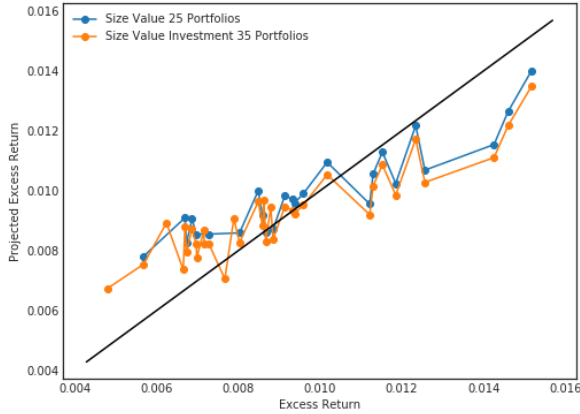
Figure 5: GAN Conditioning Function g and Portfolio Pricing



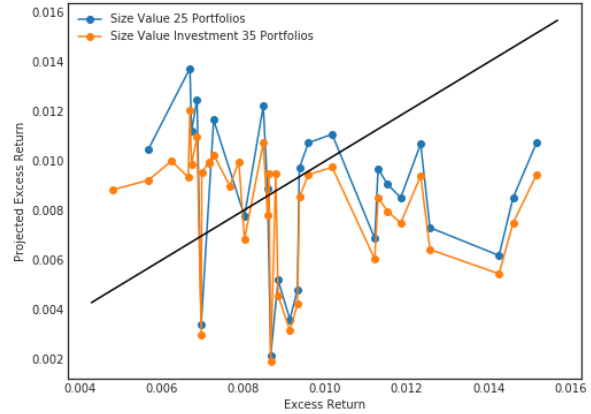
(a) Conditioning function g for GAN (SV-SV)



(b) Conditioning function g for GAN (SVI-SVI)



(c) Portfolio pricing for GAN (SVI-SVI)



(d) Portfolio pricing for UNC (SVI)

This figures show the composition of the conditioning function g and predicted vs. expected returns for the sorted portfolios. Subfigure (a) shows g based only on size and value while subfigure (b) also includes investment. Subfigures (c) and (d) show the predicted and average excess returns for the 25 and 35 sorted portfolios. The tuning parameters are chosen optimally on the validation data and are different from the general benchmark GAN.

is that the information in the test assets matters crucially for the SDF recovery. The test assets of GAN (SVI-SVI) include investment information, which results in a better model than GAN (SVI-SV) that has only size and book-to-market information for the test assets. Depending on the metric, GAN (SVI-SVI) is roughly twice as good as UNC (SVI). The top bar is the full benchmark model. Not surprisingly, the higher SR confirms that there is substantially more information that can be extracted by including the other characteristics and macroeconomic time-series. However, if the goal is to simple explain the 25 Fama-French double-sorted portfolios, GAN (SVI-SVI) already provides a good model.

Figure 5 explains why we observe these findings. The top figures show heat maps for the scalar conditioning function g . For GAN (SV-SV) the test assets become long-short portfolios with extreme weights in small value stocks and large growth stocks.³¹ When we add investment

³¹Note that the sign of g is not identified and we could multiply g by -1 and obtain the same output.

information, the test assets become essentially long-short portfolios with extreme weights for small, conservative value stocks and large, aggressive growth stocks. GAN has in a data driven way discovered the structure of the Fama-French type test assets! Not surprisingly, an asset pricing model trained on these test assets will better explain portfolios sorted on these characteristics. The bottom figures show the predicted and average excess returns for the 25 and 35 sorted portfolios for GAN (SVI-SVI) and UNC (SVI). In an ideal model the points would line up on the 45 degree line. UNC (SVI) fails in explaining small value stocks while the GAN formulation captures mean returns very well for all quantiles. The Internet Appendix contains the detailed results for all the models and test assets.

In summary, the simple example illustrates that the problem of estimating an asset pricing model cannot be separated from the problem of choosing informative test assets. In the next section we move to our main analysis that includes all firm characteristics and macroeconomic information.

C. Cross Section of Individual Stock Returns

The GAN SDF has a higher out-of-sample Sharpe ratio while explaining more variation and pricing than the other benchmark models. Table V reports the three main performance measures, Sharpe ratio, explained variation and cross-sectional R^2 , for the four model specifications. The annual out-of-sample Sharpe ratio of GAN is around 2.6 and almost twice as high as with the simple forecasting approach FFN. The non-linear and interaction structure that GAN can capture results in a 50% increase compared to the regularized linear model. Hence, the more flexible form matters, but an appropriately designed linear model can already achieve an impressive performance. The in-sample results suffer from overfitting, but the annual in-sample Sharpe ratio of GAN with 9.3 clearly stands out. The non-regularized linear model has the worst performance in terms of explained variation and pricing error. GAN explains 8% of the variation of individual stock returns which is twice as large as the other models. Similarly, the cross-sectional R^2 of 23% is substantially higher than for the other models. Interestingly, the regularized linear model based on the no-arbitrage objective function explains the time-series and cross-section of stock returns at least as good as the flexible neural network without the no-arbitrage condition. Each model here uses the optimal set of hyperparameters to maximize the validation Sharpe ratio. In case of the LS, EN and FFN this implies to leave out the macroeconomic variables.³²

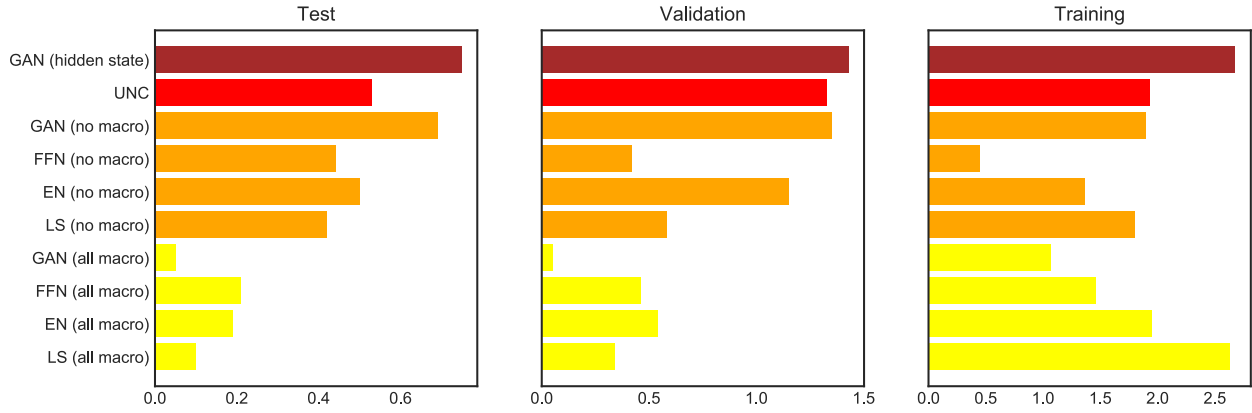
Figure 6 summarizes the effect of conditioning on the hidden macroeconomic state variables. First, we add the 178 macroeconomic variables as predictors to all networks without reducing them to the hidden state variables. The performance for the out-of-sample Sharpe ratio of the LS, EN, FFN and GAN model completely collapses. First, conditioning only on the last normalized observation of the macroeconomic variables, which is usually an increment, does not allow to detect a dynamic structure, e.g. a business cycle. The decay in the Sharpe ratio indicates that using

³²The results are not affected by normalizing the SDF weights to have $\|\omega\|_1 = 1$. The explained variation and pricing results are based on a cross-sectional projection at each time step which is independent of any scaling.

Table I: Performance of Different SDF Models

Model	SR			EV			XS- R^2		
	Train	Valid	Test	Train	Valid	Test	Train	Valid	Test
LS	1.80	0.58	0.42	0.09	0.03	0.03	0.15	0.00	0.14
EN	1.37	1.15	0.50	0.12	0.05	0.04	0.17	0.02	0.19
FFN	0.45	0.42	0.44	0.11	0.04	0.04	0.14	-0.00	0.15
GAN	2.68	1.43	0.75	0.20	0.09	0.08	0.12	0.01	0.23

This table shows the monthly Sharpe ratio (SR) of the SDF, explained time series variation (EV) and cross-sectional mean R^2 for the GAN, FFN, EN and LS model.

Figure 6: Performance of Models with Different Macroeconomic Variables

This figure shows the Sharpe ratio of SDFs for different inclusions of the macroeconomic information. The GAN (hidden states) is our reference model. UNC is a special version of our model that uses only unconditional moments (but includes LSTM macroeconomic states in the FFN network for the SDF weights). GAN (no macro), FFN (no macro), EN (no macro) and LS (no macro) use only firm specific information as conditioning variables but no macroeconomic variables. GAN (all macro), FFN (all macro), EN (all macro) and LS (all macro) include all 178 macro variables as predictors (respectively conditioning variables) without using LSTM to transform them into macroeconomic states.

only the past macroeconomic information results in a loss of valuable information. Even worse, including the large number of irrelevant variables actually lowers the performance compared to a model without macroeconomic information. Although the models use a form of regularization, a too large number of irrelevant variables makes it harder to select those that are actually relevant. The results for the in-sample training data illustrate the complete overfitting when the large number of macroeconomic variables is included. FFN, EN and LS without macroeconomic information perform better and that is why we choose them as the comparison benchmark models. GAN without the macroeconomic but only firm-specific variables has an out-of-sample Sharpe ratio that is around 10% lower than with the macroeconomic hidden states. This is another indication that it is relevant to include the dynamics of the time series. The UNC model uses only unconditional moments as the objective function, that is, we use a constant conditioning function g , but include the LSTM hidden states in the factor weights. The Sharpe ratio is around 20% lower than the GAN with hidden states. These results confirm the insights from the last subsection. Hence, it is

not only important to include all characteristics and the hidden states in the weights and loadings of SDF but also in the conditioning function g to identify the assets and times that matter for pricing.

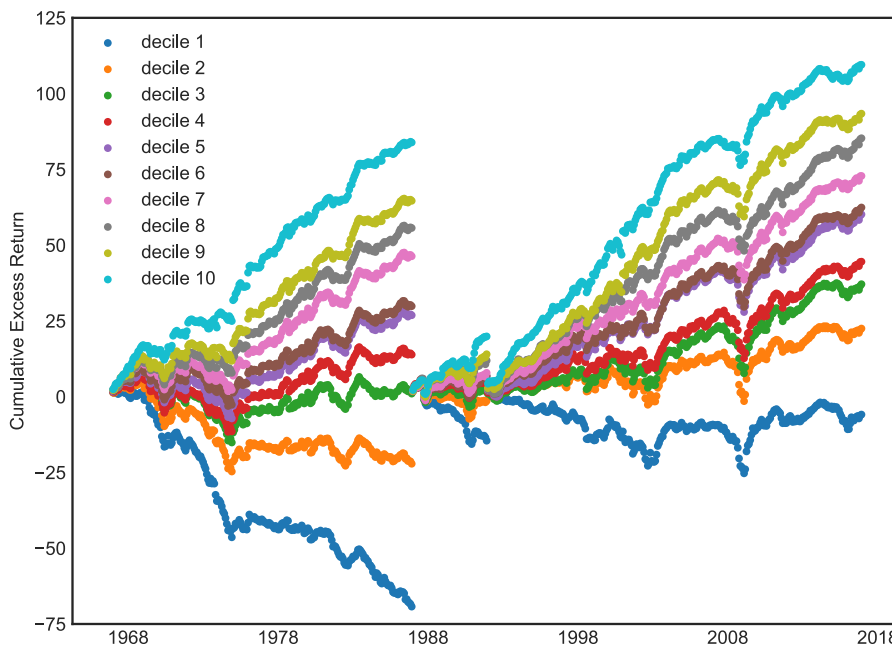
D. Predictive Performance

The no-arbitrage factor representation implies a connection between average returns of stocks and their risk exposure to the SDF measured by β . The fundamental equation

$$\mathbb{E}_t[R_{t+1,i}^e] = \beta_{t,i}\mathbb{E}_t[F_{t+1}]$$

implies that as long as the conditional risk premium $\mathbb{E}_t[F_{t+1}]$ is positive, assets with a higher risk exposure $\beta_{t,i}$ should have higher expected returns.³³ We test the predictive power of our model by sorting stocks into decile portfolios based on their risk loadings.

Figure 7: Cumulative Excess Return of Decile Sorted Portfolios with GAN

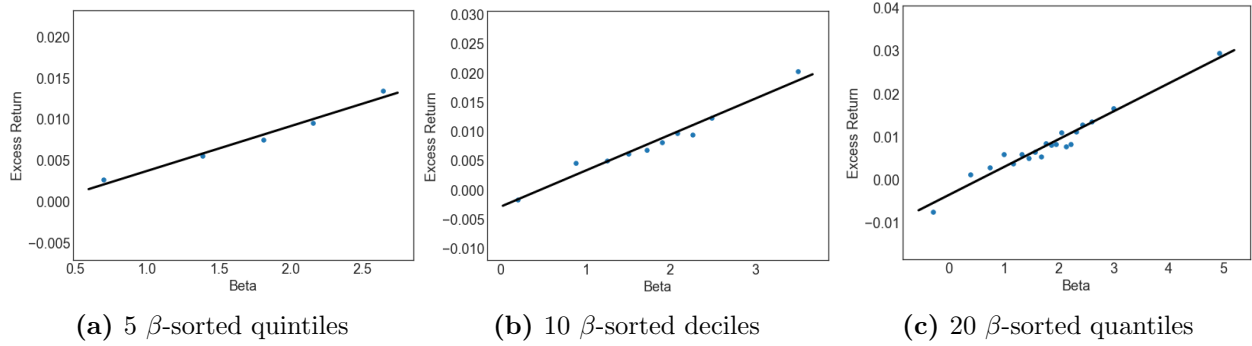


This figure shows the cumulative excess return of decile sorted portfolios based on the risk loadings β . The first portfolio is based on the smallest decile of risk loadings, while the last decile portfolio is constructed with the largest loading decile. Within each decile the stocks are equally weighted.

In Figure 7 we plot the cumulative excess return of decile sorted portfolios based on risk loadings β 's. Portfolios based on higher β 's have higher subsequent returns. This clearly indicates that risk loadings predict future stock returns. In particular, the highest and lowest deciles clearly separate. The Internet Appendix collects the corresponding results for the other estimation approaches with qualitatively similar findings, i.e. the risk loadings predict future returns.

³³We consider it to be a sensible and weak assumption that risk is compensated in the stock market and hence the conditional risk premium $\mathbb{E}_t[F_{t+1}]$ is positive.

Figure 8: Expected Excess Returns of β -Sorted Portfolios as a Function of β



This figure shows expected excess returns of β -sorted portfolios for GAN on the test sample. Stocks are sorted into 5, 10 or 20 quantiles every month. We plot them against the β of each portfolio that averages the individual stock $\beta_{t,i}$ over stocks and time within each portfolio. The linear line denotes a linear regression with intercept, which yields an R^2 of 0.98 (quintiles), 0.97 (deciles) and 0.95 (20 quantiles).

Table II: Time Series Pricing Errors for β -Sorted Portfolios

Decile	Average Returns		Market-Rf				Fama-French 3				Fama-French 5			
	Full	Test	Full		Test		Full		Test		Full		Test	
			α	t	α	t	α	t	α	t	α	t	α	t
1	-0.12	-0.02	-0.19	-8.92	-0.11	-3.43	-0.21	-12.77	-0.13	-5.01	-0.20	-11.99	-0.12	-4.35
2	-0.00	0.05	-0.07	-4.99	-0.04	-1.56	-0.09	-8.79	-0.05	-3.22	-0.09	-8.29	-0.05	-2.68
3	0.04	0.08	-0.02	-2.01	-0.00	-0.16	-0.04	-5.18	-0.02	-1.40	-0.04	-4.87	-0.01	-1.05
4	0.07	0.09	-0.00	-0.03	0.01	0.68	-0.02	-2.30	-0.00	-0.35	-0.02	-2.86	-0.01	-0.54
5	0.10	0.12	0.03	2.75	0.04	2.50	0.01	2.08	0.03	2.46	0.01	1.36	0.03	2.17
6	0.11	0.12	0.04	3.16	0.05	2.77	0.02	2.75	0.03	2.85	0.01	1.51	0.02	2.20
7	0.14	0.15	0.07	5.62	0.07	3.92	0.05	6.61	0.05	4.39	0.04	5.16	0.04	3.41
8	0.18	0.18	0.11	7.41	0.10	5.12	0.08	9.32	0.08	5.83	0.07	8.05	0.07	4.86
9	0.22	0.21	0.15	7.83	0.13	5.37	0.11	9.16	0.11	5.71	0.11	8.58	0.11	5.39
10	0.37	0.37	0.29	9.22	0.27	6.05	0.24	10.03	0.25	6.27	0.25	10.43	0.27	6.59
10-1	0.48	0.39	0.47	18.93	0.38	10.29	0.45	18.50	0.38	10.14	0.46	18.13	0.39	9.96
GRS Asset Pricing Test			GRS	p	GRS	p	GRS	p	GRS	p	GRS	p	GRS	p
			42.23	0.00	11.58	0.00	39.72	0.00	11.25	0.00	37.64	0.00	10.75	0.00

This table shows the average returns, time series pricing errors and corresponding t-statistics for β -sorted decile portfolios based on GAN. The pricing errors are based on the CAPM and Fama-French 3 and 5 factors models. Returns are annualized. The GRS-test is under the null hypothesis of correctly pricing all decile portfolios and includes the p-values. We consider the full time period and the test period. Within each decile the stocks are equally weighted.

The no-arbitrage condition does not only apply a monotonic but a linear relationship between stock β 's and conditional expected returns. An unconditional one-factor model such as the CAPM can be tested by evaluating the fit of the security market line, i.e. the relationship between expected returns and the β 's of the assets. In our case the stock specific $\beta_{t,i}$ are time-varying, but by construction the β -sorted portfolios should have a close to constant slope with respect to the SDF. In Figure 8 we plot the expected excess returns of the 10 β -sorted deciles as well as for 5 and 20 β -sorted quantile portfolios against their average β 's. No-arbitrage imposes a linear relationship and a zero intercept. Indeed, for all three plots the relationship is almost perfectly linear with a R^2 of 0.98, 0.97 and 0.95 respectively. However, the intercept seems to be slightly below zero. This

indicates a close to but not perfect fit.

The systematic return difference of the β -sorted portfolios is not explained by the market or Fama-French factors. Table II reports the time series pricing errors with corresponding t-statistics for the 10 decile-sorted portfolios for the three factor models. Obviously, the pricing errors are highly significant and expected returns of almost all decile portfolios are not explained by the Fama-French factors. The GRS test clearly rejects the null-hypothesis that either of the factor models prices this cross-section. These β -sorted portfolios equally weight the stocks within each decile. The Internet Appendix shows that the findings extend to value weighted β -sorted portfolios.

E. Pricing of Characteristic Sorted Portfolios

Our approach achieves an unprecedented pricing performance on standard test portfolios. Asset pricing testing is usually conducted on characteristic sorted portfolios that isolate the pricing effect of a small number of characteristics. We sort the stocks into value weighted decile and double-sorted 25 portfolios based on the characteristics.³⁴ Table A.III starts with four sets of decile sorted portfolios. We choose short-term reversal and momentum as these are among the two most important variables as discussed in the next sections and size and book-to-market sorted portfolios which are well-studied characteristics. GAN can substantially better capture the variation and mean return for short-term reversal and momentum sorted decile portfolios. EN and FFN have a very similar performance. The better GAN results are driven by explaining the extreme decile portfolios (the 10th decile for short-term reversal and the first decile for momentum). All approaches perform very similarly for the middle portfolios. It turns out that book-to-market and size sorted portfolios are very “easy” to price. All models have time series R^2 above 70% and cross-sectional R^2 close to 1. Hence, all models seem to capture this pricing information very well, although the GAN results are still slightly better than for the other models.

Table A.IV repeats the same analysis on short-term reversal and momentum double-sorted and size and book-to-market double-sorted portfolios. The takeaways are similar to the decile sorted portfolios. GAN outperforms FFN and EN on the momentum related portfolios, while all three models are able to explain the size and value double-sorted portfolios. Importantly, the linear EN becomes worse on the double-sorted reversal and momentum portfolios. This is due to the extreme corner portfolios, which are in particular low momentum and high short-term reversal stocks. This implies that the linear model cannot capture the interaction between characteristics, while the GAN model successfully identifies the potentially non-linear interaction effects.

Our findings generalize to other decile sorted portfolios. Table III collects the explained variation and cross-sectional R^2 for all decile-sorted portfolios. It is striking that GAN is always better than the other two models in explaining variation. At the same time GAN achieves a cross-sectional R^2 higher than 90% for all characteristics. In the few cases where the other models have a slightly higher

³⁴The Internet Appendix collects the results for additional characteristic sorts with similar findings. Here we report only the results for value weighted portfolios. The results for equally weighted portfolios are similar. The results for the unregularized linear model are the worst and available upon request.

Table III: Explained Variation and Pricing Errors for Decile Sorted Portfolios

Charact.	Explained Variation			Cross-Sectional R^2			Charact.	Explained Variation			Cross-Sectional R^2		
	EN	FFN	GAN	EN	FFN	GAN		EN	FFN	GAN	EN	FFN	GAN
ST_REV	0.43	0.58	0.70	0.45	0.79	0.94	Q	0.68	0.70	0.78	0.97	0.92	0.96
SUV	0.42	0.75	0.83	0.64	0.97	0.99	Investment	0.54	0.65	0.75	0.91	0.94	0.98
r12_2	0.26	0.27	0.54	0.66	0.71	0.93	PM	0.52	0.42	0.68	0.90	0.86	0.93
NOA	0.58	0.69	0.78	0.94	0.96	0.95	DPI2A	0.57	0.70	0.78	0.90	0.95	0.97
SGA2S	0.52	0.63	0.73	0.93	0.95	0.96	ROE	0.59	0.56	0.76	0.91	0.86	0.97
LME	0.83	0.78	0.86	0.96	0.95	0.97	S2P	0.69	0.79	0.82	0.98	0.98	0.97
RNA	0.50	0.48	0.69	0.93	0.87	0.96	FC2Y	0.56	0.71	0.76	0.91	0.94	0.95
LTurnover	0.52	0.57	0.68	0.88	0.89	0.96	AC	0.63	0.79	0.82	0.96	0.98	0.98
Lev	0.52	0.63	0.73	0.90	0.92	0.95	CTO	0.59	0.73	0.79	0.92	0.96	0.97
Resid_Var	0.52	0.27	0.65	0.84	0.73	0.97	LT_Rev	0.60	0.59	0.72	0.93	0.85	0.94
ROA	0.51	0.44	0.70	0.92	0.93	0.98	OP	0.56	0.48	0.74	0.97	0.88	0.98
E2P	0.48	0.44	0.67	0.86	0.80	0.95	PROF	0.58	0.62	0.76	0.91	0.98	0.95
D2P	0.47	0.51	0.72	0.82	0.85	0.94	IdioVol	0.43	0.27	0.66	0.79	0.72	0.97
Spread	0.49	0.32	0.60	0.76	0.71	0.92	r12_7	0.37	0.42	0.66	0.84	0.86	0.93
CF2P	0.46	0.47	0.66	0.90	0.89	0.99	Beta	0.45	0.46	0.62	0.83	0.87	0.97
BEME	0.70	0.75	0.82	0.97	0.94	0.98	OA	0.65	0.78	0.83	0.88	0.92	0.93
Variance	0.48	0.27	0.61	0.74	0.72	0.90	ATO	0.58	0.70	0.77	0.96	0.98	0.99
D2A	0.57	0.71	0.78	0.96	0.96	0.97	MktBeta	0.44	0.44	0.64	0.81	0.85	0.97
PCM	0.66	0.79	0.82	0.97	0.98	0.99	OL	0.60	0.73	0.78	0.95	0.97	0.97
A2ME	0.72	0.79	0.83	0.97	0.96	0.98	C	0.51	0.65	0.73	0.90	0.93	0.95
AT	0.77	0.70	0.83	0.77	0.89	0.92	r36_13	0.54	0.53	0.69	0.92	0.82	0.93
Rel2High	0.46	0.33	0.60	0.90	0.83	0.97	NI	0.51	0.60	0.75	0.88	0.96	0.99
CF	0.61	0.64	0.78	0.89	0.85	0.96	r2_1	0.51	0.52	0.69	0.87	0.90	0.95

This table shows the out-of-sample explained variation and cross-section R^2 for 46 decile-sorted and value weighted portfolios.

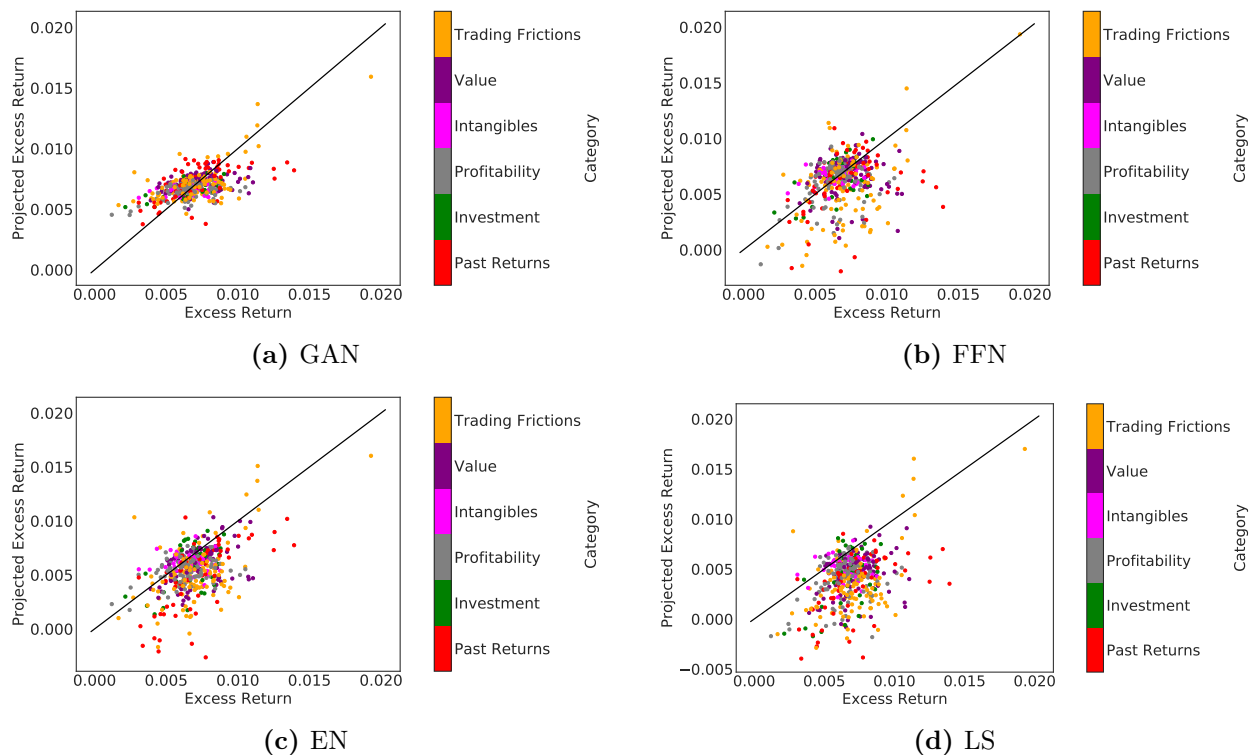
cross-sectional R^2 , this number is very close to 1, i.e. all models can essentially perfectly explain the pricing information in the deciles. In summary GAN strongly dominates the other methods in explaining sorted portfolios. The results show (1) that the non-linearities and interactions matter as GAN is better than EN and (2) the no-arbitrage condition extracts additional information as GAN is better than FFN.

Figure 9 visualizes the ability of GAN to explain the cross-section of expected returns for all value weighted characteristic sorted deciles. We plot the average excess return and the model implied average excess return. The GAN SDF captures the correct monotonic behavior, but its prediction is biased towards the mean. In contrast, the prediction of the other three models show a larger discrepancy which holds for characteristics of all groups. Figure 10 shows the prediction results for equally weighted decile portfolios. All models seem to perform slightly better, but the general findings are the same.

F. Variable Importance

What is the structure of the SDF factor? As a first step in Table A.V we compare the GAN factor with the Fama-French 5 factor model. None of the five factors has a high correlation with our factor with the profitability factor having the highest correlation with 17%. The market factor

Figure 9: Predicted returns for value weighted characteristic sorted portfolios



This figure shows the predicted and average excess returns for value weighted characteristic sorted decile portfolios for the four SDF models. We have in total 460 decile portfolios in six different anomaly categories.

has only a correlation of 10%. Next, we run a time series regression to explain the GAN factor portfolio with the Fama-French 5 factors. Only the profitability factor is significant. The strongly significant pricing error indicates that these factors fail to capture the pricing information in our SDF portfolio.

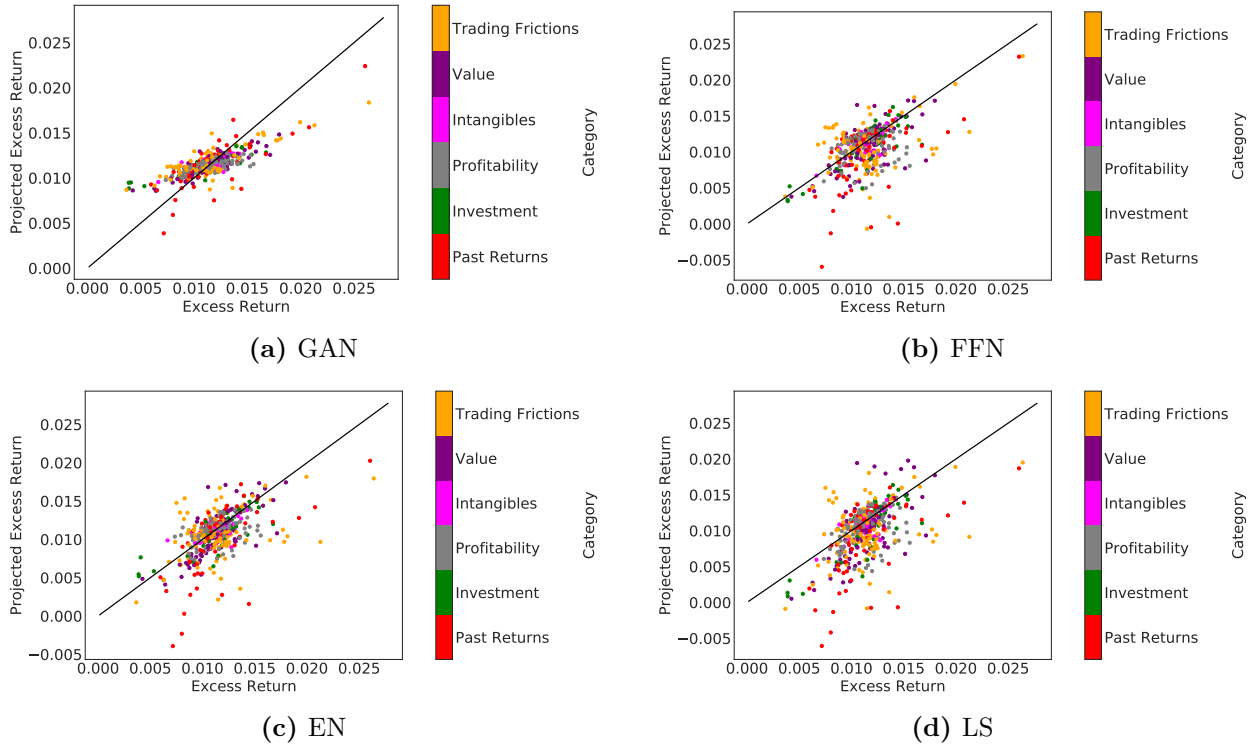
We rank the importance of firm-specific and macroeconomic variables for the pricing kernel based on the sensitivity of the SDF weight ω with respect to these variables. Our sensitivity analysis is similar to Sirignano, Sadhwani, and Giesecke (2020) and Horel and Giesecke (2020) and based on the average absolute gradient. More specifically, we define the sensitivity of a particular variable as the average absolute derivative of the weight w with respect to this variable:

$$\text{Sensitivity}(x_j) = \frac{1}{C} \sum_{i=1}^N \sum_{t=1}^T \left| \frac{\partial w(I_t, I_{t,i})}{\partial x_j} \right|,$$

where C a normalization constant. This simplifies to the standard slope coefficient in the special case of a linear regression framework. A larger sensitivity means that a variable has a larger effect on the SDF weight ω .

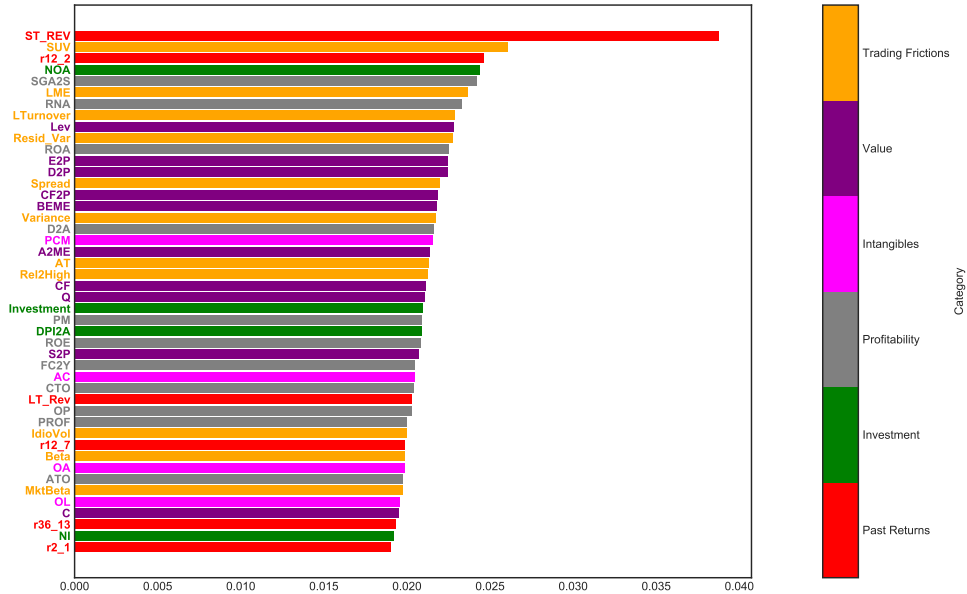
Figure 11 ranks the variable importance of the 46 firm-specific characteristics for GAN. The sum of all sensitivities is normalized to one. Figures 12, A.5 and A.6 collect the corresponding results for

Figure 10: Predicted returns for equally weighted characteristic sorted portfolios



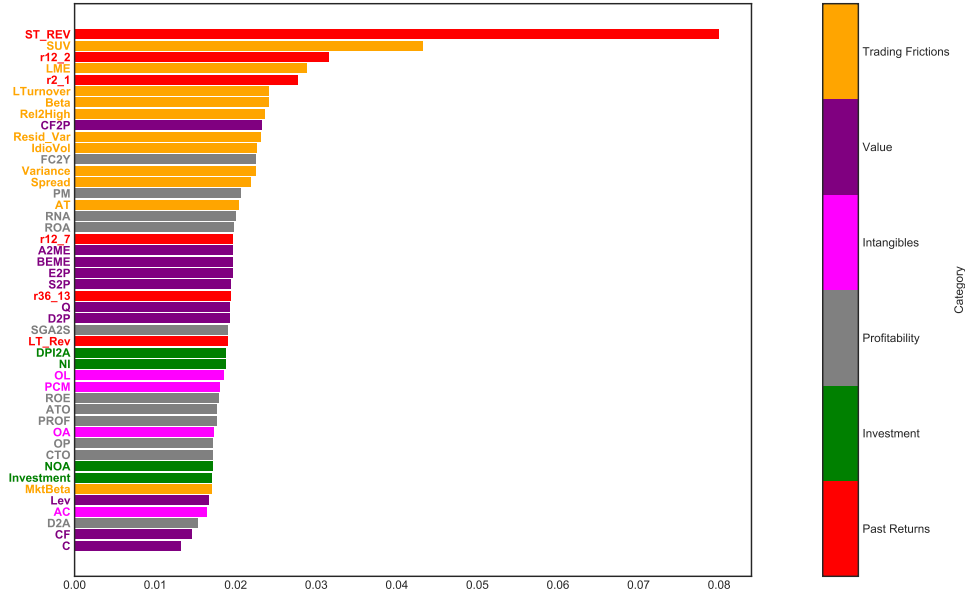
This figure shows the predicted and average excess returns for equally weighted characteristic sorted decile portfolios for the four SDF models. We have in total 460 decile portfolios in six different anomaly categories.

Figure 11: Characteristic Importance for GAN SDF



The figure shows the GAN variable importance ranking of the 46 firm-specific characteristics in terms of average absolute gradient (VI) on the test data. The values are normalized to sum up to one.

Figure 12: Characteristic Importance for FFN SDF



The figure shows the FFN variable importance ranking of the 46 firm-specific characteristics in terms of average absolute gradient (VI) on the test data. The values are normalized to sum up to one.

FFN, EN and LS. All three models GAN, FFN and EN select trading frictions and past returns as being the most relevant categories. The most important variables for GAN are Short-Term Reversal (ST_REV), Standard Unexplained Volume (SUV) and Momentum (r12_2). Importantly, for GAN all 6 categories are represented among the first 20 variables, which includes size, value, investment and profitability characteristics. The SDF composition is different for FNN, where the first 14 characteristics are almost only in the trading friction and past return category. More specifically, this SDF loads heavily on short-term reversal, illiquidity measured by unexplained volume and size, which raises the suspicion that a simple forecasting approach might focus mainly on illiquid penny stocks. The no-arbitrage condition with informative test assets seems to be necessary to discipline the model to capture the pricing information in other characteristics. Figure A.7 shows the variable importance ranking for the conditioning vector g . The GAN test assets depend on all six major anomaly categories. These test assets ensure that the GAN SDF also reflects this information. The linear model with regularization also selects variables from all six categories among the first 9 variables. Note, that the elastic net penalty removes characteristics that are close substitutes, for example, as the dividend-price ratio (D2P) and book-to-market ratio (BEME) capture similar information, the regularized model only selects one of them. The linear model without regularization cannot handle the large number of variables and not surprisingly results in a different ranking.

Figure A.4 shows the importance of the macroeconomic variables for the GAN model. These variables are first summarized into the four hidden states processes before they enter the weights of the SDF. First, it is apparent that most macroeconomic variables have a very similar importance.

This is in line with a model where there is a strong dependency between the macroeconomic time series which is driven by a low dimensional non-linear factor structure. A simple example would be the factor model in Ludvigson and Ng (2009) where the information in a macroeconomic data set very similar to ours is summarized by a small number of PCA factors. As the first PCA factor is likely to pick up a general economic market trend, it would affect all variables. If the SDF structure depends on this PCA factor, all macroeconomic variables will appear to be important (of potentially similar magnitude). It is important to keep in mind that a simple PCA analysis of the macroeconomic variables does not work in our asset pricing context. The reason is that the PCA factors would mainly be based on increments of the macroeconomic time series and hence would not capture the dynamic pattern.³⁵ The two most relevant variables that stand out in our importance ranking are the median bid-ask spread (**Spread**) and the federal fund rate (**FEDFUNDS**). These can be interpreted as capturing the overall economic activity level and overall market volatility.

We show that the hidden macroeconomic states are closely linked to business cycles and overall economic activity. Figure 13 plots the time series of the four hidden macroeconomic state variables. These variables are the outputs from the LSTM that encodes the history of macroeconomic information. Here we report one representative fit of the LSTM from the nine ensemble estimates.³⁶ The grey shaded areas indicate NBER recessions.³⁷ First, it is apparent that the state variables, in particular for the third and fourth state, peak during times of recessions. Second, the state processes seem to have a cyclical behavior which confirms our intuition that the relevant macroeconomic information is likely to be related to business cycles. The cycles and peaks of the different state variables do not coincide at all times indicating that they capture different macroeconomic risks.

G. SDF Structure

We study the structure of the SDF weights and betas as a function of the characteristics. Our main findings are two-fold: Surprisingly, individual characteristics have an almost linear effect on the pricing kernel and the risk loadings, i.e. non-linearities matter less than expected for individual characteristics. Second, the better performance of GAN is explained by non-linear interaction effects, i.e. the general functional form of our model is necessary for capturing the dependency between multiple characteristics.

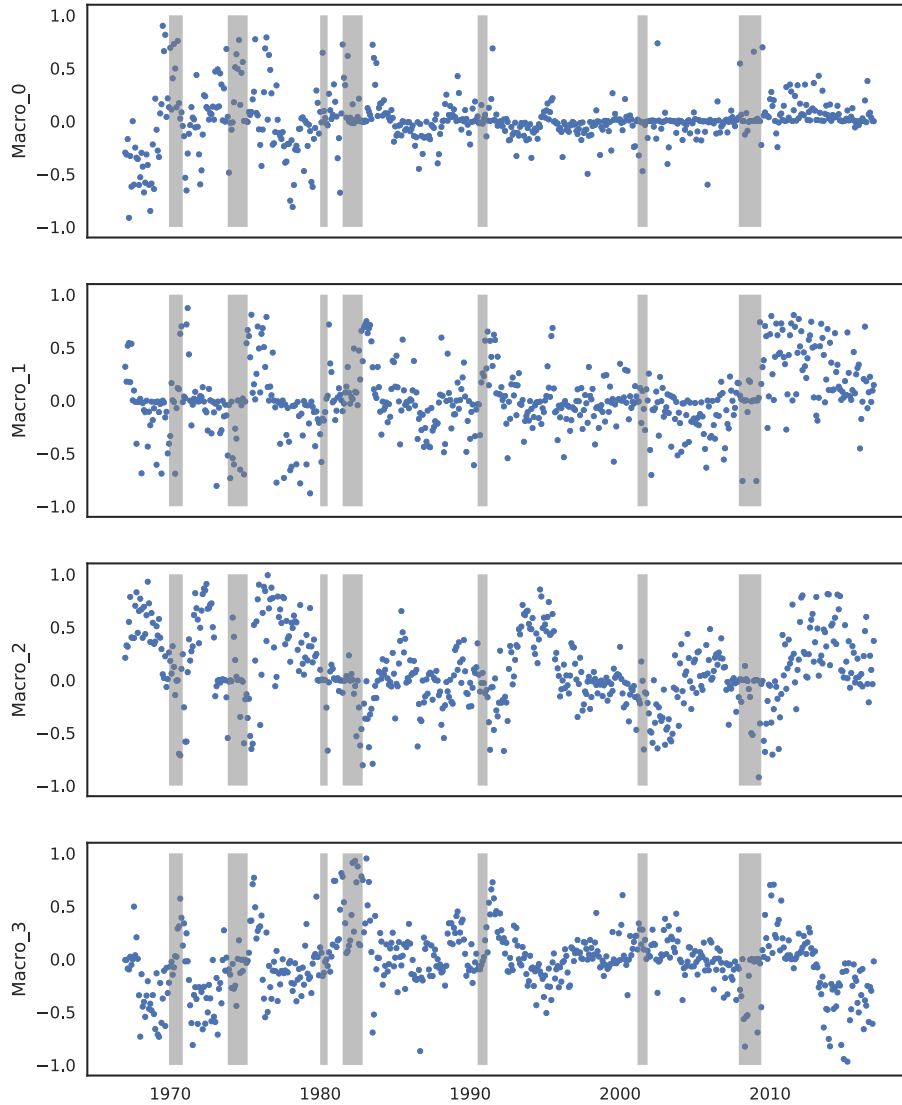
Figure A.9 plots the one-dimensional relationship between the SDF weights ω and one specific characteristic. The other variables are fixed at their mean values. In the case of a linear model these plots simply show the slope of a linear regression coefficient. As we include a separate long

³⁵The results for PCA based macroeconomic factors are available upon request. We also want to clarify that for other applications PCA based factors based on macroeconomic time series might actually capture the relevant information.

³⁶Each ensemble fit returns a four dimensional vector of the state processes. However, it is not meaningful to average these vectors as the first state process in one fit does not need to correspond to the same process in another fit. It is only meaningful to report model averages of scalar output variables.

³⁷NBER based Recession Indicators for the United States from the Peak through the Trough are taken from <https://fred.stlouisfed.org/series/USRECM>.

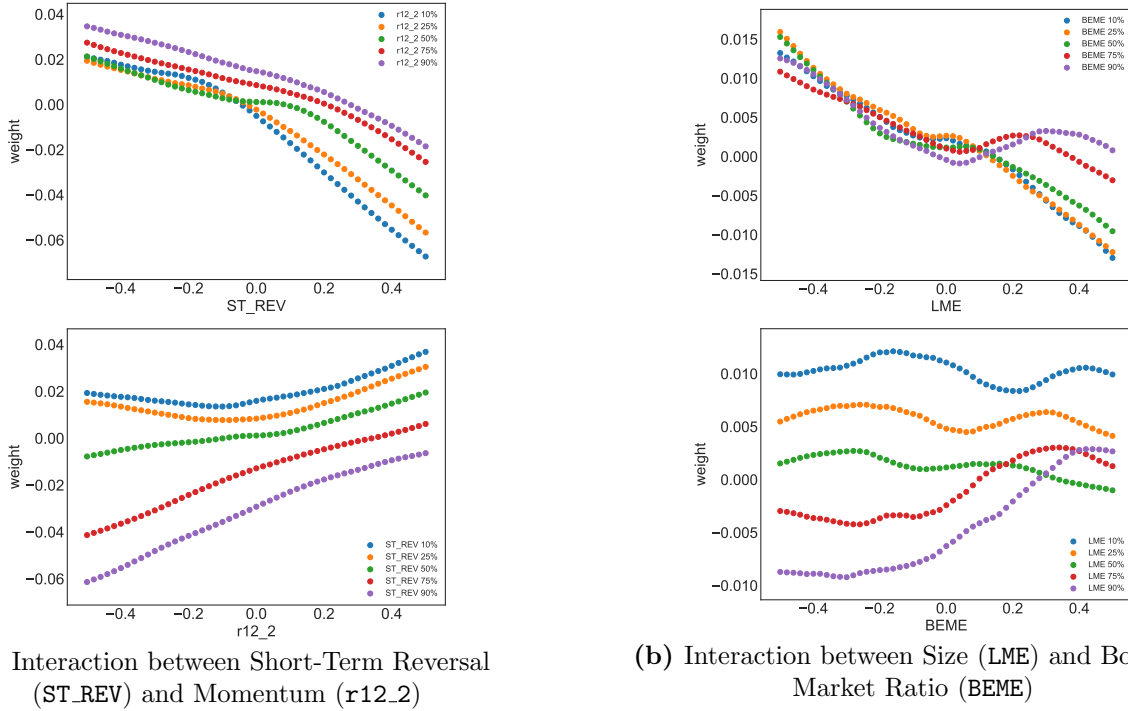
Figure 13: Macroeconomic Hidden State Processes (LSTM Outputs)



The figure shows the four macroeconomic hidden state processes extracted with LSTM in the GAN model. The gray areas mark NBER recession periods. The time-series are one representative estimation in the multiple ensemble estimations.

and short leg for the linear model, we allow for a kink at the median value. Otherwise the linear model would simply be a straight line. For the non-linear GAN and FFN the one-dimensional relationship can take any functional form. We show the univariate functional form for the three most relevant characteristics in Figure A.9, while the Internet Appendix collects the results for the other characteristics. It is striking how close the functional form of the SDF for GAN and FFN is to a linear function. This explains why linear models are actually so successful in explaining single-sorted characteristics. For a small number of characteristics, mainly short-term reversal and momentum, GAN has some non-linearities that allow for a higher slope at the extreme end. These are exactly the decile sorted portfolios for which GAN performs better than FFN and EN. However,

Figure 14: SDF weight ω as a Function of Characteristics for GAN



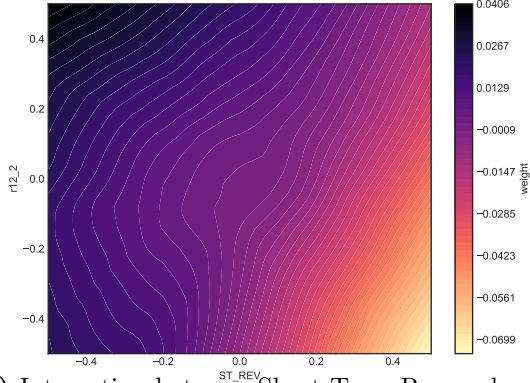
This figures show the SDF weight ω as function of short-term reversal, momentum, size and book-to-market ratio for different quantiles of the second variable while keeping the remaining variables at their mean level.

for most characteristics the pricing kernel depends almost linearly on the characteristics as long as we consider a one-dimensional relationship. However, it seems to be relevant to allow the low and high quantiles to have different linear slopes. The linear model without regularization obtains a relationship for some characteristics that is completely out of line with the other models. Given the worse overall performance of LS, this suggests that LS suffers from severe over-fitting.

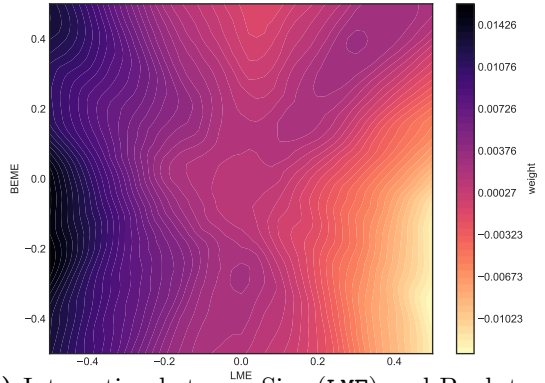
Figures 14 and 15 show the crucial finding for this section. Non-linearities matter for interactions. Here we plot the 2- respectively 3-dimensional functional form of ω when we fix all but two or three variables at their mean. A linear model like EN also assumes an additive effect of different characteristics on the pricing kernel, that is, small value stocks cannot have a different exposure to size than small stocks. Both, GAN and FNN, relax this condition and allow for general interaction effects. However, the simulation in the Internet Appendix suggests that the no-arbitrage condition of GAN helps in identifying relevant interaction effects that are not captured by FFN. Indeed, the line plots and heatmaps for GAN reveal more complex interaction patterns than for the other models.

Figure 14 plots the SDF weight of one characteristic conditioned on a quantile of a second characteristic. The corresponding plots for the other models are in the Internet Appendix. In an additive model without interaction all lines would be parallel shifts. This is exactly what we see for

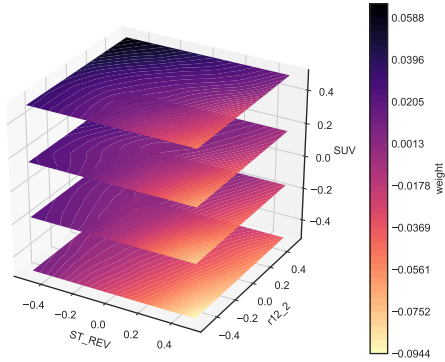
Figure 15: SDF weight ω as a Function of Characteristics for GAN



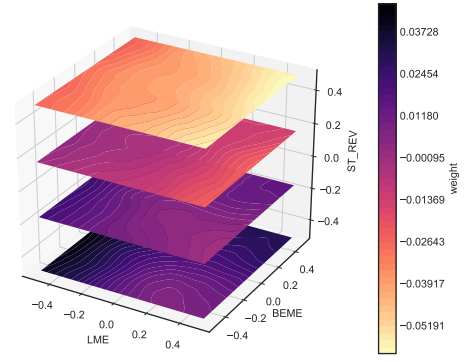
(a) Interaction between Short-Term Reversal (ST_REV) and Momentum (r12.2)



(b) Interaction between Size (LME) and Book to Market Ratio (BEME)



(c) Interaction between Short-Term Reversal (ST_REV), Momentum (r12.2) and Standard Unexplained Volume (SUV)



(d) Interaction between Size (LME), Book to Market Ratio (BEME) and Short-Term Reversal (ST_REV)

These figures show the SDF weight ω as two- and three-dimensional function of characteristics keeping the remaining variables at their mean level.

the two linear models.³⁸ Interestingly, for size and value, the FFN model also has almost parallel shifts in the SDF weights, implying that it does not capture interactions. However, for GAN small stocks have a very different exposure to value than large cap stocks. Note, that while fixing the second characteristic at the median, the lines are close to linear. However, the shape can become non-linear when conditioning the second characteristic on an extreme quantile.

Instead of conditioning on only five quantiles, we plot the two-dimensional pricing kernel for GAN in Figure 15. It confirms that the combined size and book-to-market characteristics have a highly non-linear effect on the GAN pricing kernel. The triple interaction in Figure 15 shows that low short-term reversal, high momentum and high explained volume has the highest positive weight while high reversal, low momentum and low unexplained volume has the largest negative weight in

³⁸As the linear model with regularization removes variables, it is possible that the SDF weights for one characteristic conditioned on different quantiles of the second characteristic collapse to one line.

the kernel when conditioning on these three characteristics. Low reversal and low momentum or high reversal and high momentum have an almost neutral effect independent of unexplained volume. The interaction effect for size, book-to-market and short-term reversal is even more complicated.

H. Robustness Results

Our findings are robust to small cap stocks, the choice of the tuning parameters, the time period under consideration and are not exploiting limits to arbitrage. In this subsection, we evaluate and refit the model without small cap stocks, compare the performance and structure of the SDF for different tuning parameters and time periods and control the information used to construct the test assets.

The qualitative findings are robust to small cap stocks. It is well-known that penny stocks can achieve high Sharpe ratios and are hard to price by conventional asset pricing models. However, trading in these small cap stocks is limited due to low liquidity and high spreads. Hence, the high Sharpe ratios or large alphas of small cap stocks can potentially not be exploited. Here, we compare the model performance restricted to medium and large cap stocks. Our cross-section of stocks in the test data is composed of 2,000 to 3,000 individual stocks per month. The Internet Appendix shows that the restriction to the stocks with a market capitalization larger than 0.001% of the total market capitalization leaves us on average with the largest 1,500 stocks. Restricting the sample to stocks with market cap above 0.01% of the total market cap yields on average the largest 550 stocks, that is, the sample is close to the S&P 500 index.

Table IV reports the model performance for these two subsets of the data. The SDF weights are obtained on all individual stocks, but the Sharpe-ratio and the explained time series and cross-sectional variation is calculated on stocks with market cap larger than 0.001% respectively 0.01% of the total market capitalization. As expected the Sharpe ratios decline, but GAN still achieves an annual out-of-sample Sharpe ratio of 1.4 using only the 1,500 largest stocks. In contrast, the linear models collapse. Based on the 550 largest stocks the Sharpe ratio of GAN falls to 0.9, but is still larger than for the other models. Most importantly the explained variation of GAN is two to three times higher than for the linear or deep learning prediction model. Similarly, the gap in the cross-sectional R^2 is substantially wider on the larger stocks than on the whole sample. This suggests that FFN and the linear models are mainly fitting small stocks, while GAN also finds the systematic structure in the large cap stocks.

Table IV also estimates and evaluates the different models on stocks with market capitalization larger than 0.001% of the total market capitalization.³⁹ The performance of GAN is essentially identical, suggesting that our approach finds the same SDF structure conditioned on large cap stocks if it is trained on all stocks or only the large stocks. In this sense our model is robust to the size of the companies. In contrast, the elastic net approach performs significantly better on large cap stocks when estimated on this sample. This is evidence that it overfits small stocks

³⁹We estimate the optimal tuning parameters for the model restricted to the large cap stocks. Using the same tuning parameters as for the total sample yields identical results.

Table IV: Different SDF Models Evaluated on Large Market Cap Stocks

Model	SR			EV			Cross-Sectional R^2		
	Train	Valid	Test	Train	Valid	Test	Train	Valid	Test
Evaluated for size $\geq 0.001\%$ of total market cap									
LS	1.44	0.31	0.13	0.07	0.05	0.03	0.14	0.03	0.10
EN	0.93	0.56	0.15	0.11	0.09	0.06	0.17	0.05	0.14
FFN	0.42	0.20	0.30	0.11	0.10	0.05	0.19	0.08	0.18
GAN	2.32	1.09	0.41	0.23	0.22	0.14	0.20	0.13	0.26
Evaluated for $\geq 0.01\%$ of total market cap									
LS	0.32	-0.11	-0.06	0.05	0.07	0.04	0.13	0.05	0.09
EN	0.37	0.26	0.23	0.09	0.12	0.07	0.17	0.08	0.14
FFN	0.32	0.17	0.24	0.13	0.22	0.09	0.22	0.15	0.26
GAN	0.97	0.54	0.26	0.28	0.34	0.18	0.27	0.23	0.32
Estimated and evaluated for size $\geq 0.001\%$ of total market cap									
LS	1.91	0.40	0.19	0.08	0.06	0.04	0.18	0.05	0.12
EN	1.34	0.92	0.42	0.13	0.13	0.07	0.23	0.09	0.19
FFN	0.37	0.19	0.28	0.13	0.13	0.07	0.21	0.10	0.21
GAN	3.57	1.18	0.42	0.24	0.23	0.14	0.23	0.13	0.26

The table shows monthly Sharpe ratios (SR) of the SDF factors, explained time series variation (EV) and cross-sectional R^2 for the GAN, FFN, EN and LS models. In the first two subtables the model is estimated on all stocks but evaluated on stocks with market capitalization larger than 0.01% or 0.001% of the total market capitalization. In the last subtable the model is estimated and evaluated on stocks market with capitalization larger than 0.001%.

when applied to the full sample in contrast to our approach. The prediction approach has a very similar performance on the large cap stocks when estimated on this subset or on the full data set. This is indicative that it cannot capture the structure in large cap stocks. Even when optimally trained on the subset of large cap stocks the linear and prediction approach explain substantially less time-series and cross-sectional variation than GAN.

We re-estimate the GAN model independently of our benchmark fit and list the tuning parameters of the best four models on the validation data, labeled GAN 1, 2, 3 and 4 in Table A.IX. All models have four macroeconomic states, but differ in terms of the depth of the network and the number of instruments that construct the test assets. The tuning parameters of our benchmark model would only be the second best model in this independent fit. Table V reports the performance for the different fits and tuning parameters. The asset pricing performance is essentially identical for all models. Moreover, Table A.V shows that the SDFs for the various models all have a correlation higher than 80%. The Internet Appendix collects the variable importance results and functional form of the SDF weights ω for the alternative fits. In summary, we conclude that not only the pricing performance is extremely robust to the tuning parameters, but we are actually discovering the same economic model for different tuning parameters and our results are replicable.

As another robustness test we estimate the GAN model on a rolling window of 240 months. In more detail, every year we move the training data window by one year to re-estimate the

Table V: Performance of Alternative GAN Models

Model	SR			EV			Cross-Sectional R^2		
	Train	Valid	Test	Train	Valid	Test	Train	Valid	Test
GAN 1	2.78	1.47	0.72	0.18	0.08	0.07	0.12	0.01	0.21
GAN 2	3.02	1.39	0.77	0.18	0.08	0.07	0.12	0.00	0.22
GAN 3	2.55	1.38	0.74	0.22	0.11	0.09	0.17	0.04	0.25
GAN 4	2.44	1.38	0.77	0.19	0.08	0.07	0.11	0.01	0.22
GAN Rolling	N/A	N/A	0.88	N/A	N/A	0.08	N/A	N/A	0.24
GAN No Frict	2.94	1.37	0.77	0.20	0.10	0.08	0.14	0.01	0.23

This table shows the monthly Sharpe ratio (SR) of the SDF, explained time series variation (EV) and cross-sectional R^2 for alternative GAN models. GAN 1, 2, 3 and 4 are the four best GAN models on the validation data from an independent re-estimation of the model. GAN Rolling is re-estimated every year on a rolling window of 240 months. GAN No Frict is estimated without trading frictions and past returns for the conditioning function g .

SDF weights and loadings.⁴⁰ Not surprisingly, we obtain slightly better asset pricing results, in particular for the Sharpe ratio, as reported in Table V. Overall, the results are very close and the rolling window GAN SDF has a correlation of 70% with our benchmark SDF. Figures A.10 and A.11 show the variable importance and functional form of the rolling window SDF which share the same general patterns. We conclude that a time-varying estimate of GAN does not lead to major improvements and fits a similar economic structure. In particular, this confirms that our results are robust to the time window chosen for estimation.

Our GAN is not simply capturing pricing information that is subject to limits to arbitrage. A potential concern is that GAN constructs test assets that do not represent a risk-premium but anomalies of illiquid stocks that cannot be exploited. In that case the GAN SDF would not represent the economic risk that we want to capture for asset pricing. We want to avoid that GAN explicitly targets stocks that have high trading frictions. We exclude characteristics from the trading frictions and past return category from the conditional network and re-estimate the model labeled as GAN No Frict. The resulting variable importance for g is shown in Figure A.8. This SDF has the same pricing performance and a correlation of 78% with our benchmark SDF suggesting that our results are robust to this change.

I. Machine Learning Investment

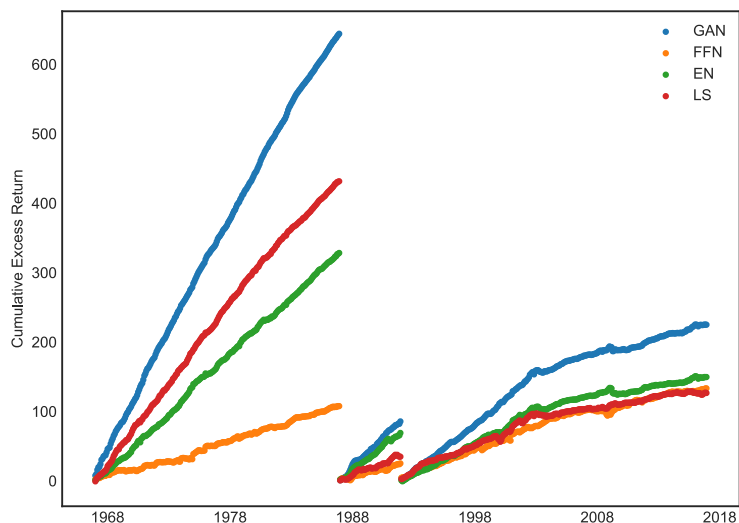
The GAN SDF is a tradeable portfolio with an attractive risk-return trade-off. Table A.VI reports the monthly Sharpe ratios, maximum 1-month loss and maximum drawdown of the four benchmark models and also the Fama-French 3 and 5 factor models.⁴¹ The number of consecutive losses as measured by drawdown and the maximum loss for the GAN model is comparable to the other models, while the Sharpe ratio is by far the highest. Figure 16 plots the cumulative return

⁴⁰The estimation of the GAN models is computationally very expensive and for this reason we are not re-estimating it every month.

⁴¹Max Drawdown is defined as the maximum number of consecutive months with negative returns. The maximum 1-month loss is normalized by the standard deviation of the asset.

for each model normalized by the standard deviation. As suggested by the risk-measures the GAN return exceeds the other models while it avoids fluctuations and large losses. Table A.VII lists the turnover for the different approaches. The GAN factor has a comparable or even lower turnover than the other SDF portfolios. This suggests that all approaches are exposed to similar transaction costs and it is valid to directly compare their risk-adjusted returns.⁴²

Figure 16: Cumulative Excess Returns of SDF



The figure shows the cumulative excess returns for the SDF for GAN, FFN, EN and LS. Each factor is normalized by its standard deviation for the time interval under consideration.

Avramov, Cheng, and Metzker (2020) raise the concern that the performance of machine learning portfolios could deteriorate in the presence of trading costs due to high turnover or extreme positions.⁴³ This important insight can be taken into account when constructing machine learning investment portfolios. Figure 17 shows the out-of-sample Sharpe ratios of the SDF portfolios after we have set the SDF weights ω to zero for stocks with either market capitalization, bid-ask spread or turnover below a specified cross-sectional quantile at the time of portfolio construction. The idea is to remove stocks that are more prone to trading frictions. There is a clear trade-off between trading-frictions and achievable Sharpe ratios. However, this indicates that a machine learning portfolio can be estimated to optimally trade-off the trading frictions and a high risk-adjusted return. For example, GAN without 40% of the smallest stocks still has an annual SR of 1.73, without 40% of the highest bid-ask spreads the SR is still 2.07, and without 40% of the stocks with the least trading activity measured by turnover the SR is 1.87. Note that these are all lower bounds

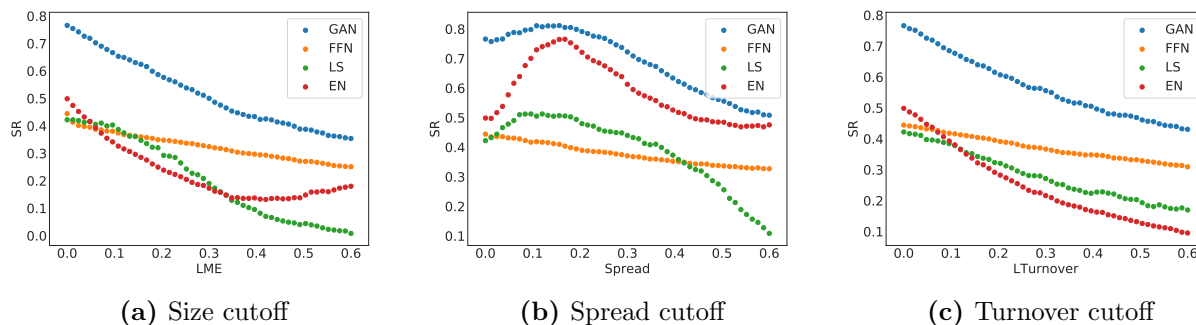
⁴²Gu, Kelly, and Xiu (2020) report high out-of-sample Sharpe ratios for long-short portfolios based on the extreme quantiles of returns predicted by FFN. The Internet Appendix compares the Sharpe ratios for different extreme quantiles for equally and value-weighted long-short portfolios with FFN. We can replicate the high out-of-sample Sharpe ratios when using extreme deciles of 10% or less and equally weighted portfolios. However, for value weighted portfolios the Sharpe ratio drops by around 50%. This is a clear indication that the performance of these portfolios heavily depends on small stocks.

⁴³In their comparison study Avramov, Cheng, and Metzker (2020) also include a portfolio derived from GAN. However, they do not consider our SDF portfolio based on ω but use the SDF loadings β to construct a long-short portfolio based on prediction quantiles.

as GAN has not been re-estimated without these stocks, but we have just set the portfolio weights of the stocks below the cutoffs to zero.

So far, most paper have separated the construction of profitable machine learning portfolios into two steps. In the first step, machine learning methods extract signals for predicting future returns or minimizing pricing errors. In a second step, these signals are used to form profitable portfolios, which are typically long-short investments based on prediction or mean-variance efficient combinations. However, if the goal is to construct optimal machine learning portfolios, these two steps should be combined and also take into account trading frictions, that is, machine learning techniques should extract the signals that are the most relevant for portfolio design under constraints. A promising step into this direction is presented in Bryzgalova, Pelger, and Zhu (2020) who propose a novel framework to combine these two steps to estimate optimal machine learning portfolios subject to trading frictions.

Figure 17: Trading Friction Cutoffs



This figure shows the out-of-sample Sharpe ratios of the SDF for GAN, FFN, EN and LS after we have set the portfolio weights ω to zero if either the market capitalization (**LME**), bid-ask spread (**Spread**) or turnover (**Lturnover**) at the time of investment is below a specified cross-sectional quantile.

J. SDF of Multi-Factor Models

Our GAN framework is *complementary* to conditional and unconditional multi-factor models. Multi-factor models are based on the assumption that the SDF is a linear combination of the multiple factors. In an unconditional multi-factor model with constant factor loadings and pricing errors, the SDF can easily be constructed as the unconditional mean-variance efficient combination of the factors. The time series regression pricing error in such a multi-factor model is identical to that of a one-factor regression on the SDF. However, this relationship does not hold out-of-sample for unconditional models and breaks down in-sample and out-of-sample for conditional multi-factor models. So far, the factor literature has mainly focused on extracting the factors and their loadings, but has been largely silent on the construction of the conditional SDF based on these factors. Our GAN framework can help to close this gap. Formula 2 is the fundamental condition to construct the SDF and can incorporate the restriction that the SDF is a linear combination of factors.

We use one of the most important conditional multi-factor models and combine it with the GAN

framework to estimate its SDF. Instrumented Principal Component Analysis (IPCA) developed by Kelly, Pruitt, and Su (2019) allows for latent factors and time-varying loadings. Both elements are key as we need a conditional factor model with time-varying loadings to explain individual stock returns and want to estimate the best performing factors without taking an a prior stand on what the factors are. Note that this model includes simple unconditional factor models as a special case. As most of the literature Kelly, Pruitt, and Su (2019) use the multi-factor framework to calculate pricing errors and report Sharpe ratios for the unconditional mean-variance efficient combination of the factors, but they do not estimate pricing errors and Sharpe ratios for the same one-factor model of the SDF. Here we show that using the additional economic structure of spanning the SDF with IPCA factors and combining it with the GAN framework can lead to an even better asset pricing model. We condition only on firm characteristics to make the results more comparable with the original IPCA framework.

IPCA assumes a K -factor model where the loadings are a linear function of the characteristics:⁴⁴

$$R_{t+1,i}^e = a_{t,i} + b_{t,i}^\top f_{t+1}^{\text{IPCA}} + \epsilon_{t+1,i} \quad b_{t,i} = I_{i,t}^\top \Gamma b.$$

Any multi-factor model assumes that the SDF is spanned by the factors, that is,

$$F = \sum_{k=1}^K \omega^f(I_{k,t}, I_t) f_{t+1,k}^{\text{IPCA}}. \quad (4)$$

The usual approach used in almost all papers is to set the weights to the unconditional mean-variance efficient portfolio weights, that is, $\omega^{\text{I-SR}} = \text{Cov}(f_{t+1}^{\text{IPCA}}, f_{t+1}^{\text{IPCA}\top})^{-1} \mathbb{E}[f_{t+1}^{\text{IPCA}}]$. An alternative approach to obtain a one-factor representation is to find a linear combination of the IPCA factors and loadings that either minimizes the cross-sectional pricing errors or the amount of unexplained variation. This means that we obtain the SDF weights $\omega^{\text{I-XS}} \in \mathbb{R}^K$ and the corresponding loading weights $v^{\text{I-XS}} \in \mathbb{R}^K$ such that the residuals $R_{t+1,i}^e - b_{t,i}^\top (v^{\text{I-XS}} \omega^{\text{I-XS}\top}) f_{t+1}^{\text{IPCA}} = \hat{e}_{t+1,i}^{\text{I-XS}}$ maximize the XS- R^2 . Similarly, we obtain $\omega^{\text{I-EV}}$ and $v^{\text{I-EV}}$ to maximize EV. If the correct one-factor representation has constant weights on the IPCA factors and their loadings, all three criteria would represent valid identification conditions to recover those weights. Note that in contrast to Kelly, Pruitt, and Su (2019) we estimate the total pricing errors and not only the component that is spanned by the characteristics. In the case of $\omega^{\text{I-EV}}$ all the weight will be put on the first IPCA factor which by construction maximizes the amount of explained variation.

The SDF loadings of the one-factor combination that maximizes the Sharpe ratio are not simply the same combination of the IPCA loadings, that is, in the above notation $\omega^{\text{I-SR}}$ does not need to equal $v^{\text{I-SR}}$. The internally consistent way to estimate the loadings of $F^{\text{I-SR}} = \omega^{\text{I-SR}} f^{\text{IPCA}}$ is to run

⁴⁴Kelly, Pruitt, and Su (2019) also allow for an error term in the loading equation. However, this does not affect the estimation procedure and our discussion, but only the confidence intervals. In order to simplify notation we leave it out.

the IPCA loading regression:

$$\Gamma_\beta = \left(\sum_{t=1}^{T-1} I_t I_t^\top \otimes (F_{t+1}^{\text{I-SR}})^2 \right)^{-1} \left(\sum_{t=1}^{T-1} (I_t \otimes F_{t+1}^{\text{I-SR}})^\top R_{t+1}^e \right), \quad \beta_{i,t}^{\text{I-SR}} = I_{i,t}^\top \Gamma_\beta,$$

where by abuse of notation $I_t \in \mathbb{R}^{q \times N_t}$ denotes here the firm-specific characteristics. This IPCA regression would simply return the IPCA loadings in a multi-factor model. In order to assess the effect of linearity between the characteristics and loadings, we also estimate the IPCA SDF loading $\beta_{i,t}^{\text{I-FFN}}$ with a feedforward neural network, that is, we estimate $\mathbb{E}_t \left[R_{t+1,i}^e F_{t+1}^{\text{I-SR}} \right]$. The combination of GAN and IPCA estimates $\omega^{\text{I-GAN}}$ using Formula 2 but restricting the SDF to a linear combination of IPCA factors based on Equation 4 and then estimates the loadings with FFN in the prediction $\beta_{i,t}^{\text{I-GAN}} = \mathbb{E}_t \left[R_{t+1,i}^e F_{t+1}^{\text{I-GAN}} \right]$.

Table VI: IPCA Asset Pricing with Different SDFs

Model	Benchmark	3	4	5	6	7	8	9	10
IPCA GAN ($\omega^{\text{I-GAN}}, \beta^{\text{I-GAN}}$)	SR	0.61	0.71	0.77	0.70	0.79	0.82	0.72	0.81
	EV	0.05	0.04	0.04	0.05	0.05	0.05	0.04	0.05
	XS- R^2	0.20	0.19	0.17	0.20	0.18	0.20	0.17	0.21
IPCA Max SR FFN Beta ($\omega^{\text{I-SR}}, \beta^{\text{I-FFN}}$)	SR	0.69	0.79	0.82	0.84	0.83	0.86	0.86	0.94
	EV	0.04	0.03	0.03	0.04	0.04	0.04	0.06	0.03
	XS- R^2	0.14	0.13	0.11	0.14	0.14	0.15	0.19	0.14
IPCA Max SR ($\omega^{\text{I-SR}}, \beta^{\text{I-SR}}$)	SR	0.69	0.79	0.82	0.84	0.83	0.86	0.86	0.94
	EV	0.01	0.01	0.01	0.01	0.01	0.01	0.01	0.01
	XS- R^2	-0.05	-0.04	-0.04	-0.04	-0.04	-0.04	-0.04	-0.04
IPCA Max EV ($\omega^{\text{I-EV}}, \beta^{\text{I-EV}}$)	SR	0.11	0.11	0.15	0.17	0.15	0.15	0.14	0.16
	EV	0.04	0.04	0.04	0.04	0.04	0.04	0.04	0.04
	XS- R^2	-0.02	-0.03	-0.03	-0.03	-0.03	-0.03	-0.03	-0.03
IPCA Max XS- R^2 ($\omega^{\text{I-XS}}, \beta^{\text{I-XS}}$)	SR	-0.06	0.15	0.12	0.41	0.33	0.37	0.34	0.41
	EV	-0.02	-0.01	-0.02	-0.02	-0.02	-0.01	-0.02	-0.02
	XS- R^2	-0.03	0.07	0.06	0.12	0.12	0.13	0.13	0.14
IPCA Multifactor ($b_{t,i} \in \mathbb{R}^K$)	SR	0.69	0.79	0.82	0.84	0.83	0.86	0.86	0.94
	EV	0.05	0.05	0.06	0.06	0.06	0.06	0.06	0.07
	XS- R^2	-0.04	-0.03	-0.02	-0.01	-0.02	-0.01	-0.02	-0.02

This table shows the out-of-sample asset pricing results for different SDFs based on IPCA. We consider $K = 3$ to 10 IPCA factors. ($\omega^{\text{I-GAN}}, \beta^{\text{I-GAN}}$) uses the GAN framework to estimate the SDF weights of IPCA factors and the SDF loading. ($\omega^{\text{I-SR}}, \beta^{\text{I-FFN}}$) is the unconditional mean-variance efficient combination of IPCA factors with flexible SDF weights. ($\omega^{\text{I-SR}}, \beta^{\text{I-SR}}$) restricts those weights to be linear. ($\omega^{\text{I-XS}}, \beta^{\text{I-EV}}$) combines the IPCA factors to maximize EV while ($\omega^{\text{I-XS}}, \beta^{\text{I-XS}}$) maximizes $XS-R^2$. The multi-factor representation obtains the residuals with a cross-sectional regression on the multiple loadings. The SDF weights and loadings are estimated on the training data and tuning parameters are chosen optimally on the validation data set.

Table VI summarizes the out-of-sample asset pricing results.⁴⁵ We can replicate the high Sharpe ratios of Kelly, Pruitt, and Su (2019) by forming the unconditional mean variance efficient combination of the IPCA factors. Note that IPCA factors use more information than our models in the main text which might explain the high Sharpe ratios. The IPCA loading regression uses the dependency structure in the characteristic variables over time which makes the factor weights and

⁴⁵Additional results are in the Internet Appendix.

loadings at each point in time a function of all past characteristics. The last subtable shows the IPCA results in a multi-factor framework, that is, we use a cross-sectional regression with multiple loadings to obtain the residual. Similar to PCA methods, IPCA captures a large amount of the variation in return, but not their means. In fact, the cross-sectional R^2 can become negative. If we construct a one-factor model that maximizes the Sharpe ratio, the explained variation of IPCA drops to around 1% without explaining more of the mean returns. The one factor that explains the most variation is simply the first IPCA factor. Similar to PCA methods, this first factor does not explain mean returns. Note that IPCA factors are not necessarily orthogonal to each other and hence estimating the factor that maximizes EV can lead to slightly different results when including more factors. As expected, the best combination for explaining mean returns leads to substantially higher $XS-R^2$, however at the cost of SR and EV . Estimating nonlinear loadings $\beta^{I\text{-FFN}}$ explains more variation and leads to smaller pricing errors. However, the best performing model among all three dimensions is IPCA combined with GAN. The Sharpe ratios are close to those of the mean-variance efficient combination and actually higher than our benchmark GAN for $K \geq 7$, while the $XS-R^2$ almost reaches the level of our benchmark GAN. The explained variation is among the highest of all models and only better for our fully flexible benchmark GAN. In summary, the GAN framework is complementary to multi-factor models and can optimally make use of the additional structure imposed on the SDF and the additional information incorporated in factors.

IV. Conclusion

We propose a new way to estimate asset pricing models for individual stock returns that can take advantage of the vast amount of conditioning information, while keeping a fully flexible form and accounting for time-variation. For this purpose, we combine three different deep neural network structures in a novel way: A feedforward network to capture non-linearities, a recurrent (LSTM) network to find a small set of economic state processes, and a generative adversarial network to identify the portfolio strategies with the most unexplained pricing information. Our crucial innovation is the use of the no-arbitrage condition as part of the neural network algorithm. We estimate the stochastic discount factor that explains all stock returns from the conditional moment constraints implied by no-arbitrage. Our SDF is a portfolio of all traded assets with time-varying portfolio weights which are general functions of the observable firm-specific and macroeconomic variables. Our model allows us to understand what are the key factors that drive asset prices, identify mis-pricing of stocks and generate the conditional mean-variance efficient portfolio.

Our primary conclusions are four-fold. First, we demonstrate the potential of machine learning methods in asset pricing. We are able to identify the key factors that drive asset prices and the functional form of this relationship on a level of generality and with an accuracy that was not possible with traditional econometric methods. Second, we show and quantify the importance of including a no-arbitrage condition in the estimation of machine learning asset pricing models. The “kitchen-sink” prediction approach with deep learning does not outperform a linear model with no-

arbitrage constraints. This illustrates that a successful use of machine learning methods in finance requires both subject specific domain knowledge and a state-of-the-art technical implementation. Third, financial data have a time dimension which has to be taken into account accordingly. Even the most flexible model cannot compensate for the problem if the data are inputted in the wrong format. Standard econometrics techniques of differencing the data to ensure stationarity might lose the information that is essential for the asset pricing model. We show that macroeconomic conditions matter for asset pricing and can be summarized by a small number of economic state variables, which depend on the whole dynamics of all time series. Fourth, asset pricing is actually surprisingly “linear”. As long as we consider anomalies in isolation the linear factor models provide a good approximation. However, the multi-dimensional challenge of asset pricing cannot be solved with linear models and requires a different set of tools.

Our results have direct practical benefits for asset pricing researchers that go beyond our empirical findings. First, we provide a new set of benchmark test assets. New asset pricing models can be tested on explaining our SDF portfolio respectively the portfolios sorted according to the risk exposure in our model. These test assets incorporate the information of all characteristics and macroeconomic information in a small number of assets. Explaining portfolios sorted on a single characteristic is not a high hurdle to pass. Second, we provide a set of macroeconomic time series of hidden states that encapsulate the relevant macroeconomic information for asset pricing. These time series can also be used as an input for new asset pricing models.⁴⁶

Last but not least, our model is directly valuable for investors and portfolio managers. The main output of our model is the risk measure β and the SDF factor weight ω as a function of characteristics and macroeconomic variables. Given our estimates, the user of our model can assign a risk measure and its portfolio weight to an asset even if it does not have a long time series available.

REFERENCES

- ARJOVKY, M., S. CHINTALA, AND B. LEON (2017): “Wasserstein GAN,” *Proceedings of the 34th International Conference on Machine Learning*.
- AVRAMOV, D., S. CHENG, AND L. METZKER (2020): “Machine Learning versus Economic Restrictions: Evidence from Stock Return Predictability,” *Working paper*.
- BANSAL, R., AND S. VISWANATHAN (1993): “No arbitrage and arbitrage pricing: A new approach,” *The Journal of Finance*, 48(4), 1231–1262.
- BIANCHI, D., M. BÜCHNER, AND A. TAMONI (2019): “Bond risk premia with machine learning,” *Working paper*.
- BLANCHET, J., Y. KANG, AND K. MURTHY (2019): “Robust Wasserstein Profile Inference and Applications to Machine Learning,” *Journal of Applied Probability*, 56(3), 830–857.
- BRYZGALOVA, S., M. PELGER, AND J. ZHU (2020): “Forest through the Trees: Building Cross-Sections of Stock Returns,” *Working paper*.

⁴⁶The data are available on <https://mpelger.people.stanford.edu/research>.

- CHAMBERLAIN, G. (1987): “Asymptotic efficiency in estimation with conditional moment restrictions,” *Journal of Econometrics*, 34(3), 305–334.
- FAMA, E. F., AND K. R. FRENCH (1992): “The Cross-Section of Expected Stock Returns,” *The Journal of Finance*, 47(2), 427–465.
- FAMA, E. F., AND K. R. FRENCH (1993): “Common Risk Factors in the Returns on Stocks and Bonds,” *Journal of Financial Economics*, 33(1), 3–56.
- (2015): “A five-factor asset pricing model,” *Journal of Financial Economics*, 116(1), 1–22.
- FENG, G., J. HE, AND N. G. POLSON (2018): “Deep Learning for Predicting Asset Returns,” *Working paper*.
- FENG, G., N. G. POLSON, AND J. XU (2019): “Deep Learning in Characteristics-Sorted Factor Models,” *Working paper*.
- FREYBERGER, J., A. NEUHIERL, AND M. WEBER (2020): “Dissecting characteristics nonparametrically,” *Review of Financial Studies*, forthcoming, 33(5), 2326–2377.
- GOODFELLOW, I., Y. BENGIO, AND A. COURVILLE (2016): *Deep Learning*. MIT Press.
- GOODFELLOW, I., J. POUGET-ABADIE, M. MIRZA, B. XU, D. WARDE-FARLEY, S. OZAIR, A. COURVILLE, AND Y. BENGIO (2014): “Generative adversarial nets,” in *Advances in neural information processing systems*, pp. 2672–2680.
- GU, S., B. KELLY, AND D. XIU (2019): “Autoencoder Asset Pricing Models,” *Journal of Econometrics*, forthcoming.
- GU, S., B. T. KELLY, AND D. XIU (2020): “Empirical Asset Pricing Via Machine Learning,” *Review of Financial Studies*, 33(5), 2223–2273.
- HANSEN, L. P. (1982): “Large sample properties of generalized method of moments estimators,” *Econometrica*, 50(4), 1029–1054.
- HEATON, J., N. POLSON, AND J. H. WITTE (2017): “Deep learning for finance: Deep portfolios,” *Applied Stochastic Models in Business and Industry*, 33(1), 3–12.
- HOCHREITER, S., AND J. SCHMIDHUBER (1997): “Long short-term memory,” *Neural Computation*, 9(8), 1735–1780.
- HOREL, E., AND K. GIESECKE (2020): “Towards Explainable AI: Significance Tests for Neural Networks,” *Journal of Machine Learning Research*, forthcoming.
- KELLY, B., S. PRUITT, AND Y. SU (2019): “Characteristics Are Covariances: A Unified Model of Risk and Return,” *Journal of Financial Economics*, 134(3), 501–524.
- KINGMA, D. P., AND J. BA (2014): “Adam: A Method for Stochastic Optimization,” *CoRR*.
- KOZAK, S., S. NAGEL, AND S. SANTOSH (2020): “Shrinking the Cross Section,” *Journal of Financial Economics*, 135(2), 271–292.
- LETTAU, M., AND M. PELGER (2020): “Factors that Fit the Time-Series and Cross-Section of Stock Returns,” *Review of Financial Studies*, 33(5), 2274–2325.
- LEWIS, G., AND V. SYRGKANIS (2018): “Adversarial Generalized Method of Moments,” *Working paper*.
- LUDVIGSON, S., AND S. NG (2007): “The empirical risk return relation: A factor analysis approach,” *Journal of Financial Economics*, 83(1), 171–222.

- (2009): “Macro factors in bond risk premia,” *Review of Financial Studies*, 22(12), 5027–5067.
- MCCRACKEN, M. W., AND S. NG (2016): “FRED-MD: A monthly database for macroeconomic research,” *Journal of Business & Economic Statistics*, 34(4), 574–589.
- MESSMER, M. (2017): “Deep Learning and the Cross-Section of Expected Returns,” *Working paper*.
- MORITZ, B., AND T. ZIMMERMAN (2016): “Tree-based conditional portfolio sorts: The relation between past and future stock returns,” *Working paper*.
- PELGER, M. (2020): “Understanding Systematic Risk: A High-Frequency Approach,” *Journal of Finance*, *forthcoming*.
- PELGER, M., AND R. XIONG (2019a): “Interpretable Sparse Proximate Factors for Large Dimensions,” *Working paper*.
- (2019b): “State-Varying Factor Models of Large Dimensions,” *Working paper*.
- ROSSI, A. G. (2018): “Predicting Stock Market Returns with Machine Learning,” *Working paper*.
- RUDER, S. (2016): “An overview of gradient descent optimization algorithms,” *CoRR*.
- SIRIGNANO, J., A. SADHWANI, AND K. GIESECKE (2020): “Deep learning for mortgage risk,” *Journal of Financial Econometrics*, *forthcoming*.
- SRIVASTAVA, N., G. HINTON, A. KRIZHEVSKY, I. SUTSKEVER, AND R. SALAKHUTDINOV (2014): “Dropout: A Simple Way to Prevent Neural Networks from Overfitting,” *Journal of Machine Learning Research*, 15, 1929–1958.
- WAGER, S., S. WANG, AND P. S. LIANG (2013): “Dropout training as adaptive regularization,” *Advances in Neural Information Processing Systems*, 26, 351–359.
- WELCH, I., AND A. GOYAL (2007): “A comprehensive look at the empirical performance of equity premium prediction,” *The Review of Financial Studies*, 21(4), 1455–1508.

Appendix A. Estimation Method

Appendix A. Feedforward Network (FFN)

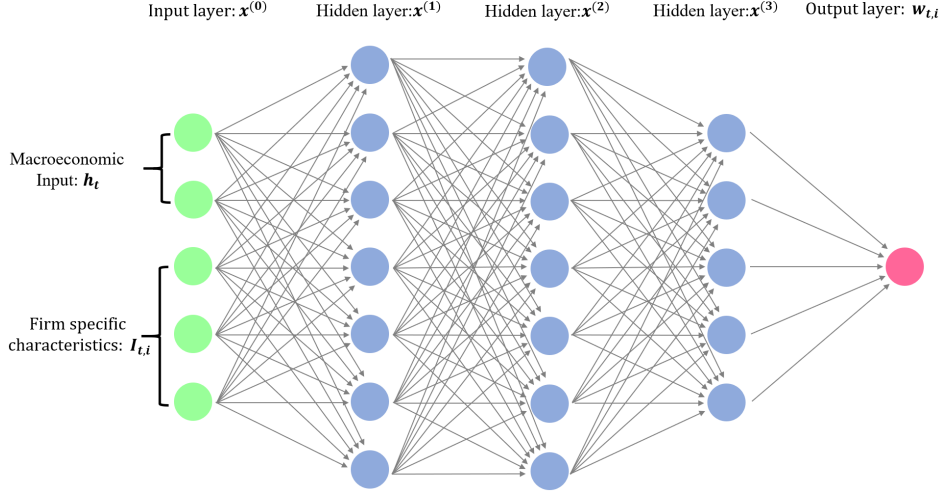
The deep neural network considers L layers as illustrated in Figure A.1. Each hidden layer takes the output from the previous layer and transforms it into an output as

$$x^{(l)} = \text{ReLU} \left(W^{(l-1)\top} x^{(l-1)} + w_0^{(l-1)} \right) = \text{ReLU} \left(w_0^{(l-1)} + \sum_{k=1}^{K^{(l-1)}} w_k^{(l-1)} x_k^{(l-1)} \right)$$

$$y = W^{(L)\top} x^{(L)} + w_0^{(L)}$$

with hidden layer outputs $x^{(l)} = (x_1^{(l)}, \dots, x_{K^{(l)}}^{(l)}) \in \mathbb{R}^{K^{(l)}}$ and parameters $W^{(l)} = (w_1^{(l)}, \dots, w_{K^{(l)}}^{(l)}) \in \mathbb{R}^{K^{(l)} \times K^{(l-1)}}$ for $l = 0, \dots, L - 1$ and $W^{(L)} \in \mathbb{R}^{K^{(L)}}$.

Figure A.1. Feedforward Network with 3 Hidden Layers



Appendix B. Recurrent Neural Network (RNN)

The LSTM is composed of a cell (the memory part of the LSTM unit) and three “regulators”, called gates, of the flow of information inside the LSTM unit: an input gate, a forget gate, and an output gate. Intuitively, the cell is responsible for keeping track of the dependencies between the elements in the input sequence. The input gate controls the extent to which a new value flows into the cell, the forget gate controls the extent to which a value remains in the cell and the output gate controls the extent to which the value in the cell is used to compute the output activation of the LSTM unit.

We take $x_t = I_t$ as the input sequence of macroeconomic information, and the output is the state processes h_t . At each step, a new memory cell \tilde{c}_t is created with current input x_t and previous hidden state h_{t-1}

$$\tilde{c}_t = \tanh(W_h^{(c)}h_{t-1} + W_x^{(c)}x_t + w_0^{(c)}).$$

The input and forget gates control the memory cell, while the output gate controls the amount of information stored in the hidden state:

$$\begin{aligned} \text{input}_t &= \sigma(W_h^{(i)}h_{t-1} + W_x^{(i)}x_t + w_0^{(i)}) \\ \text{forget}_t &= \sigma(W_h^{(f)}h_{t-1} + W_x^{(f)}x_t + w_0^{(f)}) \\ \text{out}_t &= \sigma(W_h^{(o)}h_{t-1} + W_x^{(o)}x_t + w_0^{(o)}). \end{aligned}$$

The sigmoid function σ is an element-wise non-linear transformation. Denoting the element-wise product by \circ , the final memory cell and hidden state are given by

$$c_t = \text{forget}_t \circ c_{t-1} + \text{input}_t \circ \tilde{c}_t, \quad h_t = \text{out}_t \circ \tanh(c_t).$$

We use the state processes h_t instead of the macroeconomic variables I_t as input to our SDF network.

Appendix C. Implementation

For training deep neural networks the vanilla stochastic gradient descent method has proven to be not an efficient method. A better approach is to use optimization methods that introduce an adaptive learning rate.⁴⁷ We use Adam which is an algorithm for gradient-based optimization of stochastic objective functions, based on adaptive estimates of lower-order moments to continuously adjust the learning rate. It is more likely to escape saddle points and hence is more accurate, while also providing faster convergence.

Regularization is crucial and prevents the model from over-fitting on the training sample. Although l_1/l_2 regularization might also be used in training other neural networks, Dropout is preferable and generally results in better performances. The term “Dropout” refers to dropping out units in a neural network. By dropping out a unit, we mean temporarily removing it from the network, along with all its incoming and outgoing connections with a certain probability. Dropout can be shown to be a form of ridge regularization and is only applied during the training.⁴⁸ When doing out-of-sample testing, we keep all the units and their connections.

In summary, the hyperparameter selection works as follows: (1) First, for each possible combination of hyperparameters (384 models) we fit the GAN model. (2) Second, we select the four best combinations of hyperparameters on the validation data set. (3) Third, for each of the four combinations we fit 9 models with the same hyperparameters but different initialization. (4) Finally, we select the ensemble model with the best performance on the validation data set. Table A.VIII reports the tuning parameters of the best performing model. The feedforward network estimating the SDF weights has 2 hidden layers (HL) each of which has 64 nodes (HU). There are four hidden states (SMV) that summarize the macroeconomic dynamics in the LSTM network. The conditional adversarial network generates 8 moments (CHU) in a 0-layer (CHL) network. The macroeconomic dynamics for the conditional moments are summarized in 32 hidden states (CSMV). This conditional network essentially applies a non-linear transformation to the characteristics and the hidden macroeconomic states and then combines them linearly. The resulting moments can, for example, capture the pricing errors of long-short portfolios based on characteristic information or portfolios that only pay off under certain macroeconomic conditions. The FFN for the forecasting approach uses the optimal hyperparameters selected by Gu, Kelly, and Xiu (2020) which is a 3-layer neural network with [32, 16, 8] hidden units, dropout retaining probability of 0.95 and a learning rate of 0.001.⁴⁹

⁴⁷See e.g. Ruder (2016) and Kingma and Ba (2014). We use the leading algorithm Adam. Other adaptive gradient descent methods include Adagrad or Adadelta.

⁴⁸See e.g. Srivastava, Hinton, Krizhevsky, Sutskever, and Salakhutdinov (2014) for the better performance results for Dropout and Wager, Wang, and Liang (2013) for the connection with ridge.

⁴⁹We have estimated our models on two GPU clusters where each cluster has two Intel Xeon E5-2698 v3 CPUs, 1TB memory and 8 Nvidia Titan V GPUs. We have used TensorFlow with Python 3.6 for the model fitting. A complete estimation of the GAN model with hyperparameter tuning takes around 3 days.

Appendix B. Simulation Example

We illustrate with simulations that (1) the no-arbitrage condition in GAN is necessary to find the SDF in a low signal-to-noise setup, (2) the flexible form of GAN is necessary to correctly capture the interactions between characteristics, and (3) the RNN with LSTM is necessary to correctly incorporate macroeconomic dynamics in the pricing kernel. On purpose, we have designed the simplest possible simulation setup to convey these points and to show that the forecasting approach or the simple linear model formulations cannot achieve these goals.⁵⁰

Excess returns follow a no-arbitrage model $R_{t+1,i}^e = \beta_{t,i}F_{t+1} + \epsilon_{t+1,i}$. In our simple model the SDF follows $F_t \stackrel{i.i.d.}{\sim} \mathcal{N}(\mu_F, \sigma_F^2)$ and the idiosyncratic component $\epsilon_{t,i} \stackrel{i.i.d.}{\sim} N(0, \sigma_e^2)$. We consider two different formulations for the risk-loadings:

1. *Two characteristics*: The loadings are the multiplicative interaction of two characteristics

$$\beta_{t,i} = C_{t,i}^{(1)} \cdot C_{t,i}^{(2)} \quad \text{with } C_{t,i}^{(1)}, C_{t,i}^{(2)} \stackrel{i.i.d.}{\sim} \mathcal{N}(0, 1).$$

2. *One characteristic and one macroeconomic state process*: The loading depends on one characteristic and a cyclical state process h_t :

$$\beta_{t,i} = C_{t,i} \cdot b(h_t), \quad h_t = \sin(\pi * t/24) + \epsilon_t^h, \quad b(h) = \begin{cases} 1 & \text{if } h > 0 \\ -1 & \text{otherwise.} \end{cases}$$

We observe only the macroeconomic time series with trend $Z_t = \mu_M t + h_t$. All innovations are independent and normally distributed: $C_{t,i} \stackrel{i.i.d.}{\sim} \mathcal{N}(0, 1)$ and $\epsilon_t^h \stackrel{i.i.d.}{\sim} \mathcal{N}(0, 0.25)$.

The choice of the parameters is guided by our empirical results and summarized in Table A.I. The panel data set is $N = 500, T = 600$, where the first $T_{train} = 250$ are used for training, the next $T_{valid} = 100$ observations are the validation and the last $T_{test} = 250$ observations form the test data set. The first model setup with two characteristics has two distinguishing empirical features: (1) the loadings have a non-linear interaction effect for the two characteristics; (2) for many assets the signal-to-noise ratio is low. Because of the multiplicative form the loadings will take small values when two characteristics with values close to zero are multiplied. Figure A.2 shows the form of the population loadings. The assets with loadings in the center are largely driven by idiosyncratic noise which makes it harder to extract their systematic component.

Table A.I reports the results for the first model. The GAN model outperforms the forecasting approach and the linear model in all categories. Note, that it is not necessary to include the elastic net approach as the number of covariates is only two and hence the regularization does not help. The Sharpe Ratio of the estimated GAN SDF reaches the same value as the population SDF used to generate the data. Based on the estimated loadings respectively the population loadings we project out the idiosyncratic component to obtain the explained variation and cross-sectional

⁵⁰We have run substantially more simulations for a variety of different model formulations, where we reach the same conclusions. The other simulation results are available upon request.

pricing errors. As expected the linear model is mis-specified for this setup and captures neither the SDF nor the correct loading structure. Note, that the simple forecasting approach can generate a high Sharpe Ratio but fails in explaining the systematic component.

Table A.I: Performance of Different SDF Models in Two Simulation Setups

Model	Sharpe Ratio			EV			Cross-sectional R^2		
	Train	Valid	Test	Train	Valid	Test	Train	Valid	Test
Two characteristics and no macroeconomic state variable									
Population	0.96	1.09	0.94	0.16	0.15	0.17	0.17	0.15	0.17
GAN	0.98	1.11	0.94	0.12	0.11	0.13	0.10	0.09	0.07
FFN	0.94	1.04	0.89	0.05	0.04	0.05	-0.30	-0.09	-0.33
LS	0.07	-0.10	0.01	0.00	0.00	0.00	0.00	0.01	0.01
One characteristic and one macroeconomic state variable									
Population	0.89	0.92	0.86	0.18	0.18	0.17	0.19	0.20	0.15
GAN	0.79	0.77	0.64	0.18	0.18	0.17	0.19	0.20	0.15
FFN	0.05	-0.05	0.06	0.02	0.01	0.02	0.01	0.01	0.02
LS	0.12	-0.05	0.10	0.16	0.16	0.15	0.15	0.18	0.14

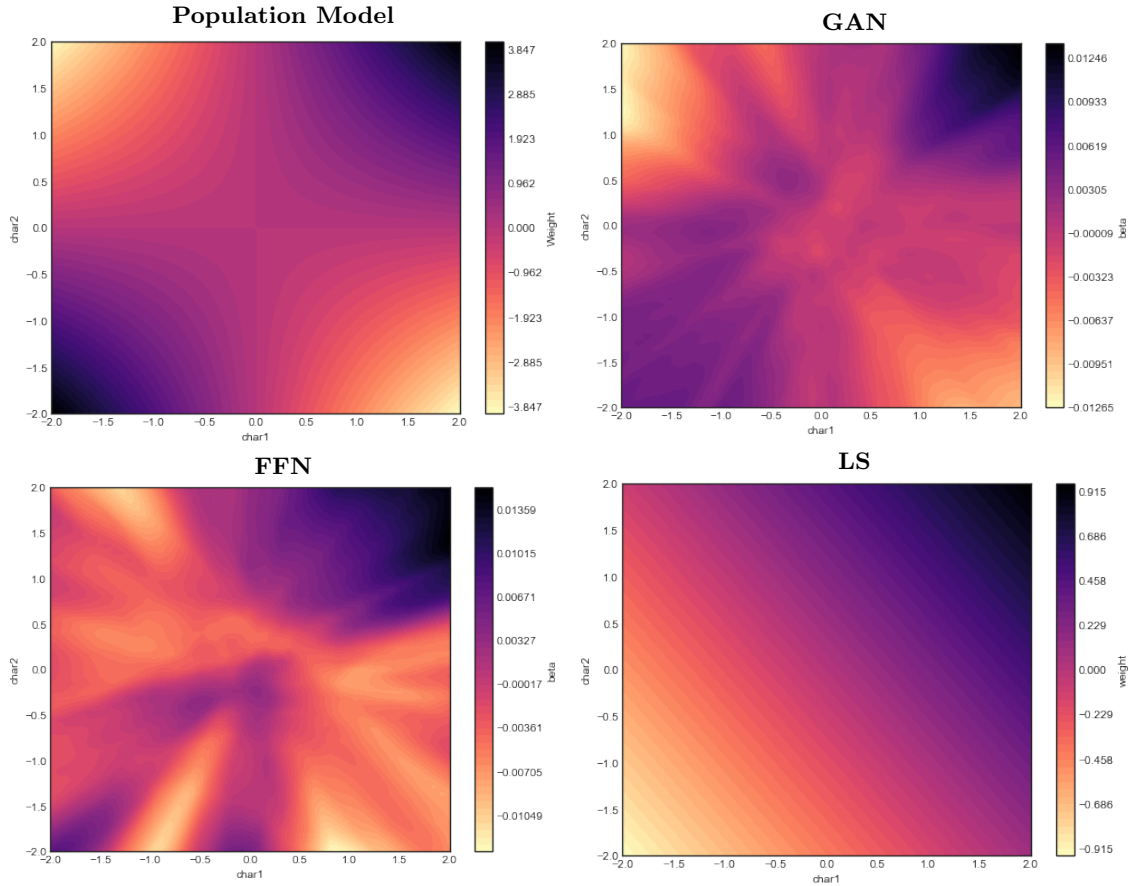
This table reports the Sharpe Ratio (SR) of the SDF, explained time series variation (EV) and cross-sectional mean R^2 for the GAN, FFN and LS model. EN is left out in this setup as there are only very few covariates. The data are generated with an SDF with Sharpe Ratio $SR = 1$ and $\sigma_F^2 = 0.1$ and the idiosyncratic noise has $\sigma_e^2 = 1$. The macroeconomic time-series has the trend $\mu_M = 0.05$. The number of observations is $N = 500, T = 600, T_{train} = 250, T_{valid} = 100$ and $T_{test} = 250$.

Figure A.2 explains why we observe the above performance results. Note, that the SDF has large positive respectively negative weights on the extreme corner combinations of the characteristics. The middle combinations are close to zero. The GAN network captures this pattern and assigns positive weights on the combinations of high/high and low/low and negative weights for high/low and low/high. The FFN on the other hand generates a more diffuse picture. It assigns negative weights for low/low combinations. The FFN SDF still loads mainly on the extreme portfolios which results in the high Sharpe Ratio. However, the FFN fails to capture the loadings correctly which leads to high unexplained variation and pricing errors. The linear model can obviously not capture the non-linear interaction.

The second model setup with a macroeconomic state variable is designed to model the effect of a boom and recession cycle on the pricing model. In our model the SDF affects the assets differently during a boom and recession cycle. Note that in our example the macroeconomic variable can by construction only have a scaling effect on the loadings of the SDF factor, but not change its cross-sectional distribution which only depends on firm-specific information.

Figure A.3 illustrates the path of the observed macroeconomic variable that has the distinguishing feature that we observe for most macroeconomic variables in our data set: (1) the macroeconomic process is non-stationary, i.e. it has a trend; (2) the process has a cyclical dynamic structure, i.e. it is influenced by business cycles. For example GDP level has a similar qualitative behaviour. The conventional approach to deal with non-stationary data is to take first differences. Figure A.3 shows that the differenced data does indeed look stationary but loses all information about the

Figure A.2: SDF Weights ω for the First Model with 2 Characteristics



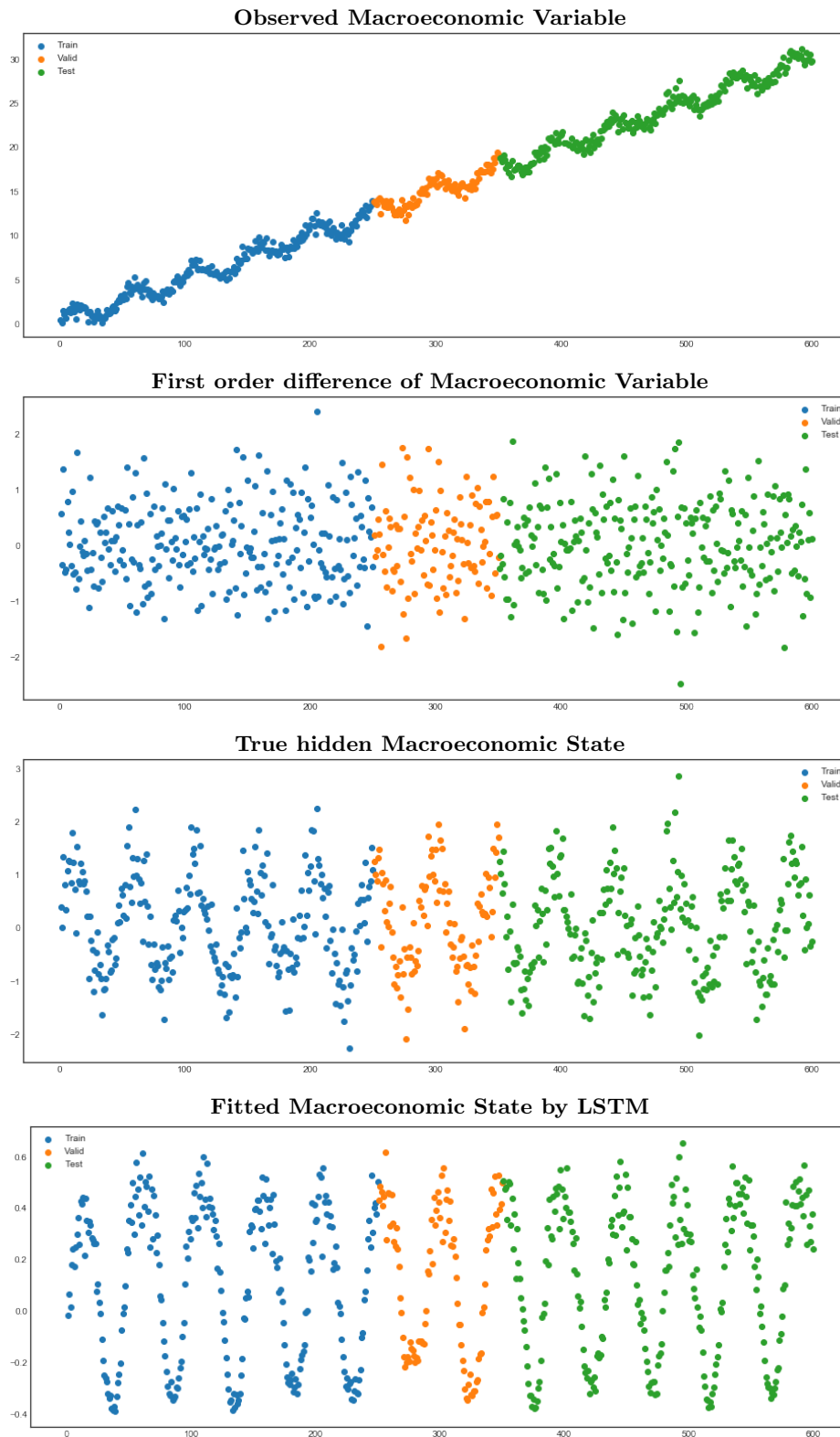
This figures shows the SDF weights ω as the function of the two characteristics estimated by different methods. Note that in our simple simulation the SDF weights ω coincide with the SDF loadings β .

business cycle. The LSTM network in our GAN model can successfully extract the hidden state process. The models based on only the most recent first differences can by construction not infer any dynamics in the macroeconomic variables.

Table A.I reports the results for the second model with macroeconomic state variable. As expected our GAN model strongly outperforms the forecasting and the linear model. Note, that the loading function here is linear and the macroeconomic state variable is only a time-varying proportionality constant for the loadings and SDF weights. As the projection on the systematic component is not affected by a proportionality constant, the linear model actually achieves the same explained variation and pricing errors as GAN. However, the Sharpe Ratio of the linear model collapses as for roughly half of the times it uses the wrong sign for the SDF weights.

The simulation section illustrates three findings: (1) All three evaluation metrics (SR, EV and XS-R2) are necessary to assess the quality of the SDF factor. (2) By conditioning only on the most recent macroeconomic observations, general macroeconomic dynamics are ruled out. (3) The no-arbitrage condition in the GAN model helps to deal with a low signal-to-noise ratio.

Figure A.3. Dynamics of the Macroeconomic State Variable



Appendix D. Asset Pricing Results for Sorted Portfolios

Table A.III: Explained Variation and Pricing Errors for Decile Sorted Portfolios

	EN	FFN	GAN	EN	FFN	GAN	EN	FFN	GAN	EN	FFN	GAN
	Short-Term Reversal						Momentum					
Decile	Explained Variation			Alpha			Explained Variation			Alpha		
1	0.84	0.74	0.77	-0.18	-0.21	-0.13	0.04	-0.06	0.33	0.37	0.39	0.11
2	0.86	0.81	0.82	0.00	-0.05	0.00	0.12	0.10	0.52	0.25	0.18	-0.01
3	0.80	0.82	0.84	0.13	0.04	0.06	0.19	0.25	0.66	0.14	0.05	-0.06
4	0.69	0.80	0.82	0.16	0.03	0.03	0.28	0.34	0.73	0.15	0.08	-0.02
5	0.58	0.68	0.71	0.13	-0.03	-0.04	0.37	0.46	0.80	0.19	0.09	0.02
6	0.43	0.66	0.75	0.22	0.05	0.01	0.45	0.58	0.78	0.02	-0.03	-0.09
7	0.23	0.64	0.77	0.20	0.03	-0.02	0.62	0.69	0.68	0.01	0.01	-0.05
8	-0.07	0.49	0.67	0.23	0.03	-0.05	0.58	0.71	0.64	-0.03	-0.04	-0.09
9	-0.25	0.29	0.58	0.30	0.09	-0.01	0.55	0.70	0.58	0.08	0.04	-0.03
10	-0.24	-0.04	0.35	0.47	0.38	0.18	0.51	0.53	0.53	0.24	0.29	0.19
All	Explained Variation			Cross-Sectional R^2			Explained Variation			Cross-Sectional R^2		
	0.43	0.58	0.70	0.45	0.79	0.94	0.26	0.27	0.54	0.66	0.71	0.93
	Book-To-Market						Size					
Decile	Explained Variation			Alpha			Explained Variation			Alpha		
1	0.38	0.66	0.70	0.03	-0.12	-0.08	0.80	0.75	0.79	0.09	-0.00	0.10
2	0.48	0.73	0.78	0.10	-0.05	-0.04	0.89	0.89	0.90	-0.11	-0.09	-0.06
3	0.71	0.84	0.86	0.07	-0.03	-0.01	0.91	0.80	0.91	-0.07	0.02	-0.02
4	0.76	0.88	0.89	0.00	-0.07	-0.07	0.90	0.77	0.91	-0.05	0.04	-0.01
5	0.82	0.87	0.88	0.05	0.02	0.01	0.90	0.78	0.91	0.01	0.10	0.04
6	0.77	0.82	0.88	0.06	0.04	0.02	0.88	0.80	0.91	0.03	0.09	0.02
7	0.81	0.81	0.87	0.03	0.08	0.03	0.84	0.81	0.89	0.04	0.05	-0.01
8	0.71	0.59	0.78	0.03	0.12	0.06	0.84	0.85	0.88	0.06	0.03	-0.02
9	0.80	0.72	0.80	-0.02	0.11	0.07	0.77	0.81	0.82	0.06	-0.01	-0.04
10	0.68	0.73	0.79	-0.05	-0.00	0.00	0.32	0.28	0.49	-0.04	-0.15	-0.10
All	Explained Variation			Cross-Sectional R^2			Explained Variation			Cross-Sectional R^2		
	0.70	0.75	0.82	0.97	0.94	0.98	0.83	0.78	0.86	0.96	0.95	0.97

This table shows the out-of-sample explained variation and pricing errors for decile-sorted portfolios based on Short-Term Reversal (**ST_REV**), Momentum (**r12.2**), Book to Market Ratio (**BEME**) and Size (**LME**).

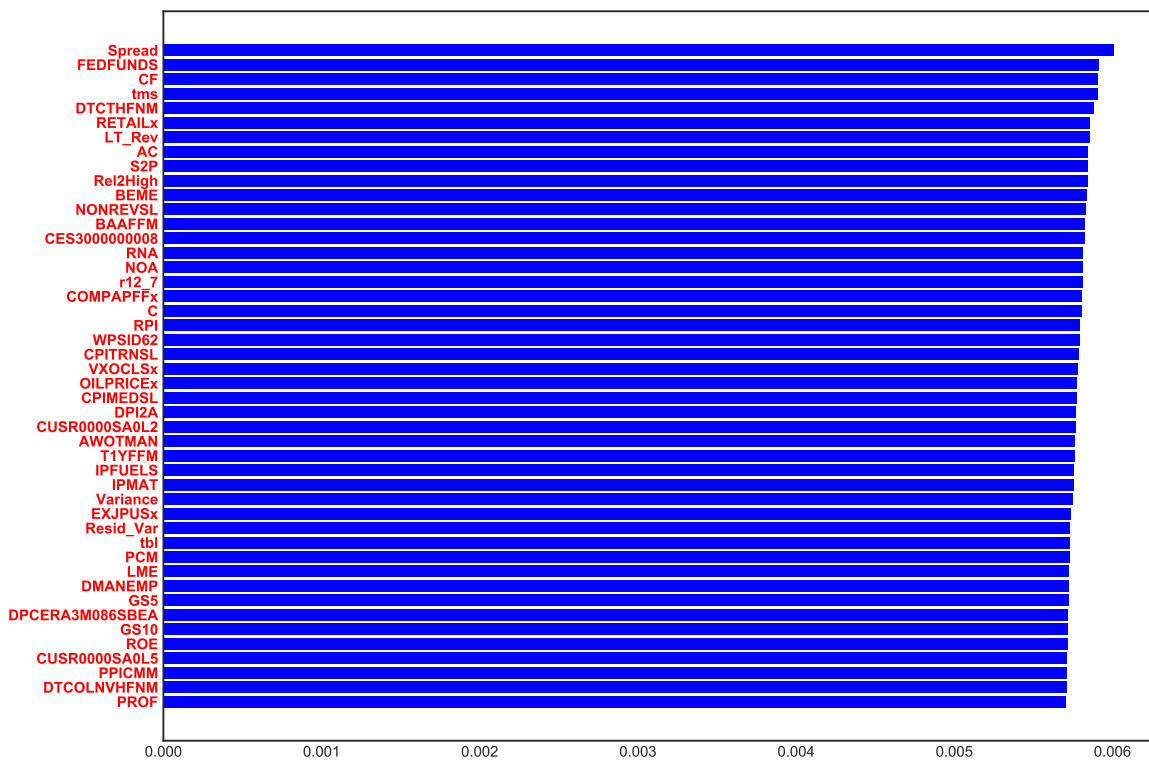
Table A.IV: Explained Variation and Pricing Errors for Double-Sorted Portfolios based on Short-Term Reversal /Momentum and Size/Book-to-Market Ratio

		Short-Term Reversal and Momentum						Size and Book-To-Market Ratio					
		EN	FFN	GAN	EN	FFN	GAN	EN	FFN	GAN	EN	FFN	GAN
ST_REV/ LME	r12.2/ BEME	Explained Variation			Alpha			Explained Variation			Alpha		
1	1	0.35	0.32	0.62	0.16	0.13	0.08	0.55	0.47	0.63	-0.01	-0.00	-0.06
1	2	0.55	0.48	0.72	-0.02	-0.04	-0.05	0.66	0.62	0.74	0.01	0.00	-0.04
1	3	0.66	0.61	0.74	-0.06	-0.07	-0.05	0.74	0.70	0.76	0.04	0.01	0.01
1	4	0.74	0.62	0.67	-0.06	-0.05	-0.02	0.77	0.69	0.75	0.01	-0.02	0.01
1	5	0.69	0.58	0.58	-0.10	-0.06	-0.03	0.70	0.66	0.76	-0.01	-0.03	0.02
2	1	0.17	0.16	0.53	0.22	0.19	0.11	0.58	0.20	0.68	0.01	0.11	-0.02
2	2	0.32	0.39	0.67	0.18	0.11	0.08	0.68	0.48	0.81	0.02	0.07	-0.01
2	3	0.59	0.61	0.71	0.08	0.03	0.01	0.82	0.74	0.86	0.04	0.06	0.03
2	4	0.72	0.74	0.59	0.00	-0.03	-0.02	0.81	0.75	0.85	-0.03	-0.00	-0.01
2	5	0.56	0.61	0.54	0.08	0.05	0.06	0.77	0.79	0.85	-0.04	0.00	0.02
3	1	-0.02	-0.01	0.48	0.18	0.16	0.01	0.53	0.25	0.73	0.08	0.12	0.02
3	2	0.13	0.33	0.65	0.12	0.02	-0.03	0.70	0.59	0.85	0.10	0.11	0.05
3	3	0.41	0.62	0.66	0.13	0.02	-0.00	0.86	0.82	0.90	0.06	0.08	0.05
3	4	0.46	0.60	0.48	0.03	-0.06	-0.07	0.86	0.82	0.88	0.01	0.05	0.02
3	5	0.39	0.53	0.42	0.08	-0.01	-0.02	0.79	0.76	0.81	-0.04	0.02	0.01
4	1	-0.24	-0.27	0.31	0.26	0.24	0.06	0.53	0.50	0.79	0.12	0.09	0.01
4	2	-0.24	0.15	0.58	0.14	0.05	-0.04	0.74	0.78	0.85	0.07	0.04	-0.00
4	3	0.02	0.51	0.68	0.11	-0.02	-0.06	0.80	0.84	0.83	0.05	0.02	0.00
4	4	0.19	0.53	0.51	0.11	-0.01	-0.04	0.83	0.81	0.85	0.02	0.03	0.01
4	5	0.17	0.47	0.51	0.14	0.02	-0.01	0.73	0.77	0.79	-0.05	-0.02	-0.01
5	1	-0.58	-0.88	0.08	0.13	0.17	-0.08	0.28	0.29	0.44	0.01	-0.09	-0.06
5	2	-0.41	-0.12	0.42	0.14	0.06	-0.06	0.54	0.53	0.58	0.00	-0.08	-0.05
5	3	-0.28	0.23	0.53	0.16	0.03	-0.03	0.51	0.56	0.57	-0.01	-0.04	-0.04
5	4	-0.06	0.31	0.44	0.12	-0.00	-0.05	0.54	0.60	0.67	-0.01	-0.00	-0.02
5	5	-0.01	0.27	0.36	0.29	0.16	0.11	0.37	0.52	0.56	-0.04	-0.03	-0.03
All		Explained Variation			Cross-Sectional R^2			Explained Variation			Cross-Sectional R^2		
All		0.20	0.26	0.53	0.50	0.77	0.92	0.67	0.60	0.76	0.94	0.91	0.98

This table shows the out-of-sample explained variation and pricing errors for double sorted portfolios based on short-term reversal (ST_REV) and momentum (r12.2) respectively size (LME) and book-to-market ratio (BEME).

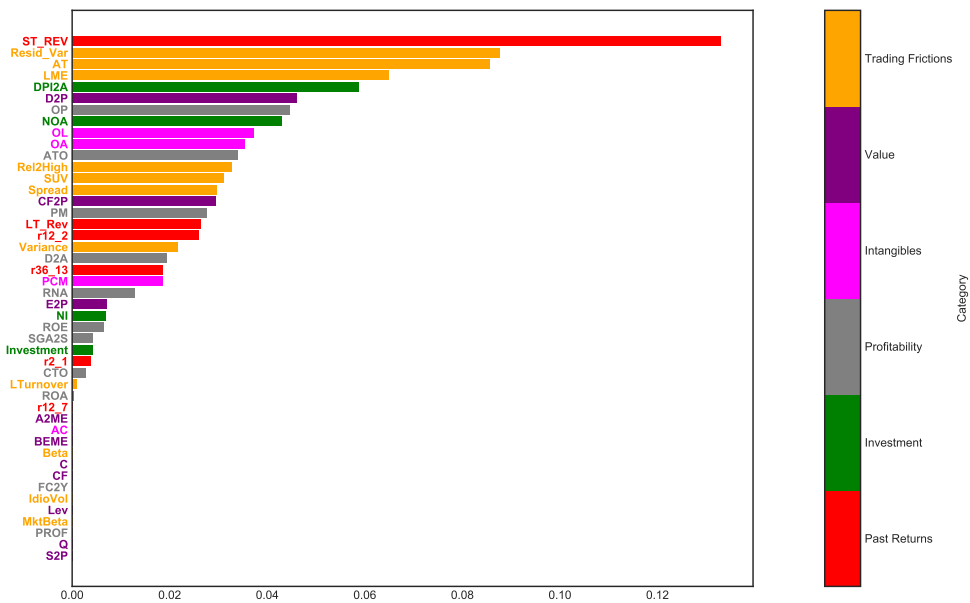
Appendix E. Variable Importance

Figure A.4: Macroeconomic Variable Importance for GAN SDF



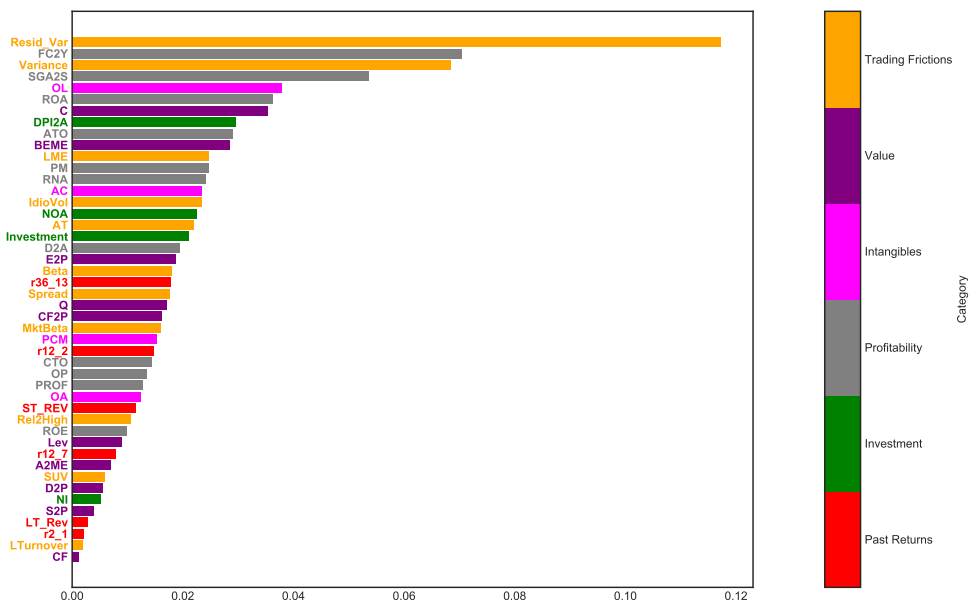
This figure shows the GAN variable importance ranking of the 178 macroeconomic variables in terms of average absolute gradient on the test data. The values are normalized to sum up to one.

Figure A.5: Characteristic Importance for EN



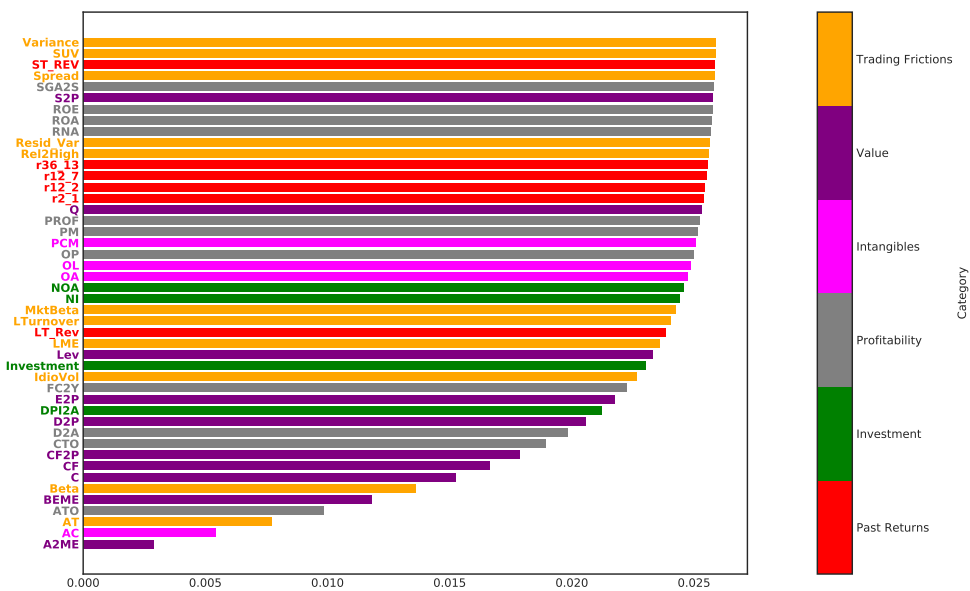
The figure shows the Elastic Net variable importance ranking of the 46 firm-specific characteristics in terms of average absolute gradient on the test data. The values are normalized to sum up to one.

Figure A.6: Characteristic Importance for LS



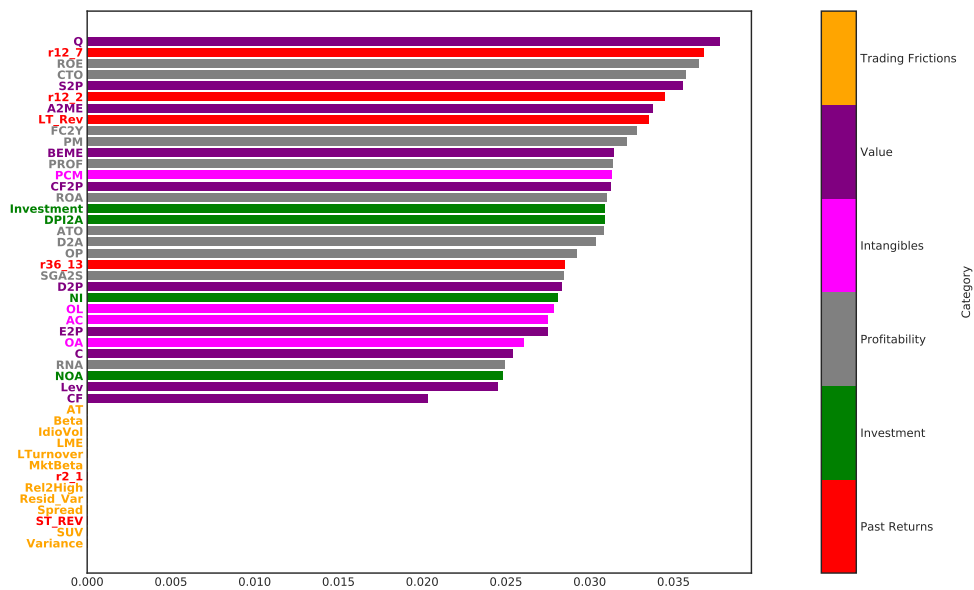
The figure shows the LS variable importance ranking of the 46 firm-specific characteristics in terms of average absolute gradient on the test data. The values are normalized to sum up to one.

Figure A.7: Characteristic Importance for Conditioning Function g for GAN



The figure shows the GAN variable importance ranking for the conditioning function g of the 46 firm-specific characteristics in terms of average absolute gradient on the test data. The ranking is the average of the absolute gradients for the nine ensemble fits. The values are normalized to sum up to one.

Figure A.8: Characteristic Importance for Conditioning Function g for GAN No Frict



The figure shows the GAN variable importance ranking for the conditioning function g of the 46 firm-specific characteristics in terms of average absolute gradient on the test data. The ranking is the average of the absolute gradients for the nine ensemble fits. This GAN model excludes trading frictions and past returns in the construction of the conditioning function g . The values are normalized to sum up to one.

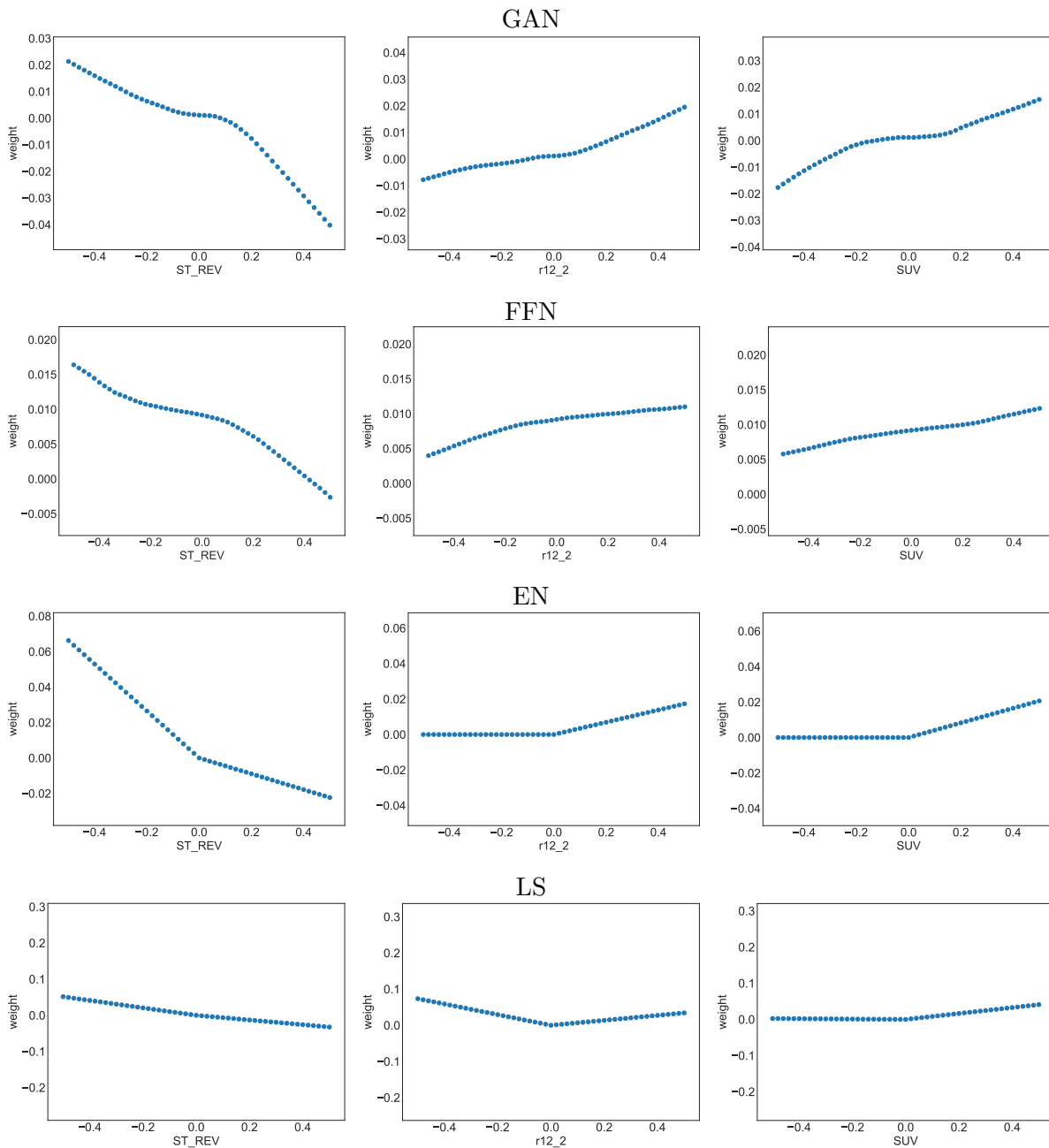
Appendix F. SDF Structure

Table A.V: Correlation of GAN SDF with Fama-French 5 Factors and Time-Series Regression

	Mkt-RF	SMB	HML	RMW	CMA	intercept
Regression Coefficients	0.00	0.00	-0.04	0.08***	0.04	0.76***
	(0.02)	(0.02)	(0.03)	(0.03)	(0.04)	(0.06)
Correlations	-0.10	-0.09	0.01	0.17	0.05	-

This table shows out-of-sample correlations and the time-series regression of the GAN SDF on the Fama-French 5 factors. Standard errors are in parenthesis. The regression intercept is the monthly time series pricing error of the SDF portfolio.

Figure A.9: SDF weight ω as a Function of Characteristics for Different Models



This figure shows the SDF weight ω as a one-dimensional function of covariates keeping the other covariates at their mean level. The covariates are Short-Term Reversal (ST_REV), Momentum (r12_2) and Standard Unexplained Volume (SUV).

Appendix G. Machine Learning Investment

Table A.VI: SDF Portfolio Risk Measures

Model	SR			Max Loss			Max Drawdown		
	Train	Valid	Test	Train	Valid	Test	Train	Valid	Test
FF-3	0.27	-0.09	0.19	-2.45	-2.85	-4.31	7	10	10
FF-5	0.48	0.40	0.22	-2.62	-2.33	-4.90	4	3	7
LS	1.80	0.58	0.42	-1.96	-1.87	-4.99	1	3	4
EN	1.37	1.15	0.50	-2.22	-1.81	-6.18	1	3	5
FFN	0.45	0.42	0.44	-3.30	-4.61	-3.37	6	3	5
GAN	2.68	1.43	0.75	0.38	-0.28	-5.76	0	1	5

This table reports the Sharpe ratio, maximum 1-month loss and maximum drawdown of the SDF portfolios. We include the mean-variance efficient portfolio based on the 3 and 5 Fama-French factors.

Table A.VII: Turnover by Models

Model	Long Position			Short Position		
	Train	Valid	Test	Train	Valid	Test
LS	0.25	0.22	0.24	0.64	0.55	0.61
EN	0.36	0.35	0.35	0.83	0.83	0.84
FFN	0.69	0.63	0.65	1.38	1.29	1.27
GAN	0.47	0.40	0.40	1.05	1.04	1.02

This table reports the turnover for positions with positive and negative weights for the SDF portfolios. It is defined as $\frac{1}{T} \sum_{t=1}^T (\sum_i |(1 + R_{P,t+1})w_{i,t+1} - (1 + R_{i,t+1})w_{i,t}|)$, where $w_{i,t}$ is the portfolio weight of stock i at time t , and $R_{P,t+1} = \sum_i R_{i,t+1}w_{i,t}$ is the corresponding portfolio return. Long and short positions are calculated separately, and the portfolio weights are normalized to $\|w_t\|_1 = 1$.

Appendix H. Implementation and Robustness Results

Appendix A. Tuning Parameters and Robustness

Table A.VIII: Selection of Hyperparameters for GAN in the Empirical Analysis

Notation	Hyperparameters	Candidates	Optimal
HL	Number of layers in SDF Network	2, 3 or 4	2
HU	Number of hidden units in SDF Network	64	64
SMV	Number of hidden states in SDF Network	4 or 8	4
CSMV	Number of hidden states in Conditional Network	16 or 32	32
CHL	Number of layers in Conditional Network	0 or 1	0
CHU	Number of hidden units in Conditional Network	4, 8, 16 or 32	8
LR	Initial learning rate	0.001, 0.0005, 0.0002 or 0.0001	0.001
DR	Dropout	0.95	0.95

This table shows the optimal tuning parameters of the benchmark GAN. The optimal SDF network has 2 layers each with 64 nodes and uses 4 hidden macroeconomic state processes. The optimal adversarial network is a generalized linear model creating 8 instruments and uses 32 hidden macroeconomic states. The Dropout parameter denotes the probability of keeping a node.

Table A.IX: Best Performing GAN Models on the Validation Data

Model	SMV	CSMV	HL	CHL	CHU	LR	SR (Train)	SR (Valid)	SR (Test)
GAN 1	4	32	4	0	32	0.001	2.78	1.47	0.72
GAN 2	4	32	2	0	8	0.001	3.02	1.39	0.77
GAN 3	4	32	4	0	16	0.0005	2.55	1.38	0.74
GAN 4	4	16	3	1	16	0.0005	2.44	1.38	0.77

This tables shows a re-estimation of the GAN model that is independent of the benchmark GAN model and reports the network structure. GAN 1 has 4 layers, 32 instruments and 4 hidden states. GAN 2 has 2 layers, 8 instruments and 4 hidden states and the hence the same architecture as our benchmark model. GAN 3 has 4 layers, 16 instruments and 4 hidden states, while GAN 4 has 3 layers, 16 instruments and 4 hidden states.

Table A.X: Correlation of Benchmark GAN SDF with SDF of Alternative GAN Estimations

	GAN	GAN 1	GAN 2	GAN 3	GAN 4	GAN Rolling	GAN No Frict
GAN	1	0.84	0.87	0.84	0.80	0.70	0.78
GAN 1	0.84	1	0.88	0.92	0.89	0.79	0.89
GAN 2	0.87	0.88	1	0.87	0.88	0.73	0.83
GAN 3	0.84	0.92	0.87	1	0.89	0.74	0.86
GAN 4	0.80	0.89	0.88	0.89	1	0.78	0.84
GAN Rolling	0.70	0.79	0.73	0.74	0.78	1	0.78
GAN No Frict	0.78	0.89	0.83	0.86	0.84	0.78	1

This table reports the factor correlations for alternative estimations of GAN. GAN is the benchmark model, GAN 1, 2, 3 and 4 are the top four performing models from a re-estimation. GAN Rolling is estimated on a rolling window of 240 months. GAN No Frict is an estimation of the GAN model without trading friction variables and past returns for the conditioning instruments g .

Figure A.10. Characteristic Importance for Rolling Window GAN

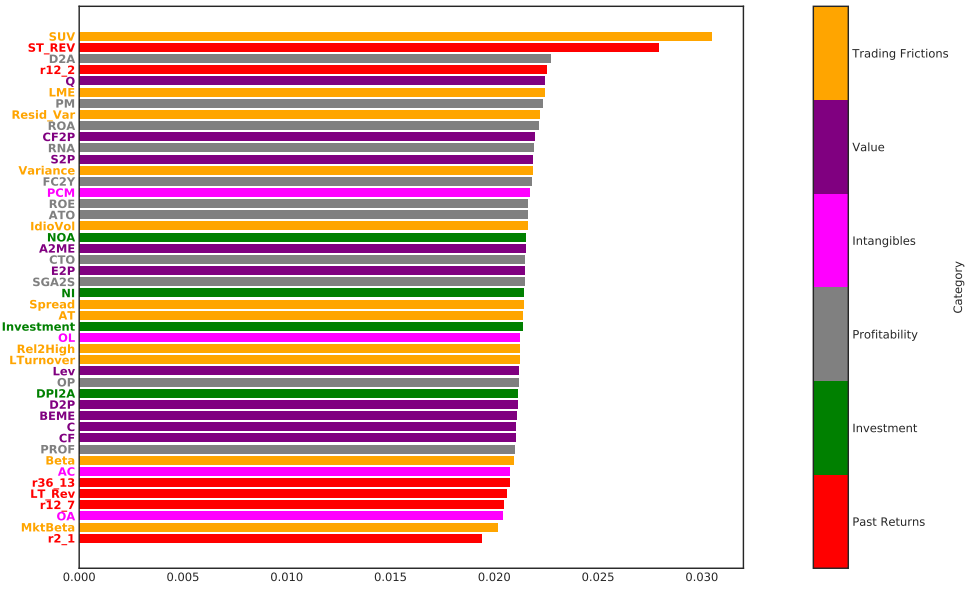
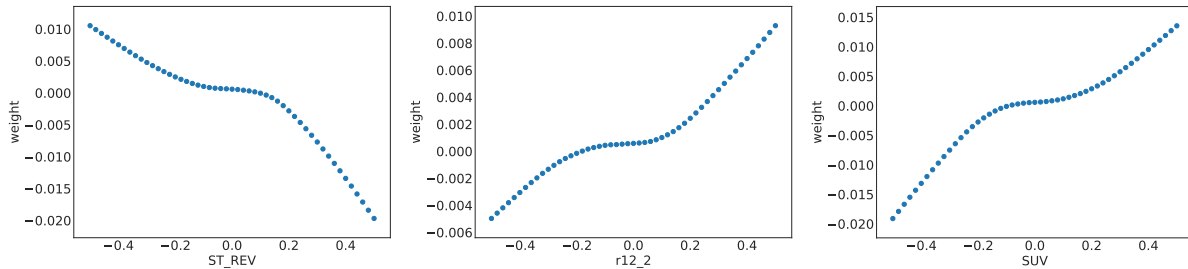
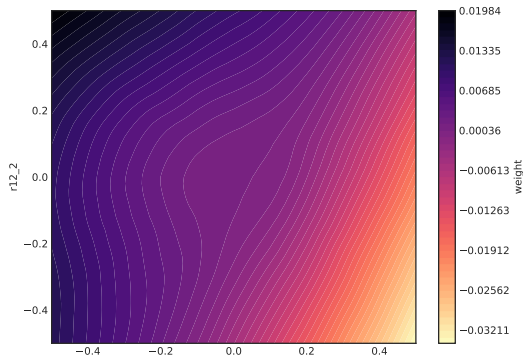


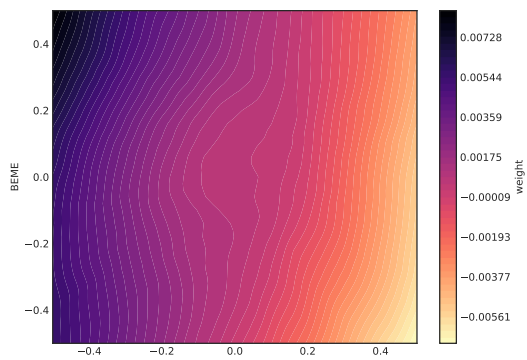
Figure A.11: SDF weight ω as a Function of Covariates for Rolling Window Fit



(a) SDF weight ω as a function of one characteristic



(b) Interaction between Short-Term Reversal (ST.REV) and Momentum (r12_2)



(c) Interaction between Size (LME) and Book to Market Ratio (BEME)

These figures show the variable importance and functional form of the SDF estimated on a rolling window of 240 months. The sensitivities and SDF weights ω are the average over those rolling window estimates.